



Fachhochschule Köln  
Cologne University of Applied Sciences



UNIVERSIDAD AUTÓNOMA DE SAN LUIS POTOSÍ  
FACULTADES DE CIENCIAS QUÍMICAS, INGENIERÍA Y MEDICINA  
PROGRAMAS MULTIDISCIPLINARIOS DE POSGRADO EN CIENCIAS AMBIENTALES

AND

COLOGNE UNIVERSITY OF APPLIED SCIENCES

INSTITUTE FOR TECHNOLOGY AND RESOURCES MANAGEMENT IN THE TROPICS AND SUBTROPICS

## **DYNAMICS OF THE COASTAL KARST AQUIFER IN NORTHERN YUCATÁN PENINSULA**

THESIS TO OBTAIN THE DEGREE OF

MAESTRÍA EN CIENCIAS AMBIENTALES

DEGREE AWARDED BY

UNIVERSIDAD AUTÓNOMA DE SAN LUIS POTOSÍ

AND

MASTER OF SCIENCE

TECHNOLOGY AND RESOURCES MANAGEMENT IN THE TROPICS AND SUBTROPICS

IN THE SPECIALIZATION: RESOURCES MANAGEMENT

DEGREE AWARDED BY COLOGNE UNIVERSITY OF APPLIED SCIENCES

PRESENTS:

**LISA HEISE**

CO-DIRECTOR OF THESIS PMPCA

DR. ANTONIO CARDONA BENAVIDES

CO-DIRECTOR OF THESIS ITT:

DR. LARS RIBBE

ASSESSOR:

DR. EDUARDO H. GRANIEL CASTRO



Fachhochschule Köln  
Cologne University of Applied Sciences



UNIVERSIDAD AUTÓNOMA DE SAN LUIS POTOSÍ  
FACULTADES DE CIENCIAS QUÍMICAS, INGENIERÍA Y MEDICINA  
PROGRAMAS MULTIDISCIPLINARIOS DE POSGRADO EN CIENCIAS AMBIENTALES

AND

COLOGNE UNIVERSITY OF APPLIED SCIENCES  
INSTITUTE FOR TECHNOLOGY AND RESOURCES MANAGEMENT IN THE TROPICS AND SUBTROPICS

## **DYNAMICS OF THE COASTAL KARST AQUIFER IN NORTHERN YUCATÁN PENINSULA**

THESIS TO OBTAIN THE DEGREE OF  
MAESTRÍA EN CIENCIAS AMBIENTALES  
DEGREE AWARDED BY  
UNIVERSIDAD AUTÓNOMA DE SAN LUIS POTOSÍ  
AND  
MASTER OF SCIENCE  
TECHNOLOGY AND RESOURCES MANAGEMENT IN THE TROPICS AND SUBTROPICS  
IN THE SPECIALIZATION: RESOURCES MANAGEMENT  
DEGREE AWARDED BY COLOGNE UNIVERSITY OF APPLIED SCIENCES

PRESENTS:

**LISA HEISE**

DR. ANTONIO CARDONA BENAVIDES

DR. LARS RIBBE

DR. EDUARDO H. GRANIEL CASTRO

---

---

---

**PROYECTO FINANCIADO POR:**

“Evaluación de la calidad del agua subterránea que subyace a la ciudad de Mérida y su impacto en la zona costera del estado de Yucatán”

Aceptado en el fondo sectorial CONAGUA-CONACYT, S0012-2010-02

Clave de Registro: 148167

PROJECT-MANAGER: DR. EDUARDO H. GRANIEL CASTRO

FACULTAD DE INGENIERÍA – UNIVERSIDAD AUTÓNOMA DE YUCATÁN

**PROYECTO REALIZADO EN:**

**PMPCA**

**FACULTAD DE INGENIERÍA**

**UNIVERSIDAD AUTÓNOMA DE SAN LUIS POTOSÍ**

**CON EL APOYO DE:**

**DEUTSCHER AKADEMISCHER AUSTAUSCH DIENST (DAAD)  
CONSEJO NACIONAL DE CIENCIA Y TECNOLOGÍA (CONACYT)**

**LA MAESTRÍA EN CIENCIAS AMBIENTALES RECIBE APOYO A TRAVÉS DEL PROGRAMA  
NACIONAL DE POSGRADOS (PNPC - CONACYT)**

## **Erklärung / Declaración**

Name / Nombre: Lisa Heise

Matri.-Nr. / N° de matricula: **11085733 (CUAS), 0204032 (UASLP)**

Ich versichere wahrheitsgemäß, dass ich die vorliegende Masterarbeit selbstständig verfasst und keine anderen als die von mir angegebenen Quellen und Hilfsmittel benutzt habe. Alle Stellen, die wörtlich oder sinngemäß aus veröffentlichten und nicht veröffentlichten Schriften entnommen sind, sind als solche kenntlich gemacht.

*Aseguro que yo redacté la presente tesis de maestría independientemente y no use referencias ni medios auxiliares a parte de los indicados. Todas las partes, que están referidas a escritos o a textos publicados o no publicados son reconocidas como tales.*

Die Arbeit ist in gleicher oder ähnlicher Form noch nicht als Prüfungsarbeit eingereicht worden.

*Hasta la fecha, un trabajo como éste o similar no ha sido entregado como trabajo de tesis.*

San Luis Potosí, den /el \_\_\_\_\_

Unterschrift / Firma: \_\_\_\_\_

Ich erkläre mich mit einer späteren Veröffentlichung meiner Masterarbeit sowohl auszugsweise, als auch Gesamtwerk in der Institutsreihe oder zu Darstellungszwecken im Rahmen der Öffentlichkeitsarbeit des Institutes einverstanden.

*Estoy de acuerdo con una publicación posterior de mi tesis de maestría en forma completa o parcial por las instituciones con la intención de exponerlos en el contexto del trabajo investigación de las mismas.*

Unterschrift / Firma: \_\_\_\_\_

## Acknowledgements

I would like to express my gratitude to all the people that accompanied and supported me during the development of this master thesis in their own particular way.

First of all I would like to thank my thesis committee conformed by Dr. Antonio Cardona Benavides from the Faculty of Engineering of the Autonomous University San Luis Potosí (UASLP), Dr. Lars Ribbe from the Institute for Technology and Resources Management in the Tropics and Subtropics (ITT) and Dr. Eduardo Graniel Castro from the Faculty Engineering (FIUADY) of who gave me the opportunity to form part of this research project and have given valuable advice and their constructive and critical attention throughout my thesis development process.

Furthermore I sincerely thank “las niñas” (Manuel, Emmanuel, Darío) of the FIUADY for their great support during my fieldwork accompanying me surviving crocodiles, mangrove worms and bogged-down vans. I thank Jazmin for her hospitality and Yucatanian culinary skills.

Thanks to Ing. Ana María Guadalupe López Hernández, Ing. Sandra Dinorah Ramos Martínez and Dra. Erika Padilla Ortega of the Laboratorio de Análisis químico de agua y suelo de la facultad de Ingeniería – UASLP for the analysis of more than 100 water samples.

Thank you MC María Elena García Arreola for the trace element analysis with ICP-MS in the Instituto de Geología – UASLP.

I thank the hardworking students and “inhabitants” of the student’s room and the Área de Ciencias de la Tierra (Hermann, Socrates, Ricardo, Isidro, Erik, Lalo, Luis, Lupita, Montse, Adriana) for their company and many valuable discussions.

Thanks to my parents who always supported me with their good and happy thoughts mostly from the other side of the “charco” as wells as my friends Lechen, Merle and Klára.

Sincere thanks are given to Sandra Avendaño, Maricela Rodriguez Díaz de Leon, Farah Ahmed, Lupita, Juanito, Dr. Claudia Raedig, Dr. Jackson Röhrig, Dr. Johannes Hamhaber and Dr. Juan Antonio Reyes Agüero for their support and motivation.

I thank Ali, Claudia, Carlos, Antonio, la señora Gilda, señora Juanina and señor Agustín and all the kind people that accompanied me on this way.

I would like to give my special thanks to my ENREM-Family alias “clique de amor” (Diana, Du, Uva with Enremesito, Teris, Firi, Maticas, Adri, Paola and Miguel) friends that are family who accompanied me over the whole two unique and unforgettable years of this master program that I will always remember.

---

**Content**

Acknowledgements .....	5
Abstract.....	10
Resumen .....	11
1 Introduction .....	13
1.1 Background & Justification .....	14
1.2 Objectives .....	16
2 Geographical setting.....	17
2.1 Physiography & Karst Morphology.....	21
2.2 Hydrology .....	22
2.3 Vegetation .....	23
2.4 Climate.....	25
2.5 Soils .....	30
2.6 Geology.....	31
2.7 Hydrogeology .....	32
2.8 Study Area .....	36
3 Methodology.....	38
3.1 Hydraulic Measurements .....	40
3.1.1 Datalogger .....	42
3.2 Water Quality.....	44
3.2.1 Hydrolab MS5 Multiprobe .....	44
3.2.2 Water Sampling .....	46
4 Results .....	49
4.1 Hydraulic Measurements .....	49
4.1.1 Datalogger .....	49
4.1.2 Hydraulic heads & Groundwater flow.....	55
4.1.3 Hydraulic gradients.....	57
4.1.4 Artesian wells .....	62
4.2 Hydrochemistry .....	68
4.2.1 Hydrolab .....	68
4.2.2 Sampling.....	77
5 Discussion & Conceptual Model.....	90
5.1 Water Chemistry .....	91
5.2 Hydraulics .....	96

6	Conclusion & Outlook.....	98
7	References .....	101
8	Appendix .....	107

## List of Figures

Figure 1:	Study area with monitoring network of observation wells and flowing artesian wells. ....	18
Figure 2:	The administrative aquifers of the Yucatán Peninsula with the location of the observation wells of this investigation (red dots). ....	19
Figure 3:	The Yucatán Peninsula with intermittent rivers in the southern and central part. ....	23
Figure 4:	Vegetation distribution of the Yucatán Peninsula in year 2005.....	24
Figure 5:	Historical records of potential annual evaporation, annual precipitation, maximal monthly precipitation, mean temperature and important hurricane events for Mérida and Progreso. ....	26
Figure 6:	Climate Diagrams for Mérida and Progreso for the historical period (1961-2012) and the period of this study from April 2012 to April 2013. Data for February Progreso are missing. ....	28
Figure 7:	Climate types according to classification by Köppen and García modified by García. ....	29
Figure 8:	Predominant soil types of the study area and the state of Yucatán.....	30
Figure 9:	Geological classification of Tertiary and Quaternary sediments, reproduced according to García Gil & Graniel Castro (2010).....	32
Figure 10:	The Ghyben-Herzberg principle under hydrostatic equilibrium conditions, based on Essaid (1986). ....	34
Figure 11:	Hydraulic conductivities represented according to Ford and Williams (2007) with the highest hydraulic conductivity for the Yucatán aquifer. ....	36
Figure 12:	Satellite image, location of the study areas with the observation wells in the urban areas of Mérida and the artesian wells at the coastline. Elaborated with Google Earth and ArcMap 10.1 (INEGI, 2013). ....	37
Figure 13:	Measurements of hydraulic heads in the flowing artesian wells. ....	41
Figure 14:	Installation of the two dataloggers at different depth in the observation wells. ....	42
Figure 15:	Installation for the capture of precipitation water in Mérida and Progreso. ....	48
Figure 16:	Difference between the water levels obtained from the two datalogger registrations in the observation well Chalmuch. ....	50
Figure 17:	Precipitation variation and hydraulic head fluctuation. ....	50
Figure 18:	Relation between precipitation and electrical conductivity. ....	51
Figure 19:	Variations of hydraulic heads and electrical conductivity. ....	51
Figure 20:	Relation between groundwater temperature and electrical conductivity. ....	52
Figure 21:	Relation between groundwater temperature and hydraulic heads. ....	52
Figure 22:	Decreasing temperature trend towards the coastline.....	54
Figure 23:	Equipotential maps for different month. ....	56
Figure 24:	Potentiometric slope obtained from hydraulic heads. ....	57
Figure 25:	Hydraulic gradient maps for four month.....	61
Figure 26:	Hydraulic heads related to the coast distance. ....	62

Figure 27: Hydraulic heads during 12 hours measurement and tidal curve, tide data from MAR V1.0 J.I. (Gonzales, 2011). .....	64
Figure 28: Groundwater discharge variations due to tidal influence. ....	65
Figure 29: Zoom to three datalogger registration days of water levels in Baag compared to tide.....	66
Figure 30: Zoom to three datalogger registration days of water levels in Dzidzilché compared to tide.....	66
Figure 31: Variation of hydraulic heads in the artesian wells Manantiales during the whole study period.....	67
Figure 32: Variation of hydraulic heads in the artesian wells Exbasurero during the whole study period.....	67
Figure 33: Schematical vertical zonation of the aquifer waters layers with different salt content.....	69
Figure 34: Quality profiles of the observation well Matemáticas. ....	70
Figure 35: Relation between mixing zone depth and coast distance of four transects. ....	74
Figure 36: Electrical conductivity profiles for six observation wells.....	75
Figure 37: Evolution of the electrical conductivity measured with the Hydrolab in the artesian wells during the investigation period.....	76
Figure 38: Errors resulting from the major ion balance of all water samples. ....	77
Figure 39: Water types of the shallow samples from September 2012 and February 2013. ....	82
Figure 40: Water types of the intermediate samples from September 2012 and February 2013.....	82
Figure 41: Water types of the deep samples (left) and the samples from artesian wells, precipitation, lagoon and ocean water (right). ....	83
Figure 42: Percentages of different water types for the shallow and intermediate water samples.....	84
Figure 43: Conceptual model of the study area.....	90

## List of Tables

Table 1: Water volumes of the administrative aquifers of the Yucatán Peninsula in $10^6 \text{ m}^3 \text{ year}^{-1}$ . ....	20
Table 2: Basic data of the observation wells. ....	39
Table 3: Basic data of the artesian wells at the study site Manantiales.....	40
Table 4: Basic data of the artesian wells at the study site Exbasurero. ....	40
Table 5: Hydraulic gradients for three transects in June. ....	58
Table 6: Hydraulic gradients for four transects in August. ....	59
Table 7: Hydraulic gradients for four transects in September.....	59
Table 8: Hydraulic gradients for three transects in November.....	59
Table 9: Hydraulic gradients for three transects in February. ....	60
Table 10: Ranges of hydraulic gradients (dimensionless) obtained for the study area from the interpolated manual measurements of hydraulic heads. ....	60
Table 11: Hydraulic gradients for study area of the artesian wells Manantiales.....	63
Table 12: Hydraulic gradients for study area of the artesian wells Exbasurero. ....	63
Table 13: Common chemical classification of waters reproduced and combined according to Robinove et al. (1958) and Moody et al. (1988).....	68

Table 14: Depth and thickness of fresh-saltwater mixing zone. a: only in January and March electrical conductivity $\geq 1,400 \mu\text{S cm}^{-1}$ was registered, b: only in August electrical conductivity $\geq 1,400 \mu\text{S cm}^{-1}$ , c: the mixing zone continues outside the scope of the observation well.....	72
Table 15: Electrical conductivity, TDS, sodium and chloride for the shallow samples during both sampling campaigns. In bold are values above drinking water standard.....	79
Table 16: Electrical conductivity, TDS, sodium and chloride for the intermediate samples during both sampling campaigns. In bold are values above drinking water standard. ....	80
Table 17: Water classification according to hardness, reproduced after Sawyer (1960). ....	81
Table 18: Alkalinity, hardness and pH for the different sample classes and sampling campaigns. a: the sampling date was 13.04.2012, b: the pH was measured in-situ. ....	81
Table 19: Percentage of samples with concentrations above Mexico's drinking water standard. ....	85
Table 20: Shallow samples, parameters exceeding the Mexican drinking water standards. February samples were not analyzed regarding coliform bacteria. ....	87
Table 21: Intermediate samples, parameters exceeding the Mexican drinking water standards. February samples were not analyzed regarding coliform bacteria. ....	87
Table 22: Deep samples, parameters exceeding the Mexican drinking water standards. February samples were not analyzed regarding coliform bacteria. ....	88
Table 23: Artesian wells samples, parameters exceeding the Mexican drinking water standards. February samples were not analyzed regarding coliform bacteria. ....	89

## Appendix

Appendix 1: Hydraulic heads [masl] obtained manually from the observation wells.....	107
Appendix 2: Ion concentrations in $\text{meq L}^{-1}$ for the September 2012 samples.....	108
Appendix 3: Ion balance errors for the September 2012 samples.....	109
Appendix 4: Ion concentrations in $\text{meq L}^{-1}$ for the February 2013 samples. ....	110
Appendix 5: Ion balance errors for the February 2013 samples.....	112
Appendix 6: Coliform concentrations for September 2012 samples.....	113
Appendix 7: Element concentrations for shallow samples. In bold values above Mexican drinking water standard. ....	114
Appendix 8: Element concentrations for intermediate samples. In bold values above Mexican drinking water standard. ....	115
Appendix 9: Element concentrations for deep samples. In bold values above Mexican drinking water standard. ....	117
Appendix 10: Element concentrations for deep samples. In bold values above Mexican drinking water standard. ....	118

**Abstract**

The Yucatán Peninsula lacks surface waters consequently groundwater resources are indispensable for human water supply. Due to the relatively high recharge rate of the shallow karst aquifer, most of the Yucatán Peninsula does not face a problem related to water scarcity but water quality, one of the most important ecosystem services. Groundwater underlying Mérida city discharges at the coastline, however several point and diffuse anthropogenic and natural (saltwater intrusion) contamination sources compromise water quality. The main objective of this research was to characterize the current status of a 1600 km<sup>2</sup> area of the coastal Yucatán karst aquifer in the northwestern region of the Yucatán Peninsula, including both quantity and quality issues, this was accomplished by investigating hydraulic conditions and water chemistry composition. This information was used to understand the systems' dynamics and its importance for the diverse ecosystems in the karst terrain.

Because of the climatic conditions and high hydraulic conductivity of the geologic material, natural recharge is highly dynamic, a direct relationship between precipitation and groundwater head evolution in the monitoring wells was identified. The spatial and temporal variations of water quality were determined. Natural discharge at the coastal zone was investigated from flowing artesian wells; influence of tidal fluctuations, natural and induced recharge by precipitation and planned and unplanned injection were identified. The results were used to develop a conceptual model describing the functioning of the aquifer flow system as a fundamental component and driving force of aquatic and terrestrial ecosystems, emphasizing the indispensable need of preservation and sustainable management of the study area is. The most serious identified problem in Yucatán is groundwater pollution due to septic tanks, sewage, pesticides and fertilizers, leaching of industrial waste water and saltwater intrusion.

Because of the karstic condition and the permeability of the geologic material a direct relationship between precipitation events in Mérida or Progreso respectively and the fluctuation of the aquifer water levels registered in the observation wells was identified. On the other hand, the variation of natural discharge at the coastal flowing artesian wells seems to correspond more with tidal fluctuation than dynamic recharge by precipitation. The relationship between the artesian wells discharge and the tide is governed by the influence of the diurnal course of the ocean over the water level in the artesian wells.

The hydraulic gradients varied temporally and spatially throughout the study area so did the contamination impacts. Overall proceeding mixing of fresh- and saltwater and degraded groundwater quality were identified. In the coastal observation wells seawater influence was reported at shallow depth and in both, deep groundwater samples from the continental

wells and samples from the discharging water at the artesian wells pollution with heavy metals was detected.

## **Resumen**

La Península de Yucatán carece de aguas superficiales por consiguiente los recursos del agua subterránea son indispensable para el abastecimiento de agua potable de la población. Debido a que la recarga del acuífero kárstico es relativamente alta, la mayor parte de la Península de Yucatán no se enfrenta a un problema de escases de agua pero de calidad de agua, uno de los servicios ambientales más importantes. El agua subterránea que subyace a la ciudad de Mérida descarga en la línea costera pero varias fuentes de contaminación puntual y difusa, antropogénica y natural (intrusión de agua salada) comprometen la calidad del agua. El objetivo principal de esta investigación fue la caracterización de la situación actual de un área de 1600 km<sup>2</sup> del acuífero kárstico costero en el noroeste de la Península de Yucatán incluyendo aspectos cuantitativos y cualitativos del agua, realizando una investigación de las condiciones hidráulicas y la composición química del agua. La información fue usada para entender las dinámicas del sistema y su importancia para los diversos ecosistemas del terreno kárstico.

Debido a las condiciones climáticas y la alta conductividad hidráulica del material geológico, la recarga natural es muy dinámica, una relación directa entre precipitación y la evolución de la carga hidráulica en los pozos de monitorización fue identificada. Se determinaron las variaciones espaciales y temporales de la calidad del agua. La descarga natural se investigó en pozos artesianos de la zona costera, la influencia de las fluctuaciones de marea, recarga natural e inducida por precipitación e inyecciones planeadas y no planeadas fue identificada. Los resultados se usaron para desarrollar un modelo conceptual describiendo el funcionamiento del sistema de flujo del acuífero como componente fundamental y la fuerza motriz de los ecosistemas terrestres y acuáticos, enfatizando la gran necesidad de preservación y manejo sustentable de la zona de estudio.

El problema más grave que se identificó es la contaminación del agua subterránea debida a fosas sépticas, aguas residuales, pesticidas y fertilizantes y lixiviación de desagües industriales e intrusión de agua salada.

Debido a las condiciones del karst y la alta permeabilidad del material geológico se identificó una relación muy directa entre eventos de precipitación en Mérida o Progreso respectivamente y la fluctuación de las cargas hidráulicas del acuífero registradas en los pozos de monitorización. Por otro lado la variación de la descarga natural de los pozos artesianos sugiere indicar que corresponde más a las fluctuaciones de la marea que a la recarga dinámica por precipitación. La relación entre la descarga de los pozos artesianos y

la marea se ve influenciada por el curso diurno del océano sobre los niveles de agua en los pozos artesianos. Los gradientes hidráulicos varían en términos temporales y espaciales a lo largo de la zona de estudio igual que los impactos de contaminación. En general se identificó la mezcla de agua dulce y salada en casi todos los pozos de observación y degradación de la calidad del agua subterránea. En los pozos de observación cercanos a la línea de costa se reportó influencia de agua salada a poca profundidad y en algunas muestras profundas de los pozos tierra adentro y del agua de descarga de los artesian wells contaminación por metales pesados fue detectada.

## 1 Introduction

During the last century the worldwide increase in water use to support human activities has been eightfold, accompanied by a fourfold increase in population and consequently a 50 % increase in water consumption per capita (Chapin et al., 2011). Groundwater resources are highly important for human water supply as in some regions surface water is absent. On the Yucatán Peninsula the only available fresh water resource is groundwater, it lacks surface water except in the southern part where some runoff is drained by intermittent rivers that disappear in the subsoil. The Yucatán Peninsula represents one of the most extensive karst terrains worldwide. With an extension of approximately 165,000 km<sup>2</sup> this trans-boundary aquifer system includes regions of Mexico, Guatemala and Belize (Bauer-Gottwein et al., 2011).

Worldwide carbonate karst landscapes occupy around 15 % of the earth's ice-free continental surface (Ford and Williams, 2007). Karst landscapes arise from the combination of high rock solubility, well developed secondary (fracture) porosity and the availability of water. Karst aquifers play an important role especially because 20-25 % of the global population depends on groundwater provided by karst aquifers (Ford & Williams, 2007). Unfortunately these resources are getting under pressure; the need of preservation and sustainable management is indispensable.

Surface karst landscape in the Yucatán Peninsula has a particular geomorphology evolving together with the groundwater flow system resulting in caves, cenotes and diverse ecosystems with a high touristic attractiveness. The constant increase of tourism and population in the last 40 years exerts pressure on the aquifer with regard to the groundwater quality and quantity. Due to the high permeability of the geologic material, karst aquifers are particularly fragile and vulnerable to contamination (Ford and Williams, 2007). The degradation of the groundwater quality beneath Mérida city and surroundings has been reported by various research studies (Graniel et al., 1999; Marín et al., 2000; Pacheco Ávila et al., 2004).

The current primary research project “Evaluation of the groundwater quality that underlies the city of Mérida and its impact in the coastal zone of the state of Yucatán” with the registration key 148167, approved in the call for proposals S0012-2010-02 and funded by the National Water Commission (CONAGUA) and the National Council on Science and Technology (CONACYT) is being developed over three years (2011-2014). The principal goal of the general project is to propose strategies for a sustainable management of the coastal aquifer region achieving a realignment to reach conservation of the water resources. During the period of the investigation project various bachelor and master thesis were

realized covering different research topics from geophysical to vulnerability analysis of the study area in Mérida and surroundings. This master thesis contributes to this project with an integral hydrogeological analysis of the study area including hydrochemical, physicochemical and hydraulic investigations, fundamental information required for the understanding of the water flow system as a socio-ecological system.

## **1.1 Background & Justification**

The hydrogeological analysis of this investigation is fundamental for the understanding of the groundwater flow system functioning in the karst aquifer, and its relation to recharge events. With the information a hydrogeological conceptual model integrating the evaluation of contamination impacts on the system can be described. This research contributes with an analysis of the contamination impacts and distribution of pollution caused in the aquifer by different kind of sources (untreated sewage, industrial wastewater and saltwater intrusion). Therefore the planned analysis is essential to understand how and to what extend the groundwater water quality beneath Mérida city, affects water discharge to coastal lagoons and the ocean.

It is not unusual to find groundwater pollution underneath any major city nowadays, but it is troubling to find it in an aquifer that serves as the sole source of drinking water (Marín et al., 2000). Furthermore increasing mean air temperature and consequently rising evapotranspiration and precipitation decrease should cause recharge of groundwater to reduce, exerting an impact to the groundwater flow regime, with decrease of discharge fluxes from land to the ocean and increase of saline intrusion (Bautista, 2011).

According to Bauer-Gottwein et al. (2011) seawater intrusion in Yucatán is an already extensive condition and reaches tens of kilometers inland, however few studies have addressed the dynamics of the fresh-saltwater interface in the northern part of the Yucatán Peninsula. Beddows (2004) reported multi-temporal observations from localities on the Riviera Maya (eastern Yucatán Peninsula) detecting both stable and dynamic interface configurations. Escolero Fuentes et al. (2007) made interface observations during hurricane Isidore aftermath (September 2002) and detected cyclic fluctuations in the interface position following the abnormal recharge event. Graniel Castro et al. (2005) analyzed the dynamics of the Yucatán coastal aquifer and the fresh-saltwater interface at the northeast coast of Yucatán for the 2002-2004 period. They detected that the fresh-saltwater interface responds to seasonal variations in recharge and discharge and that wells near the coastline are exposed to organic contamination and the saline intrusion.

In general scientists affirm that both magnitudes of groundwater recharge and coastal outflow from the Yucatán aquifer to the ocean require further research (Bauer-Gottwein et al., 2011). This study will contribute to the comprehension of the coastal discharge system and aquifer dynamics. Physicochemical analysis of water samples and determination of the fresh-saltwater interface in the densely populated region will be used for the evaluation of environmental impacts on water resources and coastal ecosystems.

Karst aquifers play an important role especially because they provide around 25 % of the worldwide human drinking water supply and in many regions they represent the only available fresh water supply for the population (Ford and Williams, 2007). The research area includes the highly populated city of Mérida, where groundwater resources are significant because there is no surface water available for drinking purposes. High permeability of the outcropping geologic material is one of the main factors that make karst aquifers very vulnerable to contamination. Detrimental impacts on groundwater quality beneath Mérida city and surroundings have been reported elsewhere due to two distinct impacts: (i) the mixing with saltwater underlying the fresh groundwater (Steinich and Marín, 1996; Marín, et al., 2000) and (ii) anthropogenic activities (septic tank leaks, improper construction of landfills and industrial or agricultural residues) that lead to water quality degradation (Pacheco A. & Cabrera S., 1997; Graniel et al., 1999; Marín et al., 2000).

Morris (1994) and Marín et al. (2000) evidenced impact from both wastewater injections from above and below fresh-saltwater interface. The freshwater body below Mérida city and outskirts is used as a receptor of wastewater, the upper 20 m of the freshwater lens are unsuitable for human consumption due to pollution from septic tanks, agricultural practices and industry; thus, currently one third of the potential water supply has been lost (Marín et al., 2003). This research will evaluate actual conditions in selected places.

In the case of the Yucatán Peninsula the main challenge for the groundwater resources is the human impact by pollution not the overexploitation of the aquifer or scarcity of water supply as recharge by precipitation in the zone is relatively high (Bauer-Gottwein et al., 2011). Nevertheless the evidence that large parts of the aquifer are affected by saltwater intrusion because of the small hydraulic heads (close to mean sea level) and the fact that groundwater use is restricted to a relatively thin freshwater lens (<10–100 m thick; Bauer-Gottwein et al., 2011) indicates the need of further research on the fresh-saltwater mixing zone and aquifer dynamics and the sustainable management of the socioecological system. Escolero et al. (2000) already recognized the need for monitoring and protecting the

aquifers in the karst region of Yucatán and proposed to establish a hydrogeological reserve zone for the karst aquifer in Mérida.

Beddows (2004) (in Bauer-Gottwein et al., 2011) measured coastal groundwater outflow in major submarine springs over a 80 km stretch of coastline in southern Quintana Roo and computed an average outflow of about  $0.73 \text{ m}^3 \text{ s}^{-1}$  per km of coastline arguing that the groundwater recharge can corresponds to 30-70 % of average precipitation.

Mérida is the largest city of the Yucatán Peninsula, with a 2010 population of 830 732 inhabitants (INEGI, 2012). There is no integrated sewage collection and drainage system for the city; domestic, industrial and medical wastes are discharged without treatment directly into the aquifer through injection wells affecting ecosystems health and services (Marín and Perry, 1994). Population growth and tourism exert additional pressure on water resources sustainable development and constitute a serious challenge for the infrastructure of drinking water supply, the sewage system and wastewater treatment of the region.

Another important fact is that sea level rise promotes salt water migration landward, however anthropogenic impacts due to increasing groundwater extraction that drive the hydraulic head of the aquifer down are prone to be more significant. However previous studies (Sherif and Singh V. P., 1999; Loáiciga et al., 2011) provide information that the impacts of water extraction and decrease in seaward discharge are more important to the landward migration of the fresh-saltwater interface than sea-level rise. Apparently this depends on a number of hydrogeological and geomorphological characteristics of the specific aquifer like the porosity and hydraulic conductivity.

## **1.2 Objectives**

The main objective of the overall research project is to investigate and characterize the contamination impacts on the Yucatán Karst aquifer in order to develop and suggest strategies for its sustainable management. The principal goal of this investigation is to understand the functioning of the groundwater flow system developing a qualitative conceptual hydrogeological model for the study area including the contamination impacts and describing the current state of the system. This is done by an integral analysis of temporal and spatial variations in the aquifer flow system of the study area due to precipitation and human induced recharge to understand the response of the flow regime to natural and anthropogenic alterations, following the five specific objectives derived from the general objective:

- Determine spatial and temporal evolution of hydraulic head and the groundwater flow net by monitoring observation wells and flowing artesian wells.
- Quantify the flow (discharge) of the artesian wells and determine its distribution and temporal changes in response to recharge events and tidal influences.
- Determine variations in the thickness and depth of the freshwater-saltwater mixing zone in the observation wells.
- Analyze the physicochemical water composition during its evolution along the hydrologic cycle in the study area.
- Analyze climatic information including precipitation and temperature data with respect to its influence on the aquifer.

The pursuance of these objectives is fundamental for the understanding of the groundwater flow system functioning, and its relation to recharge consequently it helps to obtain a hydrogeological conceptual model integrating the evaluation of contamination impacts on the aquifer system.

## **2 Geographical setting**

The Yucatán state is located in the southeast of the United Mexican States and in the north of the Yucatán Peninsula, has a land surface of 39,612.2 km<sup>2</sup> corresponding to 2 % of Mexico (INEGI, 2012). The Yucatán state borders in the north with the Gulf of Mexico, east and southeast with Quintana Roo and in the southwest with Campeche. The coastline of the state Yucatán is about 340 km long (INEGI, 2010). The study area is situated in the northern part of the state of Yucatán and lies between 20° 50' and 21° 21' north latitude and 89° 50' y 89° 20' west longitude. The research area extends over an area of approximately 1600 km<sup>2</sup>, includes the city of Mérida, its outskirts and reaches approximately 40 km north to the coastline. Figure 1 depicts the geographical location of the study area with the network of monitoring wells used to obtain information about the current status of the aquifer.

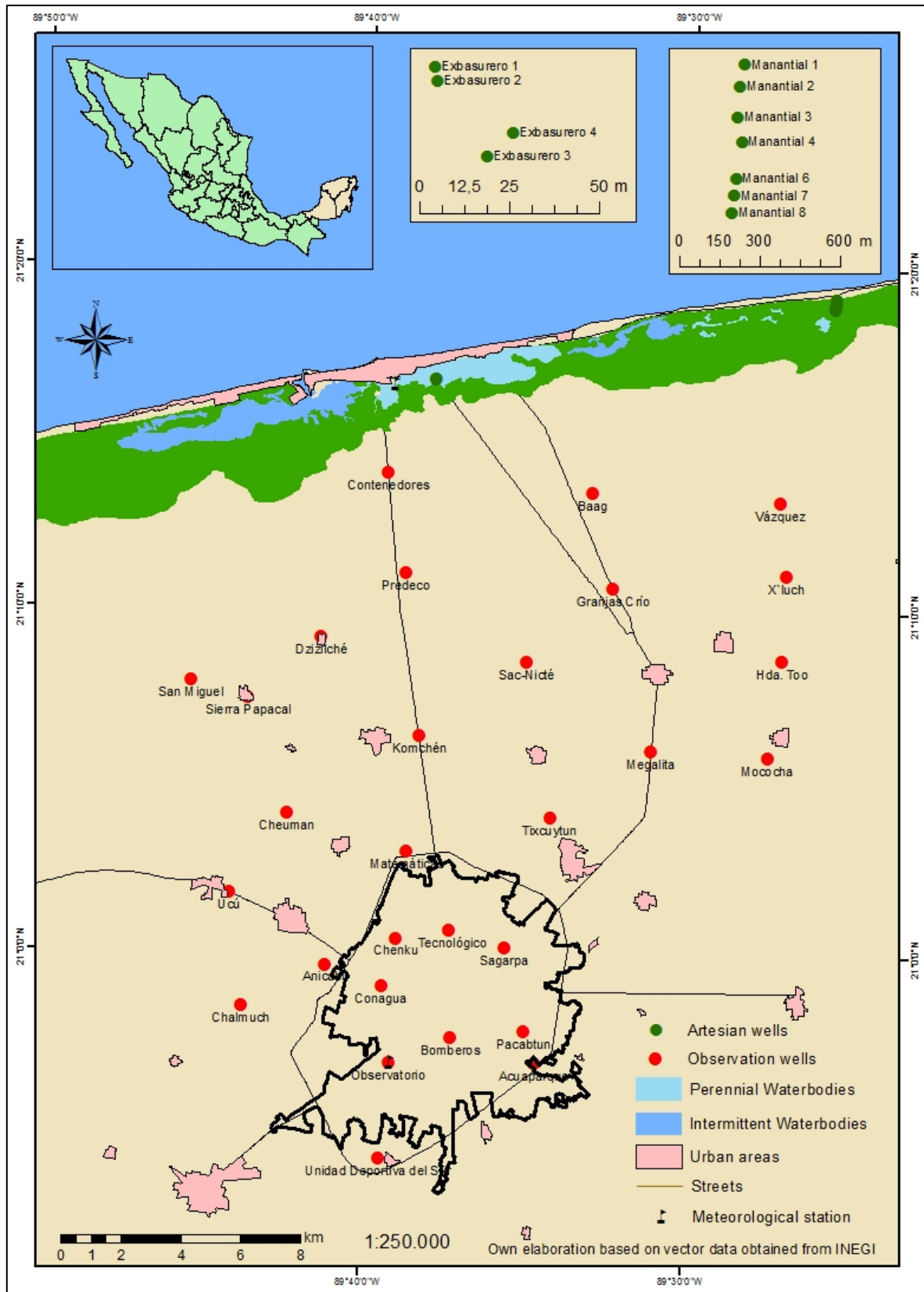


Figure 1: Study area with monitoring network of observation wells and flowing artesian wells.

The total population of the state of Yucatán is 1,955,577 with a population density of 49.5 people per km<sup>2</sup>. The capital Mérida counts with almost half of the population of Yucatán state. Besides the permanent residents in 2011 the state of Yucatán was visited by 1,746,061 tourists (DATATUR, 2013).

The United States of Mexico count with 653 administrative aquifers organized together with the river basins in 37 hydrological regions grouped into 13 hydrological-administrative regions (CONAGUA, 2011). Figure 2 shows the four administrative aquifers of the hydrological-administrative region XII “Peninsula de Yucatan” Cerros y Valles and Isla de Cozumel in the state of Quintana Roo, Xpujil in Campeche and Peninsula de Yucatan (SEMARNAT, 2009); latter comprises the most extensive part of the Peninsula, subject of investigation in which the study area of this investigation is located.

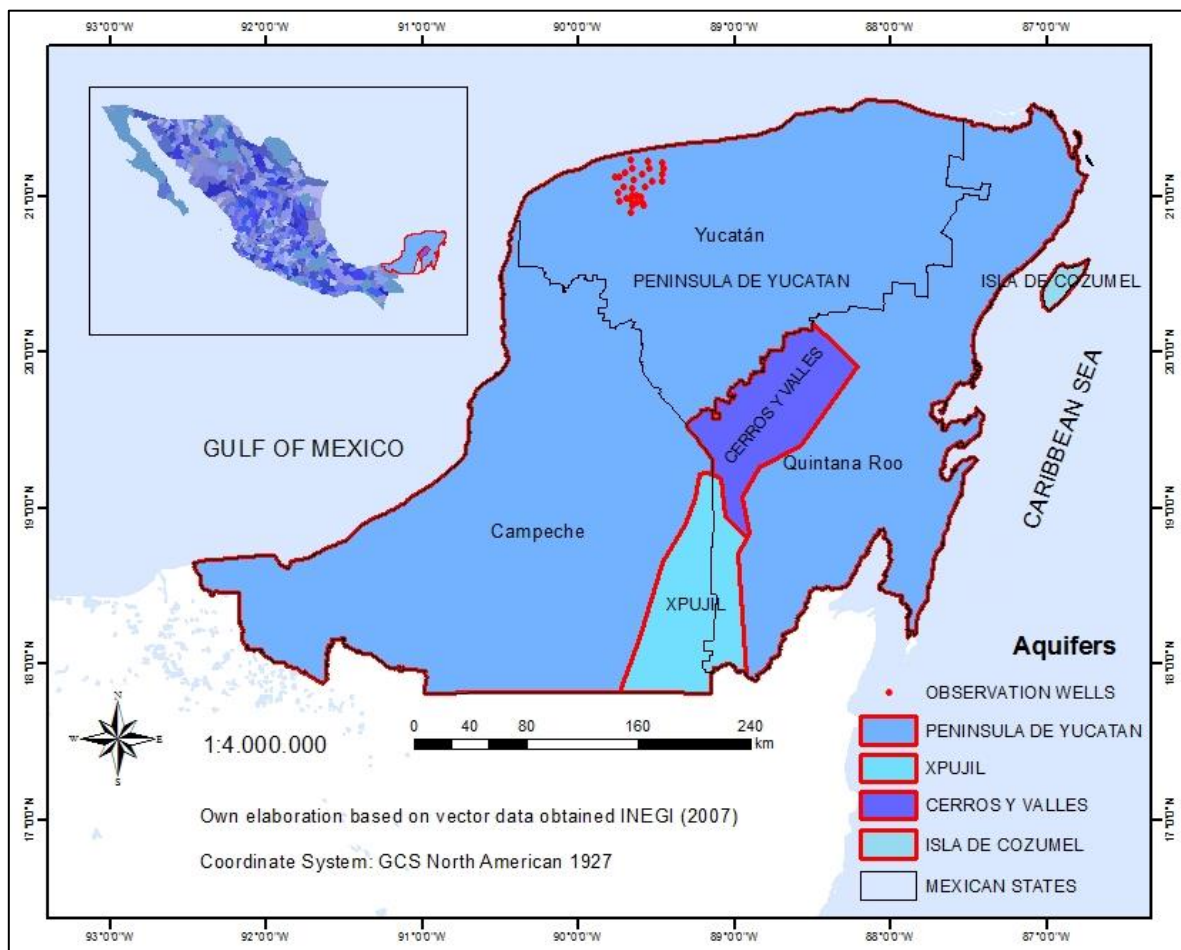


Figure 2: The administrative aquifers of the Yucatán Peninsula with the location of the observation wells of this investigation (red dots).

According to the Diario Oficial de la Federación (2009) for the hydrological-administrative region “Península de Yucatán” groundwater presents almost the only water resource for the population due to the absence of alternative sources, however calculations indicate that it does not present any deficit regarding groundwater availability. The following represented volumes of mean annual recharge (R), committed natural discharge (ND), granted volume of groundwater (VG), volume of groundwater extraction reported in technical studies (GE) and the mean annual availability of groundwater (MA) confirm that the aquifers of the Yucatán Peninsula provide sufficient groundwater resources for water supply. Values in table 1 are given in million cubic meters per year ( $10^6 \text{ m}^3 \text{ year}^{-1}$ ).

Table 1: Water volumes of the administrative aquifers of the Yucatán Peninsula in  $10^6 \text{ m}^3 \text{ year}^{-1}$ .

ID	Aquifer	R	ND	VG	GE	MA	Deficit
405	Xpujil	2,099.40	1,784.10	0.25	0.50	315.05	0.00
2301	Cerros y Valles	1,194.20	854.90	4.62	125.60	334.67	0.00
2304	Isla de Cozumel	208.70	160.40	12.96	8.20	35.34	0.00
3105	Península de Yucatan	21,813.40	4,542.20	2,265.59	1,313.30	5,005.60	0.00
Total Hydrological Region		25,315.70	7,341.60	2,283.43	1,447.60	5,690.65	0.00

The mean annual recharge of the aquifers of the hydrological region Península de Yucatán has been estimated as  $25,315.70 \text{ } 10^6 \text{ m}^3 \text{ year}^{-1}$ . According to (CONAGUA, 2010) 75 % of the total groundwater abstraction in the state of Yucatán is used for agricultural and livestock, 21 % for domestic use and 3 % in the industrial sector. The annual abstraction volume for the Mexican part of the Yucatán Peninsula is reported by CONAGUA (2010) as  $2,368 \text{ hm}^3 \text{ year}^{-1}$  corresponding to  $75.1 \text{ m}^3 \text{ s}^{-1}$ . If the mean annual precipitation for the whole Yucatán Peninsula would be like the historical mean (1961-2012) for Mérida of 1024 mm this would be equivalent to  $168,960 \text{ hm}^3 \text{ year}^{-1}$  for the entire peninsula surface, groundwater abstraction would correspond to only 1.4 % of the mean annual precipitation.

## 2.1 Physiography & Karst Morphology

The Yucatán Peninsula consists of an immense flat limestone platform (Maya Block) of marine origin that rises about 15 m above sea level covering an area of 43.000 km<sup>2</sup>. Only in the southern part of the Peninsula the relief gets more mountainous and the most important elevation is the Sierrita de Ticul (Escolero Fuentes, 2007). Located in the south of the state Yucatán this mountainous terrain reaches 275 masl and has a length of 110 km (García Gil and Graniel Castro, 2010). The study area is located in the flat northern part of the Peninsula where the relief is characterized by morphological karst forms. In the study area the density of “cenotes” (sinkholes) is very high and they represent the most characteristic topographical features.

The Yucatán Peninsula originated during the tectonic and sedimentary evolution of the marine basin of the Gulf of Mexico during which huge volumes of carbonates deposited (Padilla y Sánchez, 2007). Along the 250 km coastline of northern Yucatán, sedimentary deposits of precipitated calcium carbonate cemented (caliche) and the nearly impermeable layer leads to the confinement of the aquifer and impedes infiltration of precipitation water (Perry et al., 2002). Gerstenhauer (1987) describes the genesis of caliche driven by leachate infiltration or interflow of meteoric water that do not reach the phreatic zone, evaporation and plant transpiration lead to lime precipitation and crust formation. Field (2002) affirms that the indurated calcium carbonate layer can be formed by phreatic waters drawn to the surface by natural pressure gradients and capillarity action. Groundwater evaporates near the surface so that dissolved minerals precipitate and cement pores and fissures and compact fragments of shells y mollusks. As the precipitated calcium carbonate builds new chemical bondings, it turns insoluble. The process of case-hardening reduces the primary porosity of the surface material by a factor of 10 or more (Ford & Williams, 2007). The geologic materials below the calcrete layer are permeable limestone sands and calcareous gravel named “Sahcab” from Mayan origin (Gerstenhauer, 1987).

In the central and southern part of the state of Yucatán precipitation water infiltrates rapidly and the dissolution process of soluble limestone originates the typical landscape and hydrogeological system of the peninsula with a variety of karst formations that characterize the earth’s surface (exokarst) and subsurface (endokarst) in Yucatán. The driving force of the geomorphological processes of karstification is the water that circulates through the hydrological cycle interacting with the geological material in the subsoil and on the surface. The high degree of karstification and the absence of soil cover and surface streams at the Yucatán Peninsula cause rapid infiltration of unsaturated precipitation water with high

potential for dissolution that favors mechanical and chemical erosion in the subsoil (Lesser and Weidie, 1988). The collapsing of depressions “dolines” originated a lot of sinkholes locally called “cenotes” where groundwater becomes visible. Karst relief has mostly been fossilized by calcretes that cover marine and aeolian lime sand at the Pleistocene coastal site (Gerstenhauer, 1987).

According to various researchers (Alvarez et al., 1980; Hildebrand et al., 1991; Pope et al., 1998) at the end of the Cretaceous a big asteroid hit the Yucatán Peninsula originating the Chicxulub impact crater with a dimension of about 200 km west whose center is located offshore in the Gulf of México (Bauer-Gottwein et al., 2011). The crater after the impact became a sedimentary basin and the southern outline of the crater coincides with a characteristic fracture zone, the Ring of Cenotes that is supposed to govern groundwater flow in this region and presents surface depressions and high density of sinkholes (Perry et al., 1995).

## **2.2 Hydrology**

The only permanent rivers that reach the Mexican part of the Yucatán Peninsula are the Champeton River and the Candelaria River in the southwestern part of Campeche that open to the Gulf of Mexico and the río Hondo in the state of Quintana Roo (Kauffer Michel & Villanueva Aguilar, 2011) belonging to the border between Mexico and Belice. Figure 3 shows that in the state of Yucatán no permanent surface streams are present and most of the intermittent rivers coming from the southern part of the Peninsula disappear in the subsoil forming the karst aquifer.

In absence of surface stream erosion, extensive subsurface erosion results in the development of typical karst topography in the state Yucatán (Lesser & Weidie, 1988). In the northern coastal part of the study area shallow intermittent to perennial waterbodies mostly originated due to extreme flooding during hurricane events can be found. Due to road construction the natural water between lagoons and wetlands has been modified and interrupted. The coastal lagoons are recharged by groundwater from artesian springs and their water is extremely saline.

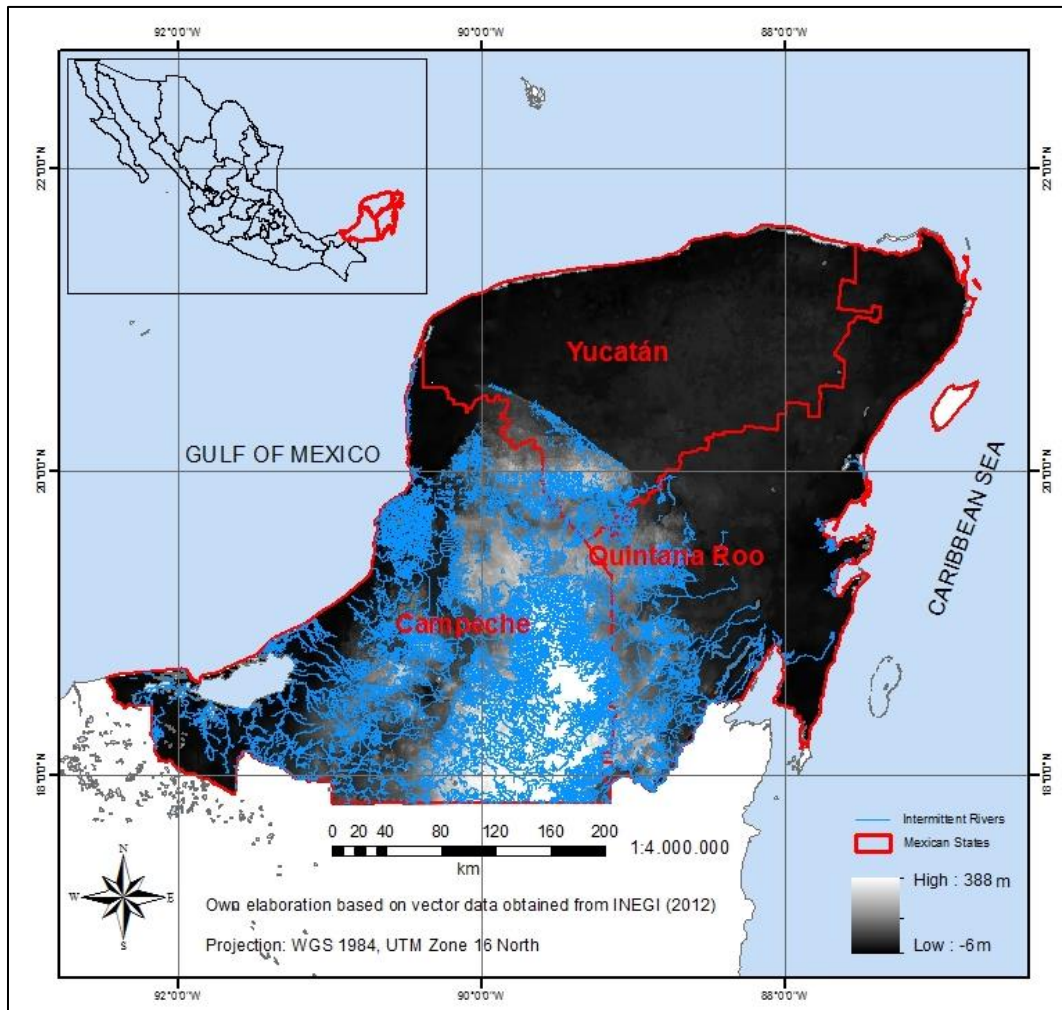


Figure 3: The Yucatán Peninsula with intermittent rivers in the southern and central part.

### 2.3 Vegetation

Along the shoreline a lot of marshlands and lagoons can be found with aquatic vegetation (INEGI, 2012). The vegetation of the wetlands along the northern Yucatán coastline is characterized by various species of mangrove with evergreen leaves (CONABIO, 2012). The adjacent regions in the northern central part of the study area are dominated by tropical and subtropical deciduous forest and agricultural terrain while in the central and southern part and the east coast evergreen tropical and subtropical forest is prevalent. According to INEGI (2012) almost 25 % of the Yucatán state surface is used for agricultural practices. Figure 4 shows the distribution of vegetation of the peninsula for the year 2005. The mangrove wetlands at the northern coastline in the study area, formed by clay, sand and calcareous mud are subjected to flooding and tidal fluctuations (Villasuso Pino et al., 2011), they are connected to the sea and to the aquifer. The Yucatán Peninsula provides more than

50 % of the total mangrove area in Mexico nevertheless there were reported great losses due to industrial activities, harbours, urban and tourism development and passing hurricanes in the valuable ecosystems (Herrera-Silveira et al., 2012). Worldwide at least 35 % of mangrove forest areas have been lost in the past two decades (Valiela et al., 2001).

Contributions of groundwater discharge and ocean water are responsible for the particular ecosystem characteristics and its water balance. The coastal wetlands and particularly the mangrove forests provide a huge variety of environmental services as they act like natural control systems, barriers against hurricanes, biological water filters, animal refuge and control coastal erosion, among others benefits (CONABIO, 2012).

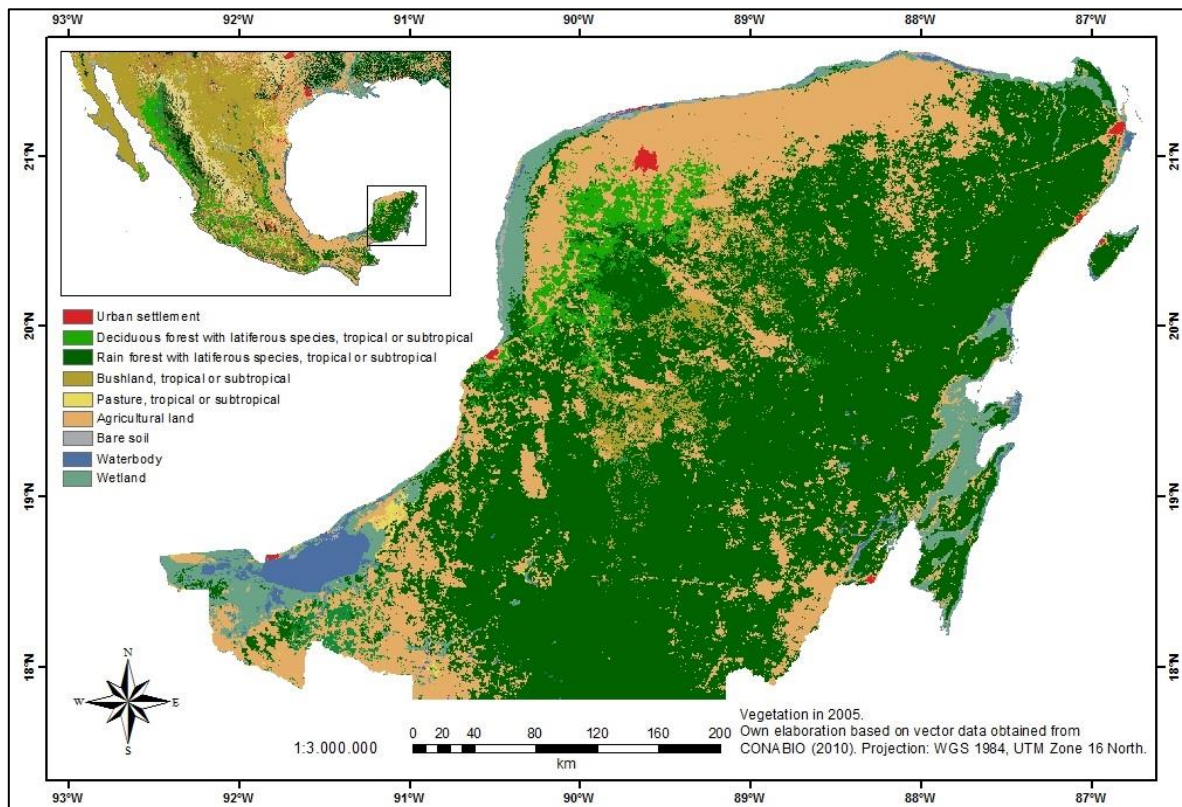


Figure 4: Vegetation distribution of the Yucatán Peninsula in year 2005.

## 2.4 Climate

Climate conditions in Mexico are diverse due to its wide spread geography, very dry regions in the north, temperate climate in the center and humid subtropical conditions in the southeast provide high biodiversity.

The Yucatán Peninsula climate is controlled by particular atmospheric circulation pattern of tropical latitudes (SEDUMA, 2010). Determining factors for the climate of the Yucatán Peninsula are (i) the absence of considerable elevations, (ii) a marked atmospheric pressure gradient, (iii) strong influence of the northern Atlantic Bermuda-Azores High/Anticyclone, (iv) summer trade winds, tropical storms, cold fronts and (v) the warm current of the Yucatán Channel between Cuba and Cancún (Orellana et al., 1999). The principal type of precipitation is convective as the Yucatán Peninsula does not present high relief or orographic obstacles that could cause clouds to ascend releasing water. As the Peninsula lies within the area of the hurricane belt of the Atlantic Ocean, it is exposed to tropical storms. The Atlantic hurricane season is from June to November, being the maximum occurrence in September (NOAA, 2007). In the hot period of the year the anticyclone is displaced to the north, prevailing easterly winds can penetrate causing precipitation events over the Peninsula (SEDUMA, 2010). During the summer months heating of the Atlantic Ocean often leads to the forming of tropical storms and hurricanes in the convection cell over the Atlantic Ocean that can have a significant contribution to the yearly precipitation amount. In September 2002 the hurricane Isidore affected the peninsula generating the highest monthly precipitation registered in Mérida within the period 1961-2012 of 697.8 mm. In Progreso the highest documented monthly precipitation amount (369 mm) occurred during the hurricane Katrina in October 1999. Figure 5 shows the temporal progress of temperature, precipitation and evaporation and depicts some of the hurricanes that impacted the Yucatán Peninsula.

There is a strong correlation between the distribution of the vegetation present in the Yucatán Peninsula and the climatological subtypes (CONABIO, 2012). High air temperatures and abundant vegetation produce evapotranspiration to be about 85 % while the remaining 15 % infiltrate to the subsoil providing recharge of the aquifer (Lesser & Weidie, 1988).

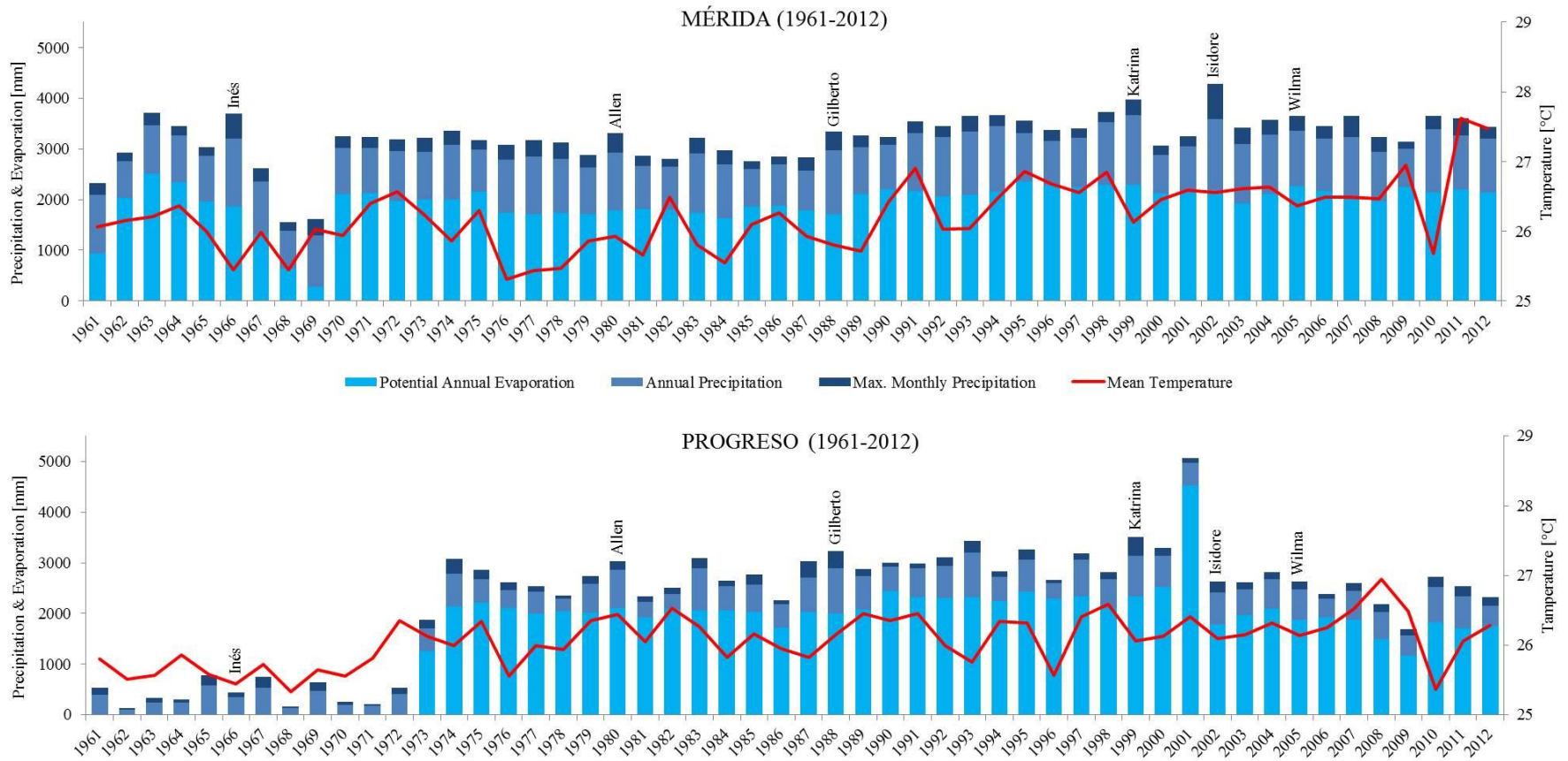


Figure 5: Historical records of potential annual evaporation, annual precipitation, maximal monthly precipitation, mean temperature and important hurricane events for Mérida and Progreso.

According to the global climate classification developed by Köppen and Geiger in the 20<sup>th</sup> century, the Yucatán peninsula in its mayor extend is classified as tropical savanna climate (*Aw*) with the mean temperature of the coldest month  $> 18\text{ }^{\circ}\text{C}$  (Köppen, 1936) while in a narrow band at the northern coast hot semi-arid steppe climate (*BSh'*) predominates. García (1964) characterized the climate for the whole Mexican country implementing more precise subunits as the general system of Köppen is not able to represent subtle differences. Two meteorological stations of CONAGUA in Mérida and Progreso provide representative climatological and meteorological data for both dominate climate types present in the study area. The meteorological station in Mérida is located in the region classified as subhumid or savanna climate (*Aw*) while the station in Progreso belongs to the arid zone (*BS*).

At Yucatán Peninsula the rainy season takes place in summer from June to October and dry season lasts from November to May. The mean annual precipitation for the historical measurement period (1961-2012) is about  $1024\text{ mm year}^{-1}$  for Mérida representing more than the double amount of precipitation registered in Progreso ( $500\text{ mm year}^{-1}$ ). Considering the long-term average data for the observatory in the city of Mérida 76 % of the precipitation is registered during the rainy season (June to October) 72 % at the coastal observatory Progreso. The mean annual temperature for both observatories is about  $26\text{ }^{\circ}\text{C}$  and temperature ranges between the extreme values  $5\text{ }^{\circ}\text{C}$  (February 2006) and  $43.5\text{ }^{\circ}\text{C}$  (May 2009) in Mérida City. After CONAGUA the annual potential evaporation for Mérida and Progreso is  $1942\text{ mm year}^{-1}$  and  $2089\text{ mm year}^{-1}$  respectively. The average actual evapotranspiration for the Yucatán Peninsula varies spatially between 350 and 2500  $\text{mm year}^{-1}$  (2004-2008) with a mean evaporation of about  $950\text{ mm year}^{-1}$  presenting higher values along the coastline where the groundwater tables is close to earth surface and average actual evapotranspiration can exceed annual recharge by precipitation (Gondwe et al., 2010).

Figure 6 shows four climograms for Mérida and Progreso for the study period from April 2012 to April 2013 and the historical record for the period 1961-2012. The climograms indicate, that during the study period (2012-2013) the precipitation did not follow the historical pattern for all month and, the registered rainfall was less than the historical mean. For arid *BSh'* climates with summer rain regime applies that the amount of precipitation in the most humid month of the warm half of the year (April to September) corresponds at least to 10 fold the amount of rain during the driest month.

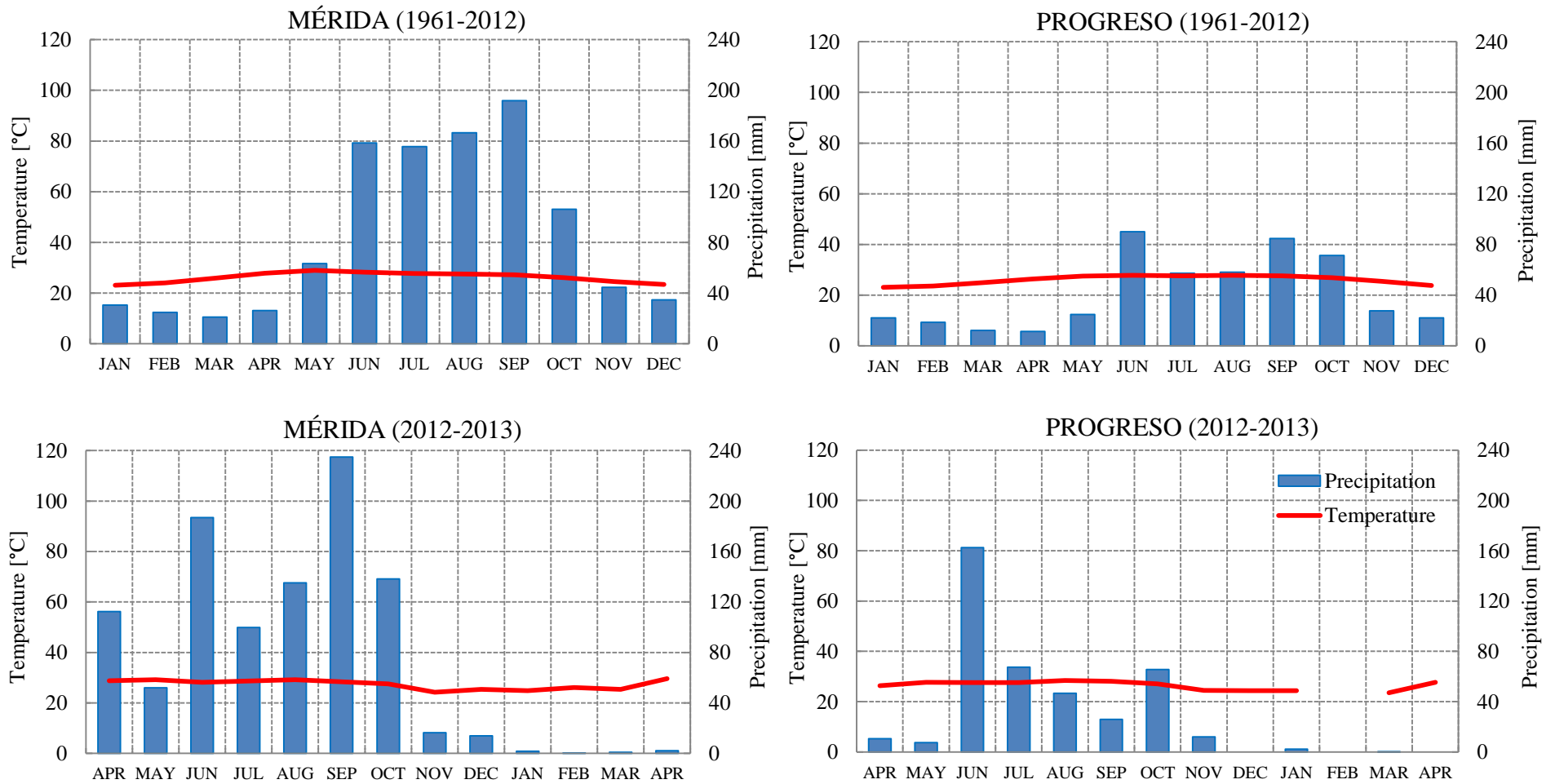


Figure 6: Climate Diagrams for Mérida and Progreso for the historical period (1961-2012) and the period of this study from April 2012 to April 2013. Data for February Progreso are missing.

Climate type  $Aw$  is described as subhumid or savanna climate with a rainy season in summer but in Yucatán there can be found marked differences in climatological pattern within relatively small distances (García, 2004). By García the  $Aw$  climate was classified into three subdivisions ( $Aw_0$ ,  $Aw_1$  and  $Aw_2$ ) with increasing humidity using *Lang's* humidity index known as the ratio between the total annual precipitation and the mean annual temperature (Mohr & van Baren, 1954). The Yucatán Peninsula as well as the study area, presents a gradient regarding the humidity that increases both from north to south and from west to east. Mérida city is located near the dry edge, the dry  $BS$  climate and classified as  $Aw_0$ . The northern coastal part of the Yucatán Peninsula where the flowing artesian wells are located presents drier conditions with mean annual temperatures  $> 22\text{ }^\circ\text{C}$  ( $h'$ ).  $BS$  climate describes steppe or dry savanna climate, being the northwest coast near the town Progreso with arid climate  $BS_0(h')w(x')$  the driest part of the study area. Climates with summer rain regimes ( $w$ ) that present more than 10.2 % of the annual rain in winter were denominated  $w(x')$  by García to emphasize the presence of precipitation in winter and the proximity to regimes with precipitation throughout the whole year ( $x'$ ). Consequently  $BS_1(h')w(x')$  and  $BS_1(h')w$  classify semiarid zones in the northern and northwestern coastal part of the Yucatán Peninsula. Figure 7 shows the climatic units of Yucatán state.

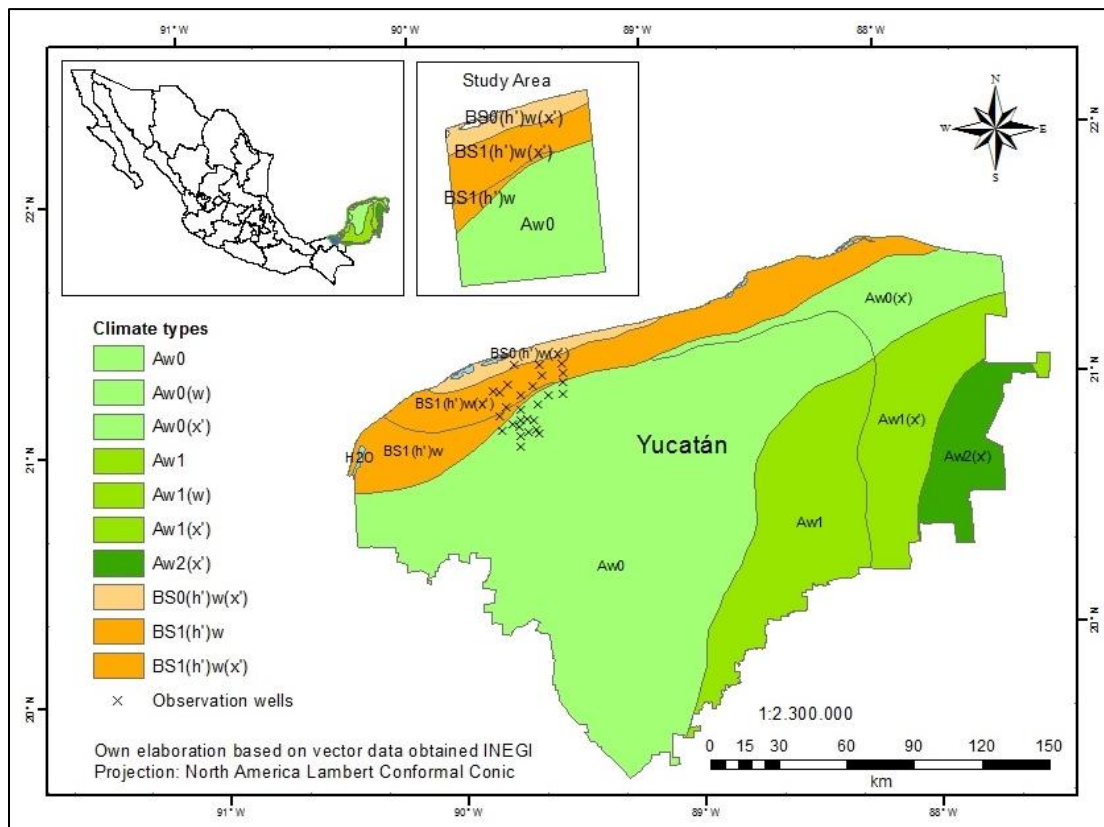


Figure 7: Climate types according to classification by Köppen and García modified by García.

## 2.5 Soils

The thin soil layer that covers the surface in the state of Yucatán mainly consists of immature, poorly developed soils. Rendzina is the most abundant soil type typically overlying carbonate material, followed by Litosol and Luvisol. In the coastal part a narrow band covered by Regosols can be found (Figure 8). In many national soil classifications Rendzina and Litosol are subtypes of the Leptosoles used to indicate shallow soils on firm or loose bedrocks (IUSS, 2007). Rendzina soils are very typical for karst and mountainous terrain and develop during the solution decomposition and weathering process (Scheffer/Schachtschabel, et al., 2010). Their thickness reaches 10-15 cm typically consisting of a single humus-rich layer developed directly on carbonate material (Scheffer/Schachtschabel et al., 2010). Litosols develop on firm and continuous bedrocks and can be found on cemented carbonate layers (caliche) in the study area (INEGI, 2013). The Regosol soils predominate on loose rocks and sand with low calcium content and are more than 30 m thick (Scheffer/Schachtschabel et al., 2010).

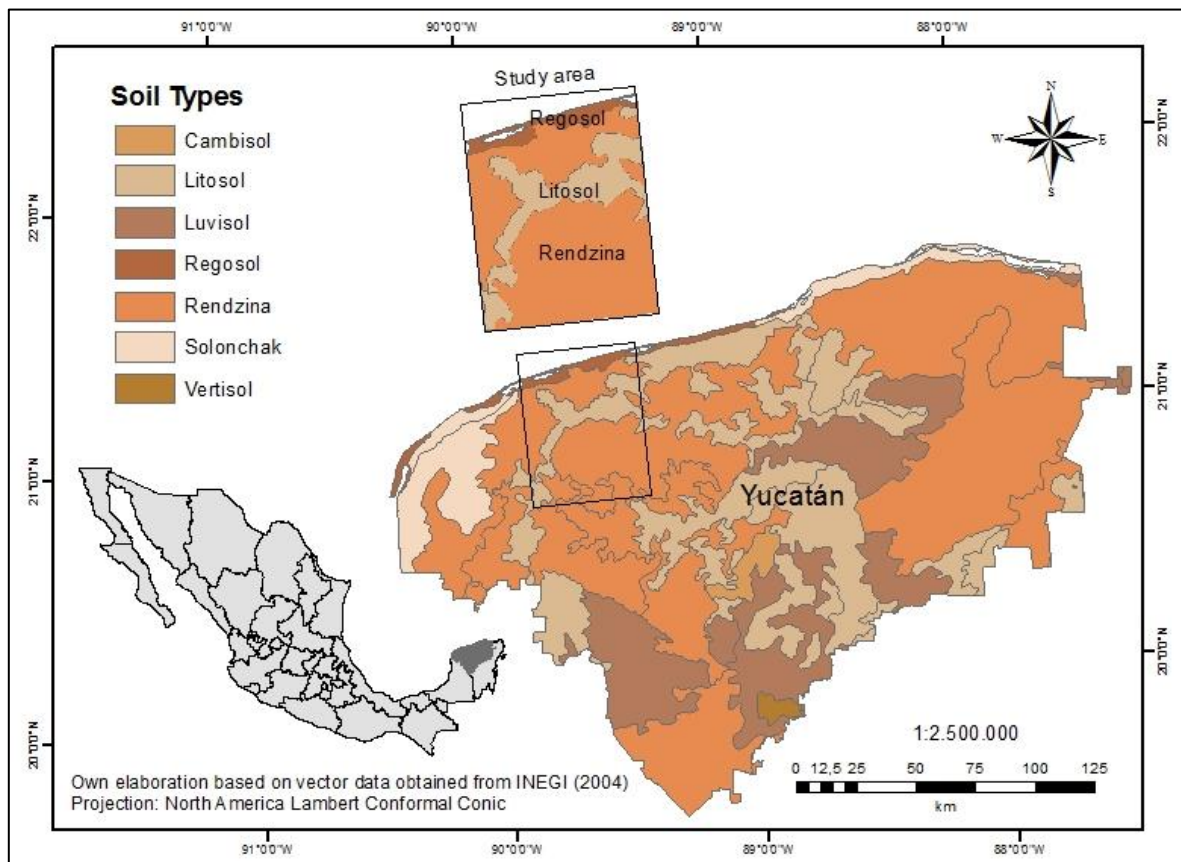


Figure 8: Predominant soil types of the study area and the state of Yucatán.

According to Pope, et al. (1996) there is a clear relationship between the soil types and the bedrock age at Yucatán Peninsula. The scarce soil cover exceptionally reaches a thickness of more than one meter and in combination with the highly fractured subsoil of porous and permeable rocks it favors the rapid infiltration of meteoric waters directly into the aquifer (Perry et al., 2003) in the southern and central part of the state of Yucatán.

## **2.6 Geology**

The immense limestone platform that forms the Yucatán Peninsula in the state of Yucatán is composed mainly of calcareous rocks of marine origin from Tertiary and Quaternary. Nevertheless the platform is built from limestones developed from the Cretaceous period (144 to 165 million years ago) to the Cenozoic period in the Quaternary era (65 million year till present) (Beddows et al., 2007a). A temporal gradient from north (youngest) to south (oldest) is reflected in the deposits of the Yucatán Peninsula and the Quaternary rocks are restricted to a narrow band along the coastline. The Chicxulub impact crater formation presents the limit between Cretaceous and Tertiary (Beddows et al., 2007a).

The rocks that form the Sierrita de Ticul are of the oldest recrystallized formation from Paleocene-Eocene. The Paleocene-Eocene limestones and dolomite rocks have enclosed evaporite lenses and are covered by sediments from Middle-Eocene, crystalline and fossiliferous limestones from the member Pisté. In the central part of the study area limestones of Pliocene and Miocene (Tertiary) origin dominate while in a narrow band along the coastline Holocene (Quaternary) limestones of mollusks emerge (García Gil & Graniel Castro, 2010). This white to cream-colored band of marine origin is of approximately 80 m and overlies the limestones of the Carrillo Puerto Formation originated in Miocene and Upper-Pliocene. The Carrillo-Puerto Formation is between 163 and 240 m thick and contains foraminifera. The mayor part of the geology (82 %) of the Yucatán Peninsula is of Tertiary origin and approximately 13 % correspond to the Quaternary period whose calcareous deposits arise in the coastal part after a small emersion of the peninsula (García Gil & Graniel Castro, 2010). The maximum thickness of the Tertiary carbonates is about 1000 m (Lesser & Weidie, 1988). At the coast the Tertiary rocks are covered by thin Quaternary carbonate layers (Holocene, Pleistocene) and by a very thin soil horizon inland (Perry et al., 2003). The stratification of the Tertiary sediments in its mayor extend is horizontally and approximately the first 120 m are composed of massive recrystallized limestone that present high fracturing and cavernous subsoil (García Gil & Graniel Castro, 2010). The Quaternary deposits along the northern coastline consist of limestone with mollusks and are highly compacted and contribute to the confinement of the aquifer.

Figure 9 shows the geological classification of the Tertiary and Quaternary deposits of the Yucatán Peninsula according to García Gil and Graniel Castro (2010).

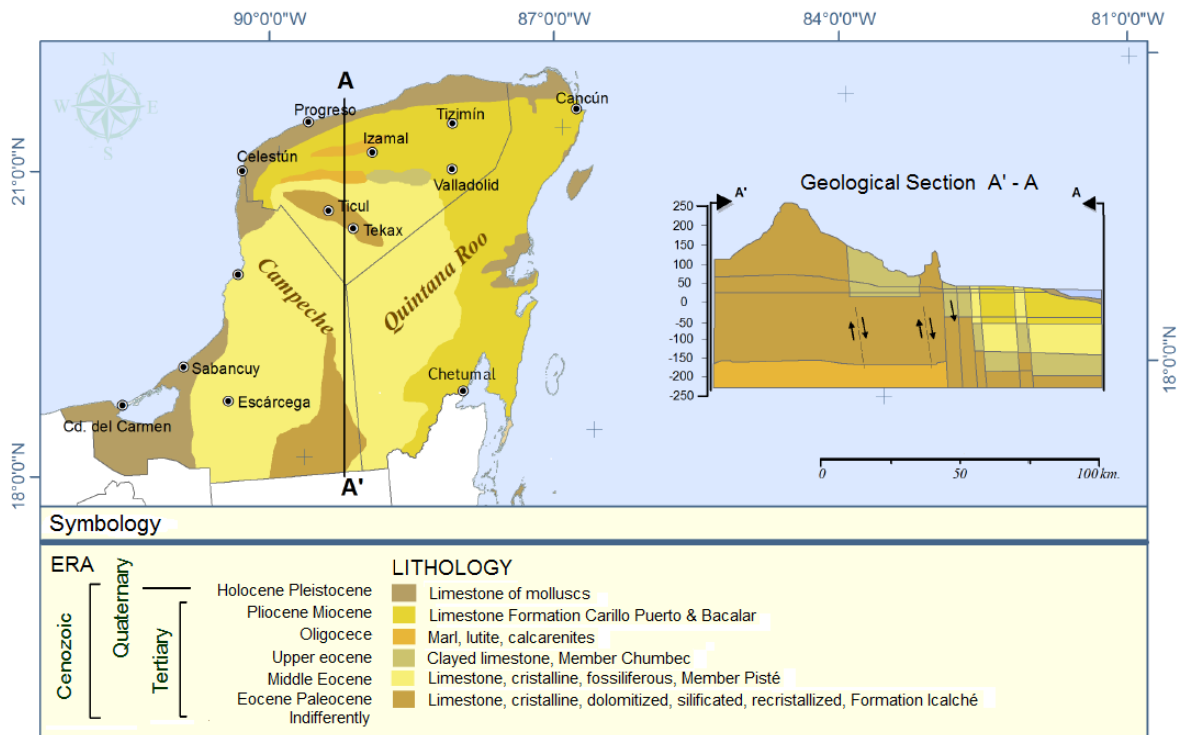


Figure 9: Geological classification of Tertiary and Quaternary sediments, reproduced according to García Gil & Graniel Castro (2010).

## 2.7 Hydrogeology

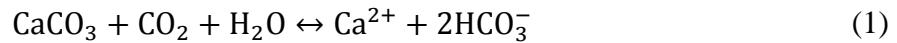
The aquifer in the state of Yucatán to a large extent is unconfined but along the entire northern coast the groundwater is confined due to a thin impermeable cemented calcareous aquitard layer (caliche) that reaches from the Isla Arena, Campeche to Holbox, Quintana Roo (Perry et al., 2003) and determines the coastal flow system (Perry et al., 2002).

Karst is the term used to describe a particular kind of landscape originated by dissolution and denudation of soluble rocks due to the natural interaction between water in the subsoil and the earth's surface which presents an extensive subsurface hydrology system. The karst denudation rate depends on climate conditions (temperature and precipitation), as well as on particular geological and morphological characteristics. The motor of the karstification process is the water of the global hydrological cycle originating formations of caves, cenotes, dolines and large dissolution conduits that favor turbulent flow. The solubility of calcite highly depends on the concentration of dissolved  $\text{CO}_2$  present in the water and the

partial atmospheric CO<sub>2</sub> pressure (Sanz et al., 2011). As the Yucatán Peninsula consists mainly of limestone the solubility of the mineral calcite is a limiting factor for karstification. Ford and Williams (2007) affirm that karst becomes abundant in terrains where more than 40 mg L<sup>-1</sup> of dissolved calcium are found in meteoric waters. The solubility of calcite in water at 25 °C and 1 bar pressure is 60 mg L<sup>-1</sup> (Ford & Williams, 2007).

Mixing of different groundwaters in equilibrium with calcite produce undersaturated mixed water that can favor calcite dissolution (Sanz et al., 2011). In aquifers near the coast the mixing of fresh water and seawater can favor dissolution due to the phenomenon of mixing corrosion that turns the solution calcite-aggressive.

Both electrical conductivity and calcium dissolution process are temperature dependent. The calcium carbonate-carbonic acid equilibrium varies between different waters and the layers of an aquifer. With input of carbon dioxide or increasing temperature the equilibrium shifts into the direction of calcium carbonate solution. The reversible dissolution and precipitation reaction of calcite in water is described by equation 1.



The most lithofacies at Yucatán Peninsula have good permeability (Lesser & Weidie, 1988) and rapid infiltration of precipitation water into the subsurface is favored by conduits and fractures due to dissolution of the soluble limestone. According to Ford and Williams (2007) the well-developed cave systems conduct 99.7 % of the groundwater flow.

Because of the highly heterogeneous development of the aquifer flow conduits and preferential flow paths, turbulent groundwater flow dominates (Bauer-Gottwein et al., 2011).

Between fresh and salt water in coastal zones there is a sensible dynamic balance. The scientists Ghyben (1889) and Herzberg (1901) were the first that investigated the phenomenon of the freshwater-saltwater interface (halocline) (Ford & Williams, 2007). In coastal aquifers like the Yucatán karst aquifer a less dense freshwater lens overlies the salt water that penetrates the aquifer from the seaside. Ghyben and Herzberg discovered that the depth of the freshwater-saltwater interface below sea level  $h_s$  and the fresh water head above sea level  $h_f$  are directly related and depend on the water density holding the following relationship (Essaid, 1986)

$$h_s = \frac{\rho_f}{\rho_s - \rho_f} \cdot h_f \quad (2)$$

Out of the common values for freshwater  $\rho_f$  and saltwater  $\rho_s$  densities ( $1.0 \text{ kg L}^{-1}$  and  $1.025 \text{ kg L}^{-1}$  respectively) it results that the depth of the interface below sea level  $h_s$  is approximately 40 times the fresh water head  $h_f$  above sea level (Essaid, 1986) illustrated in Figure 10.

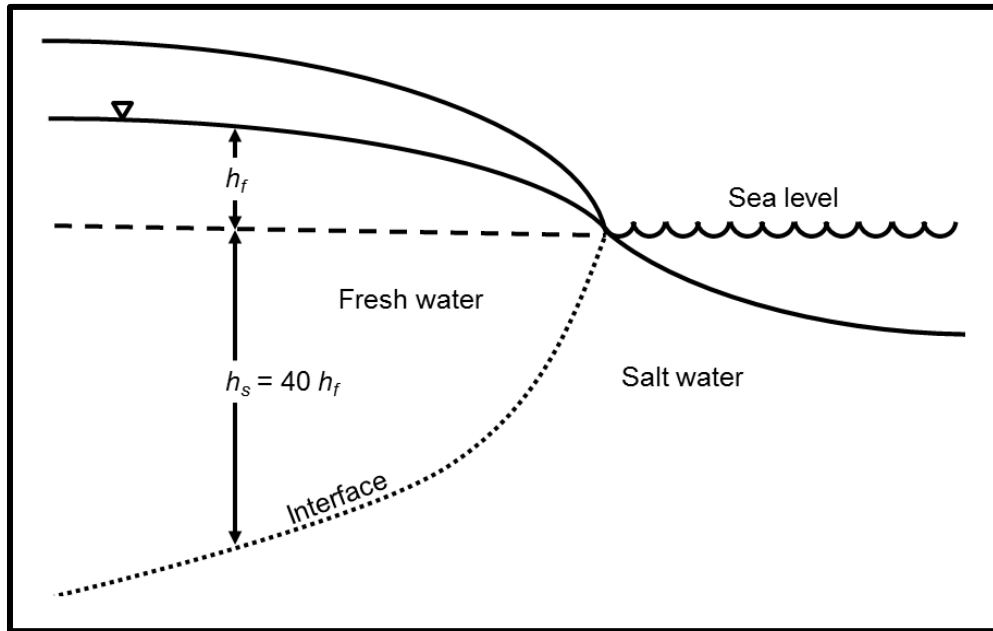


Figure 10 The Ghyben-Herzberg principle under hydrostatic equilibrium conditions, based on Essaid (1986).

The Ghyben-Herzberg principle of gravitational equilibrium is based on static groundwater conditions and simplifies the relationship found in nature, treating the two fluids as immiscible, leading to a sharp interface (Ford & Williams, 2007). Groundwater conditions rarely follow hydrostatic equilibrium and in coastal aquifers there is a transition zone between salt and freshwater where the waters are mixed by hydrodynamic dispersion and molecular diffusion due to different densities (Papadopoulou, 2011). The Ghyben-Herzberg model provides a theoretical basis to explain the configuration and hydrology of coastal karst aquifers, but a lot of field studies have revealed that varying boundary conditions (e.g. sea level) and secondary porosity can be important controlling factors for the fresh and saline groundwater flow (Ford & Williams, 2007). In anisotropic and heterogeneous karst aquifers the form and location of the interface are difficult to predict and depend highly on the karst permeability and the coastal geology (Elkhatib & Günay, 1993). With decreasing water table towards the coastline, the depth of the fresh-saltwater interface also decreases. The inflow of the underlying salt water at depth is induced by the dynamic circulation of

groundwater towards the coast that often results in the inflow of saline water at depth, forming a mixing zone of saline and fresh water and the discharge of brackish water along the coast (Ford & Williams, 2007). Along the northern coast of the Yucatán Peninsula artesian springs can be observed where the brackish water discharges naturally to the surface due to the confinement of the aquifer along the coastline. In the northern coastal part where swamp and estuary ecosystems dominate, outlets connect the aquifer system to the ocean through groundwater discharges into the sea in form of submarine springs (Villasuso Pino et al., 2011) or in coastal lagoons through upward diffuse discharge. The water of the coastal aquitard discharges naturally to the coastal wetlands, because it is subjected to a relatively higher pressure in the subsoil than the atmospheric pressure of the environment due to the confining caliche bed.

As the study area is located close to the ocean, seawater has a direct influence on the hydrogeology. The tide regime for the Yucatán Peninsula is mixed (diurnal and semidiurnal) but the diurnal tides predominate ranging between 0.1 and 0.8 m during neap and spring tide (Cuevas-Jiménez & Euán-Ávila, 2009).

A thin fresh water lens overlies saline water that originates either from dissolution of evaporite deposits embedded in the carbonate sediments or from seawater that penetrates the aquifer (Lesser & Weidie, 1988; Bauer-Gottwein et al., 2011).

Most karst aquifers present triple porosity resulting in three flow components; matrix, fracture and channel flow that follow different flow laws (Darcy, Hagen-Poiseuille and Darcy-Weisbach respectively) that can occur as turbulent and laminar flow (Ford & Williams, 2007). Darcy's Law alone cannot describe the flow through the whole karst aquifer basin because the majority of the suppositions that apply for flow through Darcian media are not fulfilled (Ford & Williams, 2007). The hydraulic conductivity of the geological material present in the Yucatán karst aquifer system has a high variability but is relatively high due to well-connected channel networks and pores (Ford & Williams, 2007) and leads to an extremely low hydraulic gradient of the order of 7-10 mm km<sup>-1</sup> (Steinich & Marín, 1997) or (Marín et al., 2000). Figure 11 reproduced from (Worthington et al., 2002) depicts the hydraulic conductivity of different carbonate aquifers worldwide, being the Yucatán karst aquifer the one with the highest conductivity. The preferential flow paths in the Yucatán karst aquifer have to be analyzed over a large range of scales. The general pattern for the groundwater flow direction in the region of Mérida are described in various research studies (Marín & Perry, 1994; Steinich & Marín, 1996; Perry et al., 2003) as being from the south to the north or northwest coastline.

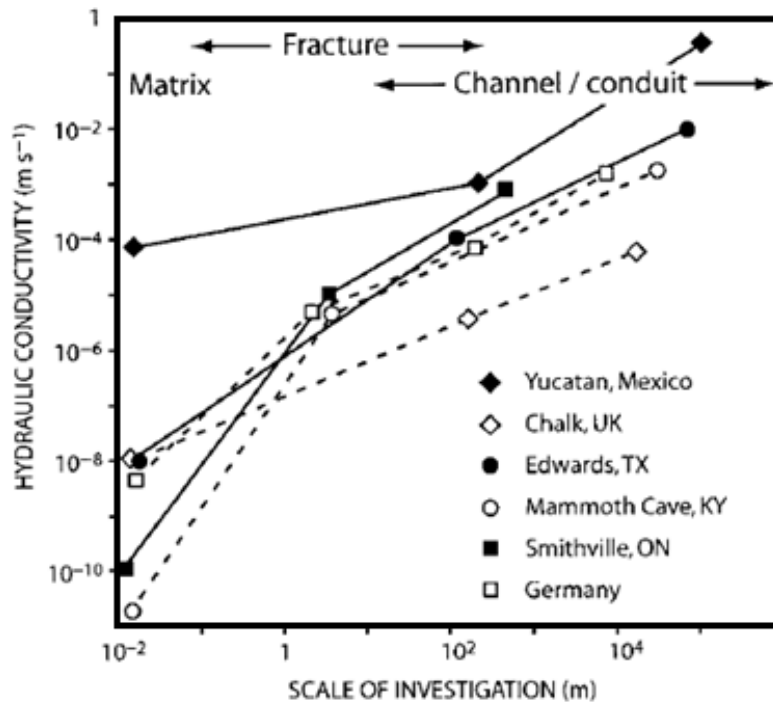


Figure 11: Hydraulic conductivities represented according to Ford and Williams (2007) with the highest hydraulic conductivity for the Yucatán aquifer.

## 2.8 Study Area

As previously mentioned, the study area, where the observation wells are located, in its greatest extent, comprises an area of approximately 1600 km<sup>2</sup>. The 29 observation wells that are subject of this investigation are spatially distributed between the southern part of Mérida city and the coastline given that half of the wells are situated within the urban area and the other half in sparsely populated regions. Furthermore the study area comprises two sites at the coast near the port city Progreso, located within a distance of 1,400 m to the Gulf of Mexico. Here 11 artesian wells are located in the mangrove wetlands that separate the beach from the continent.

Two meteorological stations of CONAGUA in Mérida and Progreso that provide reliable climatological and meteorological data for the analyses are located within the study area.

Figure 12 shows a satellite image of the study area that depicts the different zones forming part of this investigation, the observation wells in Mérida city and surroundings and the artesian wells at the study site named “Exbasurero” and “Manantiales”.

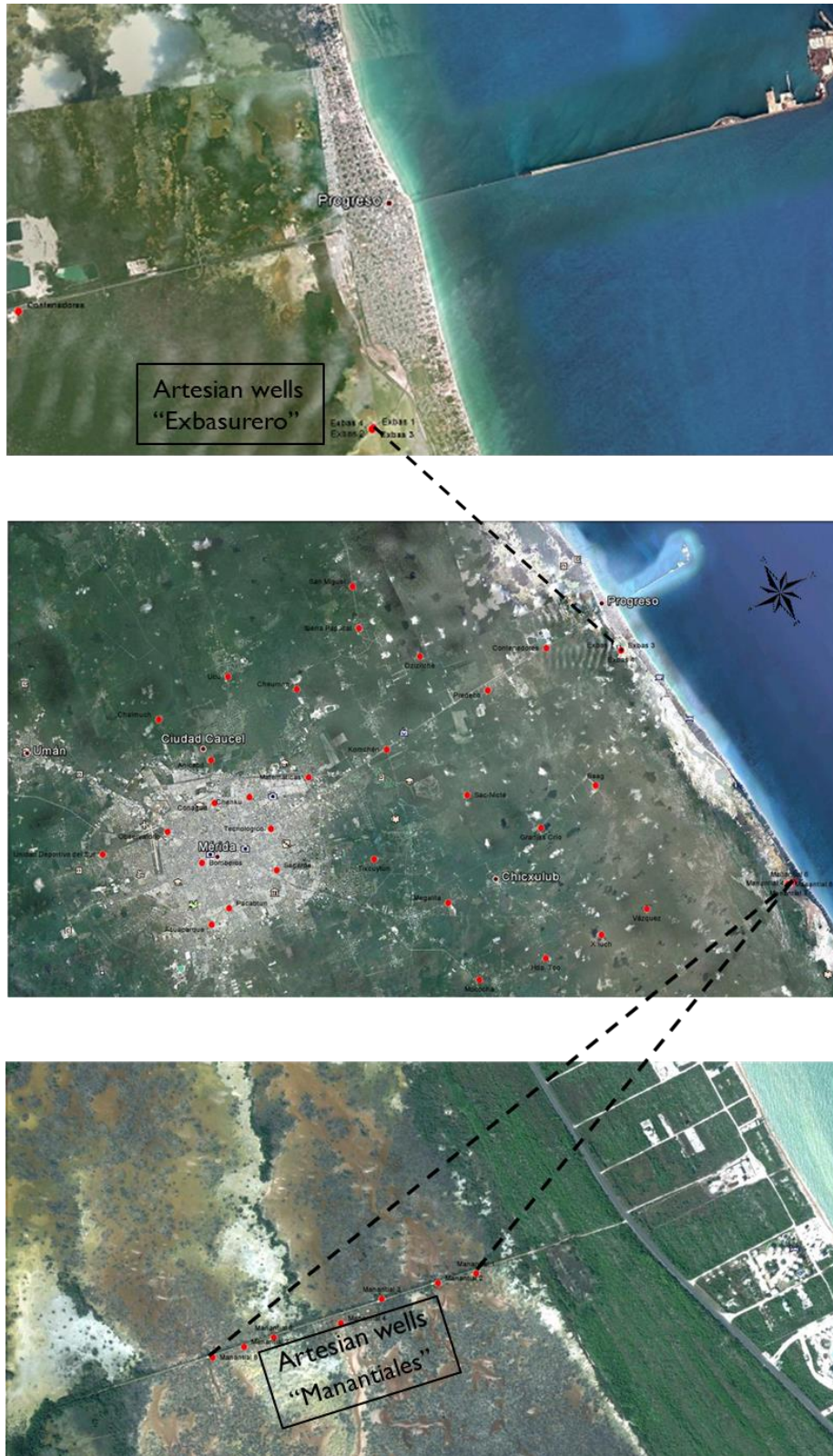


Figure 12: Satellite image, location of the study areas with the observation wells in the urban areas of Mérida and the artesian wells at the coastline. Elaborated with Google Earth and ArcMap 10.1 (INEGI, 2013).

### 3 Methodology

For the research project various methods were applied insitu and exsitu to obtain information about the aquifer characteristics, its hydrodynamic conditions and water quality. A groundwater monitoring network has been established within the framework of the primary research project, which includes 29 observation wells (10 - 60 m deep) as well as 11 flowing artesian wells at the two coastal study sites “Manantiales” and “Exbasurero” (Figure 12). Most of the deep wells were drilled within the project and some are previously perforated wells of CONAGUA. The observation wells were drilled with a diameter of 10 inch and the upper 6 m consist of a PVC tube of 8 inch diameter that is enclosed by cement to avoid water infiltration from the surface. The artesian wells were constructed by the “Secretaría de Desarrollo Urbano y Medio Ambiente” (SEDUMA) and consist of a steel tube with a diameter of 10 and 15 cm respectively that penetrates the sediment. The artesian wells reach depth between 0.89 and 4.64 m.

Worldwide groundwater converges towards the coastal areas, therefore the sea level (masl) is the benchmark analyzing the water movement along hydraulic gradients towards the coast. Within the project period all the observation wells and artesian wells that form part of the piezometric monitoring network were geopositioned and leveled with a Receptor GPS Trimble 5700 using a geodetic reference point of the National Institute of Statistics, Geography and Informatics (INEGI) using up to eleven satellites to obtain the exact location of the measuring points.

Furthermore the distance between every well or artesian spring and the coastline was estimated with help of the geographic information systems mapping software ArcMap 10.1.

For the climatological assessment reliable data were obtained from two meteorological stations of CONAGUA in the City center of Mérida and Progreso at the coastal study site. The basic information for the observation wells and artesian wells of the study sites “Manantiales” and “Exbasurero” are represented in tables 2, 3 and 4 respectively.

Table 2: Basic data of the observation wells.

ID	Location	UTM Zone 16 N		Z Altitude [masl]	Depth [m]	Distance Coast [m]	Meteorological Station	Dist. Metro. Station [m]
		X East	Y North					
1	Megalita	238350.967	2335222.111	6.712	51.52	23,000	Mérida	21,891
2	Granjas Crío	236296.583	2343980.274	4.930	42.26	14,013	Progreso	16,048
3	Baag	235198.280	2349086.984	3.680	36.985	8,796	Progreso	12,113
4	Sac-Nicté	231623.292	2340055.099	5.004	51.74	17,142	Progreso	16,495
5	Dzizilché	220586.328	2341397.613	4.492	35.01	14,028	Progreso	14,179
6	Sierra Papacal	216653.948	2338173.181	4.233	39.57	16,338	Progreso	18,609
7	San Miguel	213592.808	2339115.080	4.034	40.26	14,670	Progreso	19,330
8	Cheuman	218755.194	2331956.315	4.560	45.82	22,853	Mérida	14,531
9	Ucú	215633.109	2327693.013	4.781	58.03	26,258	Mérida	12,589
10	Anicabil	220785.554	2323798.185	7.408	28.08	31,255	Mérida	6,323
11	UDS	223635.865	2313336.386	9.795	60.04	42,076	Mérida	5,193
12	Bomberos	227497.324	2319812.503	8.569	43.3	36,413	Mérida	3,524
13	Tecnológico	227441.049	2325618.009	7.682	49.9	30,672	Mérida	7,814
14	Sagarpa	230459.102	2324656.822	8.097	55.77	32,184	Mérida	8,763
15	Pacabtun	231492.370	2320171.325	8.581	51.72	36,768	Mérida	7,454
16	Tixcuytun	232927.638	2331629.805	6.157	56.19	25,668	Mérida	15,754
17	Observatorio	224228.852	2318495.173	9.064	53.285	37,174	Mérida	0
18	Chalmuch	216274.632	2321580.445	7.189	50.94	32,372	Mérida	8,532
19	Acuaparque	232033.301	2318438.629	8.443	55.52	38,559	Mérida	7,805
20	Chenku	224573.049	2325195.308	6.701	41.24	30,687	Mérida	6,709
21	Conagua	223822.555	2322637.614	7.593	56.37	33,047	Mérida	4,162
22	Matemáticas	225170.910	2329868.559	6.407	62.2	26,138	Mérida	11,412
23	Komchén	225850.596	2336083.687	5.132	36.16	20,089	Mérida	17,663
24	Predeco	225145.596	2344882.639	3.977	25.6	11,330	Progreso	10,122
25	Contenedores	224190.832	2350250.427	1.268	10.98	5,886	Progreso	4,760
26	Mococha	244639.028	2334820.057	7.242	49.27	24,603	Mérida	26,136
27	Hda. Too	245362.799	2340024.815	5.888	41.56	19,560	Progreso	25,577
28	X'luch	245599.701	2344583.144	4.487	24.69	15,084	Progreso	23,418
29	Vázquez	245319.680	2348516.612	4.182	20.3	11,143	Progreso	21,687

Table 3: Basic data of the artesian wells at the study site Manantiales.

Location	UTM Zone 16 N		Z Altitude [masl]	Depth [m]	Distance Coast [m]	Dist. Meteo. Progreso [m]
	X East	Y North				
Manantial 1	248356.276	2359453.754	-0.560	3.07	645	24,151
Manantial 2	248337.694	2359370.767	-0.497	3.19	725	24,117
Manantial 3	248329.297	2359257.927	-0.565	2.73	837	24,089
Manantial 4	248344.639	2359164.151	-0.627	3.20	932	24,088
Manantial 6	248322.502	2359027.942	-0.452	4.64	1,065	24,043
Manantial 7	248317.005	2358964.966	-0.204	4.38	1,127	24,027
Manantial 8	248307.625	2358899.981	-0.208	2.29	1,191	24,007

Table 4: Basic data of the artesian wells at the study site Exbasurero.

Location	UTM Zone 16 N		Z Altitude [masl]	Depth [m]	Distance Coast [m]	Dist. Meteo. Progreso [m]
	X East	Y North				
Exbasurero 1	226798.016	2355263.618	-0.290	1.90	1,364	2,194
Exbasurero 2	226798.586	2355259.597	-0.298	2.40	1,368	2,194
Exbasurero 3	226812.388	2355238.544	-0.206	0.89	1,391	2,205
Exbasurero 4	226819.602	2355245.292	-0.300	1.41	1,385	2,213

The measurement campaigns for this thesis include hydrodynamic, hydrochemical and physicochemical investigations and started with a preliminary phase in April 2012. The procedure of the measurements was of different temporal dynamics according to the specific methods of obtaining the required data and is described in the following section.

### 3.1 Hydraulic Measurements

To identify the spatial distribution of the water table and the groundwater flow direction the water table elevation (hydraulic heads) throughout the study zone was determined. The hydraulic heads or water potentials were obtained based on manual measurements made with the help of an electrical tape (Solinst 101 Water Level Meter) and Solinst Levelloggers in the deep observation wells and with help of a conventional PVC tube and in the coastal artesian wells. To obtain the real elevation above sea level of the water table (static level) the measured values had to be subtracted from the height of the benchmark obtained from the leveling of each measuring point.

Figure 13 shows how the measurements in the coastal artesian wells were performed. The three determined parameters A, B and C were measured with a regular measuring tape. To achieve the measurement of the hydraulic head (A) a PVC-tube of the diameter ( $d$ ) of 10 cm was introduced into the steel pipe of the flowing artesian wells, sealed with a

polystyrene ring, to measure the rising water. In July 2012 and March 2013 there were realized hourly measurements of the artesian water levels over a period of 12 hours to monitor the daily fluctuations of the aquifer in the discharge zone while the majority of the remaining measurements was performed twice a day (am and pm).

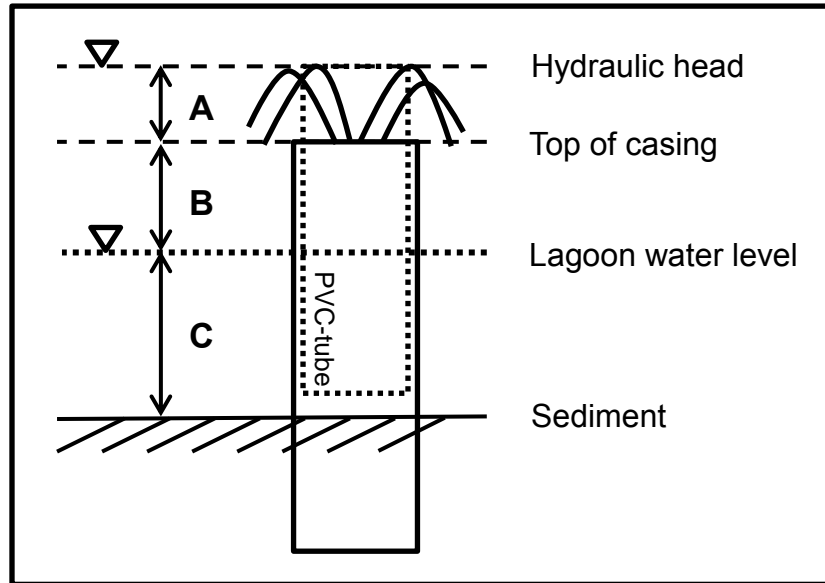


Figure 13: Measurements of hydraulic heads in the flowing artesian wells.

To estimate the discharge of the flowing artesian wells a propeller flowmeter was used to measure the flow velocity of the discharging groundwater in the steel tube. From the measured velocity  $v$  in  $\text{m s}^{-1}$  the discharge rate  $Q$  in  $\text{L s}^{-1}$  was calculated, using the cross section with the pipe radius  $r$  of 0.05 m at the top end of the tube, following equation 3. It has to be emphasized that it was challenging to obtain the exact radius of the steel pipe as it is often overgrown with algae or corroded. The flow velocity measurement accompanied the 12 hours monitoring campaign in June 2012 and March 2013.

$$Q = \pi \cdot r^2 \cdot v \quad (3)$$

With help of the manually obtained water levels from the observation wells equipotential maps were developed and the hydraulic gradients of different transects in the study area were calculated from manual and automatically conducted measurements. The hydraulic gradients were obtained from the hydraulic head measurements in the observation wells and the distance between them applying the following equation 4 to calculate the slope of the

water table. Being  $h_1$  and  $h_2$  the hydraulic heads of the two observation wells whose gradient should be obtained and  $(l_1 - l_2)$  the distance between them.

$$\frac{dh}{dl} = \frac{(h_1 - h_2)}{(l_1 - l_2)} \quad (4)$$

Gradients and equipotential lines were also obtained with help of the Golden Software Surfer 9 using the interpolation method Kriging to obtain a more comprehensive geographical distribution of the data from the individual manual hydraulic head measurements at the observation wells. The maps of equipotentials are used to determine the groundwater flow direction of the karst aquifer.

### 3.1.1 Datalogger

The automatic registration of the water table fluctuations was conducted with the help of dataloggers. For the continuous measurements of the electrical conductivity, temperature and water levels automated dataloggers were installed in 20 observation wells at different depth. Figure 14 illustrates the installation of the two dataloggers in the observation wells.

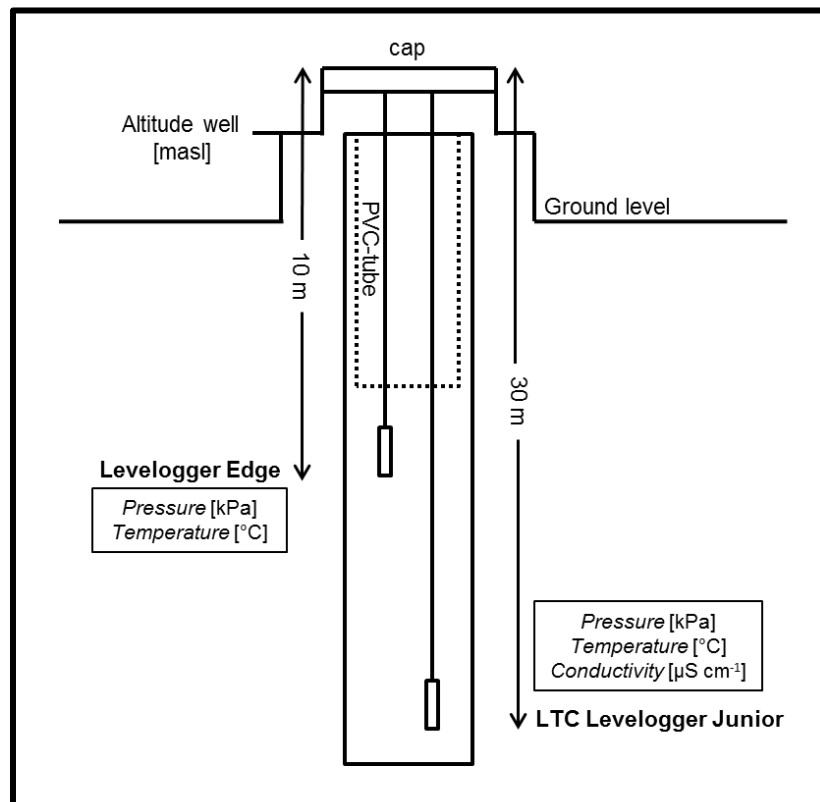


Figure 14: Installation of the two dataloggers at different depth in the observation wells.

In the wells Sagarpa and Sac-Nicté additionally two barologgers were installed to report the fluctuations of atmospheric pressure. The Barologgers are required to make a barometric compensation of the pressure registered by the Leveloggers that vary due to atmospheric pressure fluctuations, to obtain the net values of the hydraulic head elevation. According to (Solinst, 2012) the atmospheric pressure data from a Barologger can be used to compensate Leveloggers that are located within a radius of 30 km. Under this principle the data of the closest Barologger were selected to compensate the measurements of each well.

The Datalogger used are manufactures by Solinst and the types LTC Levelogger Junior, Levelogger Edge and Barologger Edge respectively. The registration of the parameters started on June 17, 2012 and the divers are currently operating. The sensors register values every 6 hours and the measurement period considered for this investigation lasts from the beginning of the measurements till mid-May 2013.

The Levelogger registers the sum of pressures that exert the water column and the atmospheric pressure at a certain point below water level where the transducer is collocated. To obtain the real elevation of the hydraulic heads ( $h$ ) at the observation wells with respect to sea level (masl) equation 5 was applied in order to make the barometric compensation of the data from the Leveloggers.

$$h [\text{masl}] = z_w - (l_0 - p_0 \cdot 0.1022 + w_0 - c) - (l_1 - p_1 \cdot 0.1022) \quad (5)$$

$$l_0 - p_0 \cdot 0.1022 + w_0 - c = \text{constant}$$

The factor 0.1022 is used to convert the reported pressure data from kilopascal (kPa) to water column equivalent in meters. The first term that is subtracted from the altitude  $z_w$  of the observation well in masl stays constant within the same well. The variable  $l_0$  is the first reported water pressure (level) in kPa and  $p_0$  represents the initial value of atmospheric pressure in kPa that is recorded by the Barologger. The parameter  $w_0$  is the water table in meters measured manually in the observation well during the installation of the datalogger and  $c$  stands for the height of the cap covering the observation well in meters.

Additional information like climatological and meteorological data, tide data and geographic information among others was obtained from the institutions CONAGUA, CICESE, INEGI and CONABIO. The results and received data were analyzed and visualized in graphic and cartographic form, regarding subject matter, using the Geographic Information System tool GIS-Software ArcMap 10.1 and Surfer 9, Aquachem 4.0 for the water quality analysis and Microsoft Excel 2010.

## 3.2 Water Quality

The chemical water composition considered in the analysis of the karst environment depends on various intrinsic and external factors like the geology, climatic conditions, natural and anthropogenic recharge or land use practices among others.

The analysis of the physical and chemical properties and the quality of the groundwater was carried out by different kinds of methods that are described below. Besides precipitation water, coastal lagoon water and ocean water were analyzed.

### 3.2.1 Hydrolab MS5 Multiprobe

The Multiparameter Water Quality Sonde Hydrolab MS5 Multiprobe was used insitu for an undisturbed physicochemical screening of the groundwater layers in the deep observation wells and for punctual measurements in the flowing artesian wells, the coastal lagoons and the ocean. The MS5 is designed and distributed by HACH Company, Loveland, Colorado. The device is connected to a notebook via a pluggable waterproof cable. With the user software Hydras 3LT the data are directly displayed and can be exported for further processing (HACH, 2006). Before every measurement campaign and after every battery change the sensors of the MS5 device were calibrated with a specific solution. The two parameters to calibrate are pH and electrical conductivity, two standards were used for each parameter to make a two point calibration.

The screening of the deep wells with the Hydrolab has been carried out every two or three month from April 2012 to March 2013. This thesis will regard six profiling campaigns at the observation wells for the month in April, May, August, November, January and March. The Hydrolab can measure up to 10 water quality parameters simultaneously that are ammonia, chloride, chlorophyll a, rhodamine WT, conductivity, depth, dissolved oxygen, nitrate, ORP, pH, temperature, total dissolved gas, turbidity, and blue-green Algae (HACH, 2006). Of the possible parameters the following, specified according to HACH (2006) were measured for the investigation of this thesis.

**Depth [m]:** The depth describes the vertical distance between the water surface and the multiprobe sensors, measured in meter. Via a pressure recording system the absolute hydrostatic pressure is measured from an internal diaphragm and converted into meters of water column. The maximum immersion depth of the Hydrolab is 225 meters and the accuracy  $\pm 0.05$  meters.

**Temperature [°C]:** Water temperature is of high importance for the analysis because it is responsible for many biochemical processes like the dissolution of calcium carbonate as it modifies its solubility. The operating temperature ranges from -5 to 50 °C with an accuracy of  $\pm 0.10$  °C and can be displayed in [°C], [°F] or [K].

**pH:** The pH is a very important parameter regarding water quality as certain chemical processes like chlorine reactions can only take place in a determined pH range. The pH sensor uses a glass bulb that is impregnated with KCl and permeable for hydrogen ions. A reference electrode filled with 3 molar KCl solution originates the forming of a salt bridge between sensor and reference electrode, a potential can be measured. The accuracy is of  $\pm 0.2$  units.

**Electrical conductivity [ $\mu\text{S cm}^{-1}$ ]:** The electrical conductivity is the capacity of the water to conduct electricity due to dissolved substances and is a method to determine water salinity. The conductivity sensor contains four graphite electrodes in an open cell to measure the current between two electrodes held at a fixed potential. The accuracy for this value is  $\pm 0.001$  mS  $\text{cm}^{-1}$  or 1 % of the reading.

**Total Dissolved Solids (TDS) [ $\text{g L}^{-1}$ ]:** The TDS are derived from the conductivity readings. As default factor 0.64 is used to calculate the TDS but it can be user defined if measured data indicate the need for a different factor.

**Dissolved Oxygen (DO) [ $\text{mg L}^{-1}$ , %]:** The actual concentration of dissolved oxygen in a water sample refers to the amount of oxygen dissolved in water at a certain temperature and pressure. Adequate oxygen concentrations are indispensable for good water quality, very low concentrations indicate poor quality. Temperature influences the maximum dissolved oxygen content of water, by increasing environmental temperature the amount of dissolved oxygen is reduced (EPA, 2012). The accuracy is  $\pm 0.1$  mg  $\text{L}^{-1}$  and  $\pm 0.2$  mg  $\text{L}^{-1}$  for concentrations lower than 8 mg  $\text{L}^{-1}$  and above 8 mg  $\text{L}^{-1}$  respectively.

**Oxidation-Reduction Potential (ORP) [mV]:** The ORP is a measure of the capacity of the water to oxidize or to reduce elements present in the water. The more positive the ORP value the more oxidized are the chemical compounds of a solution. In polluted ecosystems were microorganisms consume the available oxygen the ORP is low. The accuracy is  $\pm 20$  mV.

During the measuring process the Hydrolab MS5 was lowered slowly meter for meter, checking the depth via the frontend to register the parameters in order to plot them against the depth to obtain quality profiles of the groundwater. In intervals of one meter the Hydrolab equipment measured for one minute to ensure stabilization of the measurement values before registration. During every measuring campaign at the deep wells the groundwater table was determined.

At the coastal study site in the shallow artesian wells one measurement per spring at depth of approximately one meter was performed per measuring campaign, additionally the Hydrolab was used to measure the physicochemical parameters of the coastal lagoon water.

### 3.2.2 Water Sampling

One sampling campaign of the observation wells and artesian springs was conducted during the rainy season (September 21 to October 2, 2012) and the second campaign was realized in the dry season of the study period (February 14 to 19, 2013).

For the water sampling a *WILDCO Water Sample Bottle* with a volume of 1.2 L was used. In most of the deep wells samples were taken from two different depths in order to capture different water layers. To conserve the element concentrations some water samples were acidified with nitric acid. Besides an aliquot of 50 ml ( $V_{sample}$ ) was taken to measure the alkalinity insitu by titration directly after the extraction of the groundwater sample to avoid disturbance. The total alkalinity is defined as the acid neutralizing capacity of a solution and was determined by titration. It is equivalent to the sum of bases that can be titrated with a strong acid as the non-conservative bases  $\text{HCO}_3^-$ ,  $\text{CO}_3^{2-}$  and  $\text{OH}^-$  change their concentration while they react with  $\text{H}^+$  during titration (Kehew, 2001). For the titration with sulphuric acid (1.6 N  $\text{H}_2\text{SO}_4$ ) a *HACH Alkalinity Test Kit*, Model AL-DT was used. The pipet with a mechanical counter allows adding small volumes of  $\text{H}_2\text{SO}_4$  to the sample drop by drop. This procedure was carried out till the sample reached a pH of 4.3. To measure the current pH during the addition of the strong acid to the 50 ml aliquot a portable pH meter was used. By the number of recorded digits (drops) and the corresponding pH ( $\text{H}^+ = 10^{-\text{pH}}$ ) the alkalinity can be determined by means of the graphical method using the equation 6 of the Gran Function (*GF*) (König, 2009) that is plotted against the volume of sulphuric acid  $V_{acid}$  added during the titration till reaching a pH of 4.3.

$$GF = \frac{V_{sample} + V_{acid}}{V_{sample}} \cdot [\text{H}^+] \quad (6)$$

The total hardness in  $\text{mg L}^{-1}$  of  $\text{CaCO}_3$  was calculated from the different molar masses of the elements (equation 7).

$$\text{Hardness} [\text{CaCO}_3] = \frac{M_{\text{CaCO}_3}}{M_{\text{Ca}}} \cdot [\text{Ca}^{2+}] + \frac{M_{\text{CaCO}_3}}{M_{\text{Mg}}} \cdot [\text{Mg}^{2+}] \quad (7)$$

The ratios of the molar masses for  $\text{CaCO}_3/\text{Ca}^{2+}$  and  $\text{CaCO}_3/\text{Mg}^{2+}$  are 2.5 and 4.1 respectively.

Furthermore the ion balance errors [%] of the analytical results have been obtained in the laboratory of San Luis Potosí by equation 8 in order ensure the analytical reliability. Cations ( $\text{Na}^+$ ,  $\text{K}^+$ ,  $\text{Ca}^{2+}$ ,  $\text{Mg}^{2+}$ ,  $\text{Si}^{4+}$ ,  $\text{Fe}^{2+}$ ,  $\text{Mn}^{3+}$ ) and anions ( $\text{CO}_3^{2-}$ ,  $\text{HCO}_3^-$ ,  $\text{Cl}^-$ ,  $\text{SO}_4^{2-}$ ,  $\text{NO}_3^-$ ,  $\text{F}^-$ ) are used in the unit  $\text{meq L}^{-1}$ .

$$\text{Error} [\%] = \frac{\sum \text{Cations} - \sum \text{Anions}}{\sum \text{Cations} + \sum \text{Anions}} \cdot 100 \quad (8)$$

A total of 103 samples were considered for this analysis being the majority (96) from groundwater. For the analysis of the water chemistry the samples were classified according to the sampling depth into shallow samples ( $< 20$  m), samples from the intermediate zone ( $\geq 20 < 30$  m) and deep samples ( $\geq 30$  m). The samples of the flowing artesian wells, lagoon water, meteoric waters and ocean water were analyzed independent of the depth.

For the recollection of precipitation water samples two PVC-Canisters were installed at the meteorological stations in Mérida and Progreso respectively, Figure 15 shows the arrangement at the observatory in Progreso. The canisters previously were covered with an anti-reflective coating and furthermore 220 ml of glycerin were added to avoid evaporation of the precipitation water. The samples were taken in rainy and dry season at beginning of September and end of January respectively.



Figure 15: Installation for the capture of precipitation water in Mérida and Progreso.

All water samples were analyzed in the chemistry laboratory of the UASLP determining the concentrations of major anions and cations, heavy metals and trace elements. Inductively Coupled Plasma Mass Spectrometry (ICP-MS) was employed to identify heavy metals and trace elements; due to the high sensitivity of the analytical method it is possible to detect very small element concentrations in the range of  $\text{ng L}^{-1}$ . Various approaches were employed to determine major anions, such as spectrophotometry and volumetric method among others. Cation concentrations were obtained via Atom Absorptions Spectroscopy (AAS) making use of the specific light wavelengths absorbed by the elements. The bacteriological analysis was done in the laboratories of the UADY in Mérida.

## 4 Results

In the following chapters the results of the investigation are presented and analyzed.

### 4.1 Hydraulic Measurements

The following section reports the results of the hydraulic measurements and the data obtained from the continuous datalogger registration and manual measurements at the deep observation wells and the flowing artesian wells.

#### 4.1.1 Datalogger

The continuous measurement of the hydraulic heads with help of the dataloggers presented significant difference between the pressure readings obtained from the two different dataloggers that were positioned at different water horizons in the wells. The readings of the Leveloggers LTC Junior installed deeper (> 15 m deep) in order to register electrical conductivity besides water pressure, in the majority of the cases reported lower hydraulic heads than the Leveloggers Edge. Comparing with the manual measurements of hydraulic heads, Leveloggers Edge showed consistent values and in the further process of the analysis almost exclusively the electrical conductivity data of the Levelogger LTC Junior were considered. The difference between shallow and deep dataloggers eventually occurred due to a vertical water flow downwards in the observation wells or even because of violating the recommended installation range of 10 to 30 m in many cases. However Figure 16 depicts that the phenomenon of displacement for the observation well Chalmuch was registered the other way round.

Regarding the measured information obtained from the dataloggers for the period of 17.06.2012 to 21.05.2013 in Figure 17 the data of Chalmuch observation well are presented together with daily precipitation data obtained from the meteorological station in Mérida (located 8.5 km to the south-east from Chalmuch).

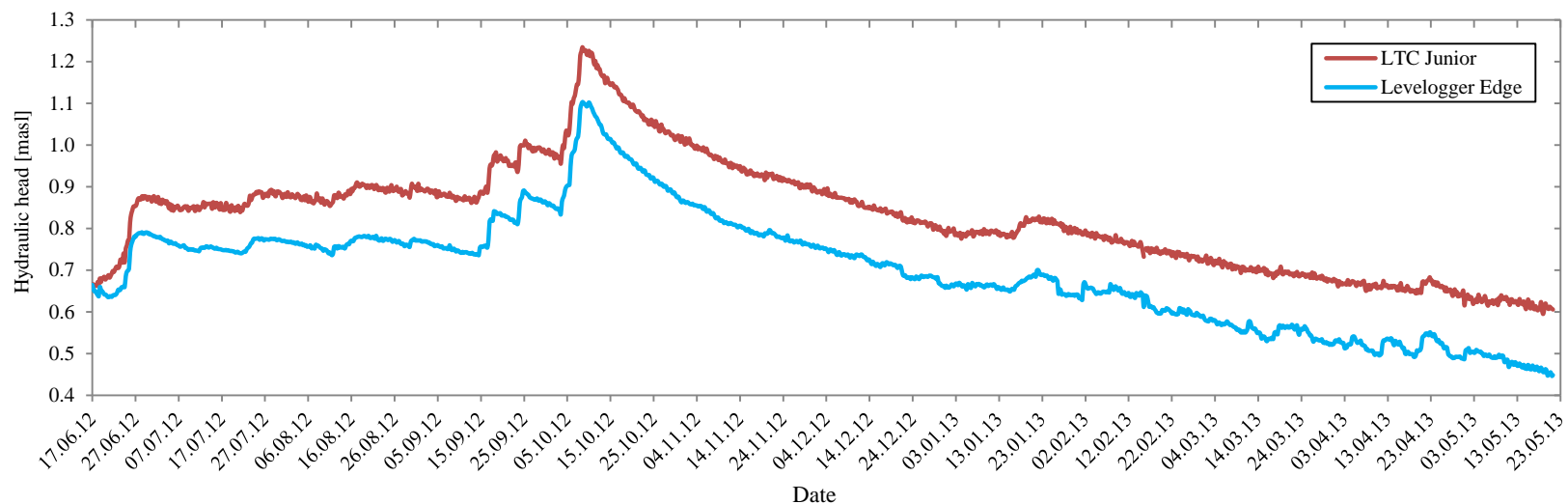


Figure 16: Difference between the water levels obtained from the two datalogger registrations in the observation well Chalmuch.

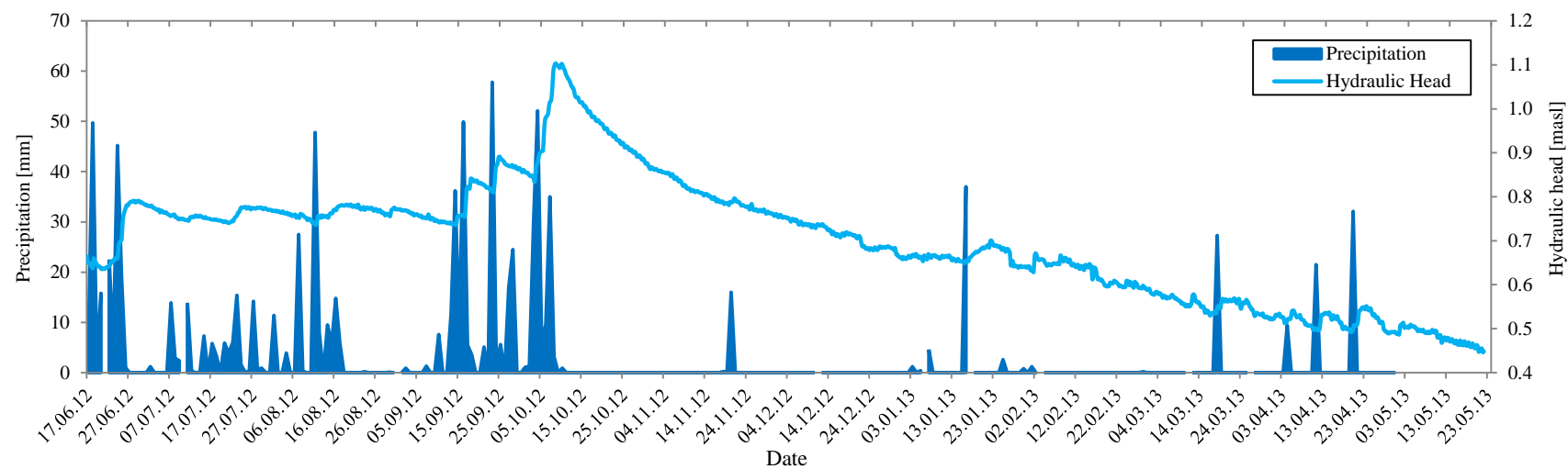


Figure 17: Precipitation variation and hydraulic head fluctuation.

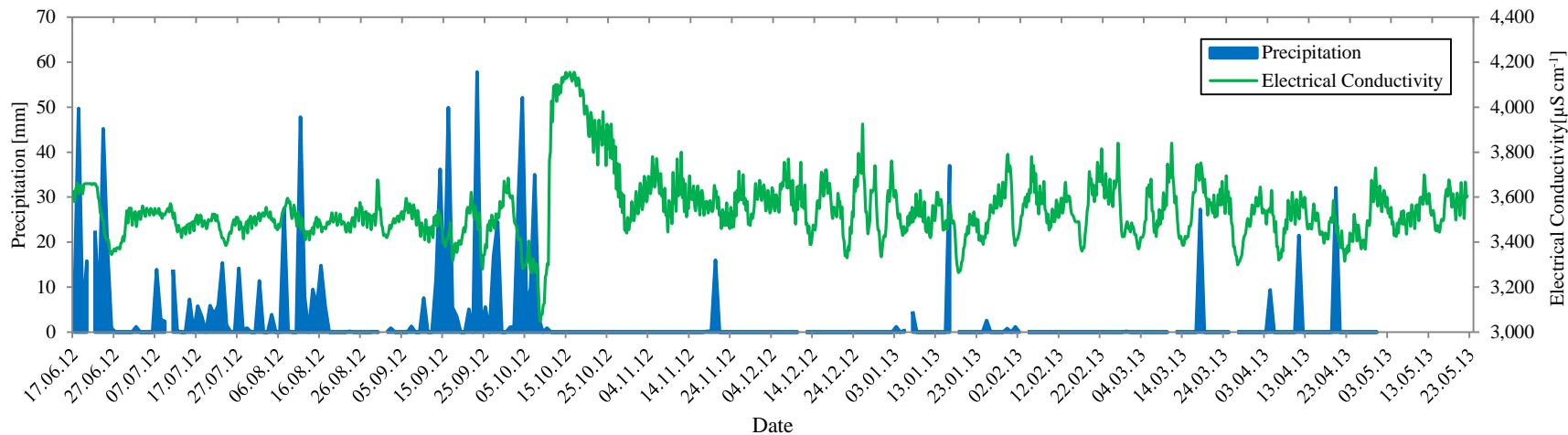


Figure 18: Relation between precipitation and electrical conductivity.

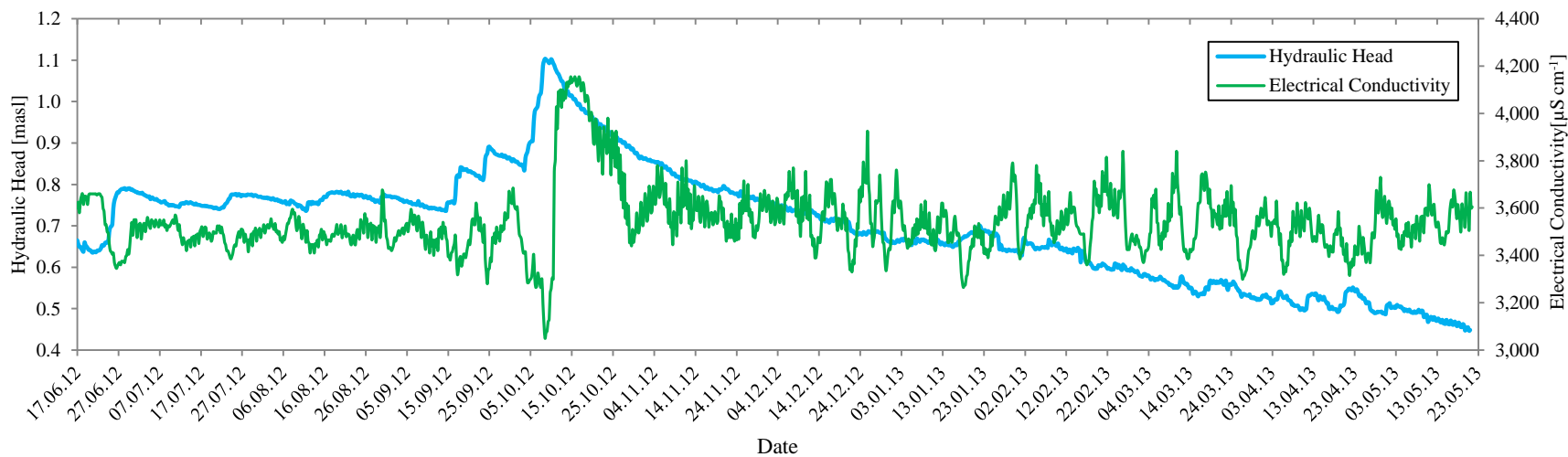


Figure 19: Variations of hydraulic heads and electrical conductivity.

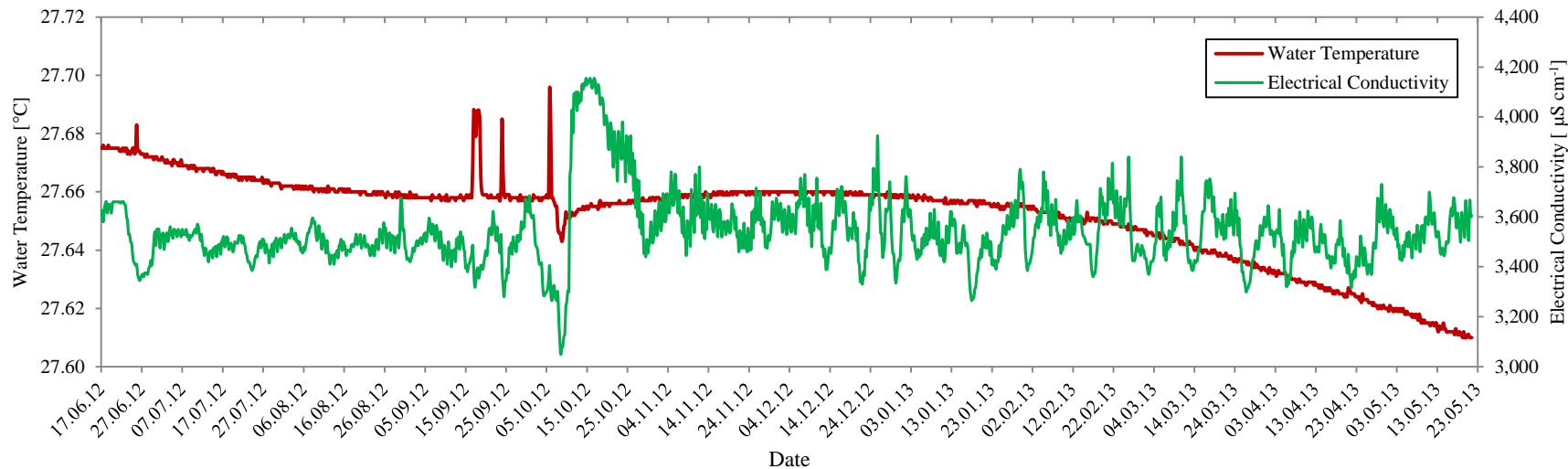


Figure 20: Relation between groundwater temperature and electrical conductivity.

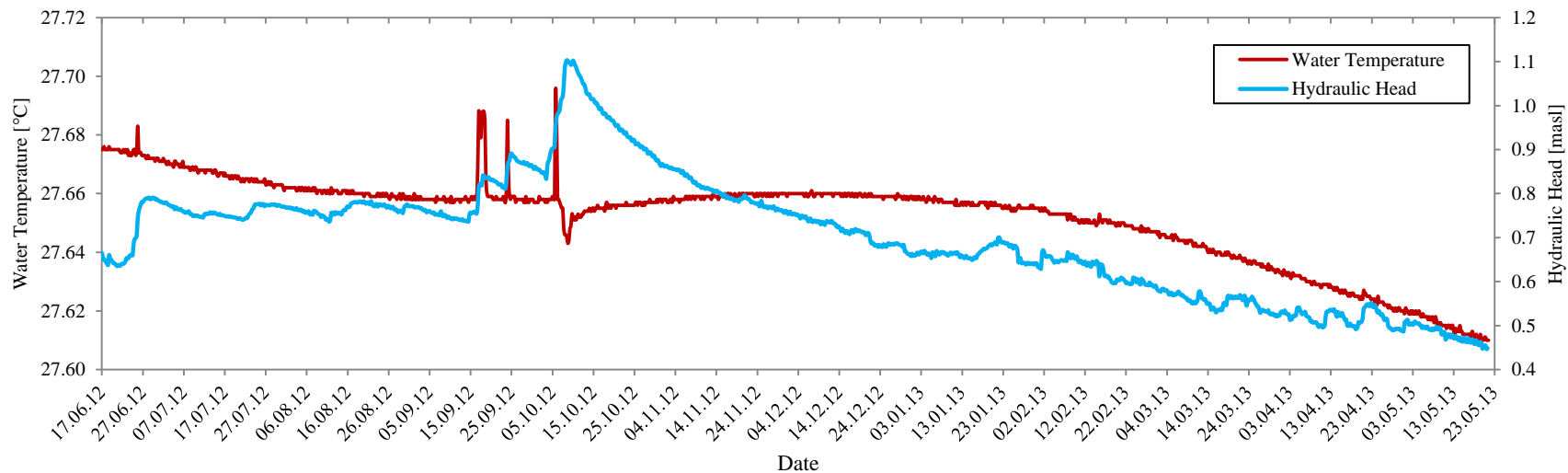


Figure 21: Relation between groundwater temperature and hydraulic heads.

There could be observed a clear correlation between precipitation events and fluctuation of the water table in the observation wells. The relationship indicated a relatively quick response of the water level to rainfall. The overall highest head registered by the dataloggers for Chalmuch was 1.1 masl for October 8, 2012. This elevation was reached after a steep increase that started October 3, 2012 from a hydraulic head of 0.83 masl. It was assumed that the described rise of about 27 cm to the highest elevation of documented hydraulic heads is largely due to the accumulated precipitation events reported in the meteorological station in Mérida at the end of September and beginning of October. There were reported 29 mm of precipitation for October 3, 52 mm for October 4, and 35 mm of rainfall for October 7, 2012 that are supposed to be reflected in the overall highest peak of hydraulic head, assumed to be subjected to a small retarded effect due to the time it takes the water to infiltrate through the subsoil and to reach the watertable. From this date on precipitation started to decrease and so did the hydraulic head. Also very small amounts of precipitation seemed to have a very direct influence of the hydraulic heads of the karst aquifer. For November 20, 2012 for instance a precipitation event of 16 mm was reported and the hydraulic head indicated a little local peak reflecting an increase of approximately 9 mm. For January 22, 2013 there was registered an intermediate peak in hydraulic head from 0.65 masl (January 16, 2013) to 0.70 masl (January 22, 2013) probably reflecting the precipitation event of 37 mm on January 16, 2013. The retarded effect for the rise in hydraulic head of almost 5 cm was approximately six days. Of course there has to be taken into account that the described variations are subjected to the accuracy of the divers that can be up to 0.05 % of the measured value.

Figure 18 illustrates the precipitation events in Mérida during the study period together with the electrical conductivity data obtained from the LTC Junior datalogger 30 m deep. Overall there could be observed variations in the electrical conductivity values in the range of  $3,050 \mu\text{S cm}^{-1}$  to  $4,155 \mu\text{S cm}^{-1}$  as the sensor was placed at the depth of brackish water. After the aforementioned precipitation events registered at the end of September and beginning of October the electrical conductivity rose steeply from the overall lowest to the highest value.

In Figure 19 the electrical conductivity is related to the hydraulic head and it becomes clear, that the steeply increasing hydraulic head on October 8, 2012 resulted in an immediate decrease of the electrical conductivity to the lowest value ( $3,500 \mu\text{S cm}^{-1}$ ) at the same day. Nevertheless a steep rise in electrical conductivity to the overall highest value ( $4,100 \mu\text{S cm}^{-1}$ ) was registered only four days after the increment of hydraulic head. The increase in electrical conductivity a few days after the highest precipitation events cannot be explained with the warming effect that the rainfall exerts over the groundwater and the high

temperature dependency of the electrical conductivity alone (Figure 20). Theoretical conditions suggest that increasing hydraulic head causes the interface fresh-saltwater to drop down and consequently the electrical conductivity should decrease. A steep decrease of electrical conductivity was only evidenced at the same time the highest hydraulic head was reported. The latter electrical conductivity increase, inconsistent with the theory, is probably due to a modification of groundwater flow and the preferential flow paths in the karstic conduct system because of the increased hydraulic heads. This could provoke important vertical flow components and changing velocity that cause mixing of fresh and deep saltwater. The vertical flow probably could also generate a piston effect that causes the water to behave like a coiled spring, moving down initially, to later bounce back until the energy dissipates and the system returns to its original state (Escolero, et al., 2006).

After main precipitation events during the study period the hydraulic head showed an overall decreasing trend after the highest water level in October, with decreasing water levels, the water temperature also decreased (Figure 21). With a few variations the described pattern was identified in almost all the observation wells that were equipped with dataloggers. Groundwater levels of the karst aquifer obtained from the observation wells are highly influenced by rainfall.

The groundwater temperature measured with help of the dataloggers and the Hydrolab decreased towards the shoreline (Figure 22). The artesian wells showed a steeper temperature increase in a small area suggesting that the groundwater is governed by a different system than the observation wells.

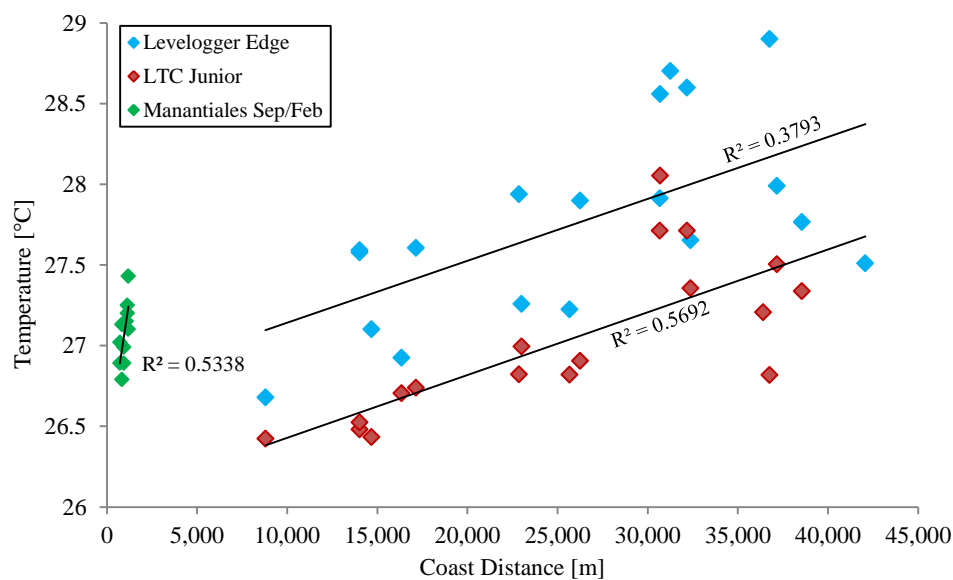


Figure 22: Decreasing temperature trend towards the coastline.

### 4.1.2 Hydraulic heads & Groundwater flow

The maps in Figure 23 depict the equipotential lines obtained from the manual measurement of the hydraulic heads for different month during wet and dry season. Overall the regional groundwater flow in the study area, being streamlines orthogonal to the equipotential lines, was determined as from south to north, slightly north-west oriented.

Lowest hydraulic heads were documented in August and the overall lowest water tables were measured in the northern coastal region (Contenedores -0.13 masl). The highest precipitation amount was registered for Mérida in September and for Progreso in June. Unfortunately manual hydraulic head measurements were not carried out neither in September nor in October but the groundwater levels registered by the leveloggers documented the increase of hydraulic heads during wet season.

For the manual measurements in November the overall highest water levels were registered in the observation wells being all hydraulic heads above sea level, ranging from 1.13 masl (Unidad Deportiva del Sur) to 0.13 masl (Baag). The high water table in November is assumed to reflect the increased aquifer recharge by precipitation in September and October. Comparing the results to the diver measurements it becomes clear that the overall highest water tables were reached in October but manual data are missing for this month. Around the observation well Sac-Nicté (4), Komchén (23) and X'Luch (28) very high hydraulic gradients could be observed as the interpolated equipotentials were closer together. This is probably an effect of local precipitation events in this area. For the equipotential map of January two outliers were eliminated for the observation wells Chenku and Mococho as they presented very extreme and probably erroneous values. The map looks very similar to the one for November and for both month there could be observed higher hydraulic gradients around the same observation wells Sac-Nicté (4) and Granjas Crío (2) being the groundwater flow the most northward oriented. For May 2013 when hydraulic heads were among the lowest during the study period, as very little precipitation amounts were reported for Mérida and Progreso, the obtained flow direction for the study area was stronger oriented from south to north-west than during the other months. The hydraulic heads measured manually within the research project can be found in Appendix 1.

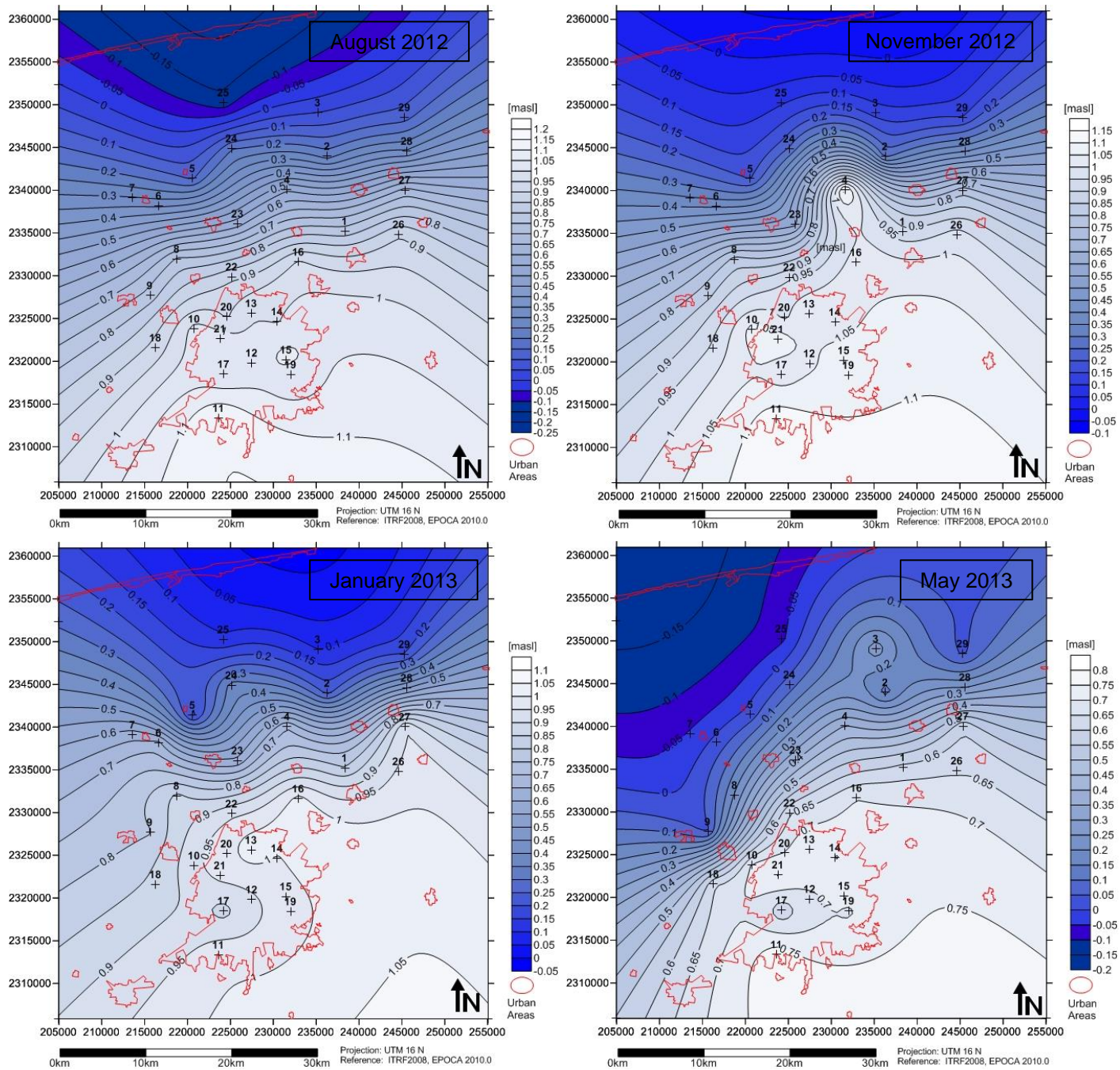


Figure 23: Equipotential maps for different month.

### 4.1.3 Hydraulic gradients

Measured hydraulic heads showed an increase with distance from the coastline and it becomes clear that there is a correlation between the distance of the observation wells from shore and the water table elevation. The regression lines of the described relationship were determined for the different month of the investigation. For the month July there could be obtained the best fit of the regression line and consequently the strongest correlation while January showed the poorest correlation and also lower hydraulic gradients were reported. Figure 24 depicts the hydraulic heads that were obtained according to the manual and automatically processing of the data in relation to the coast distance. It illustrates that the overall potentiometric slope varied according to the different data acquisition methods and between the different months of the study period.

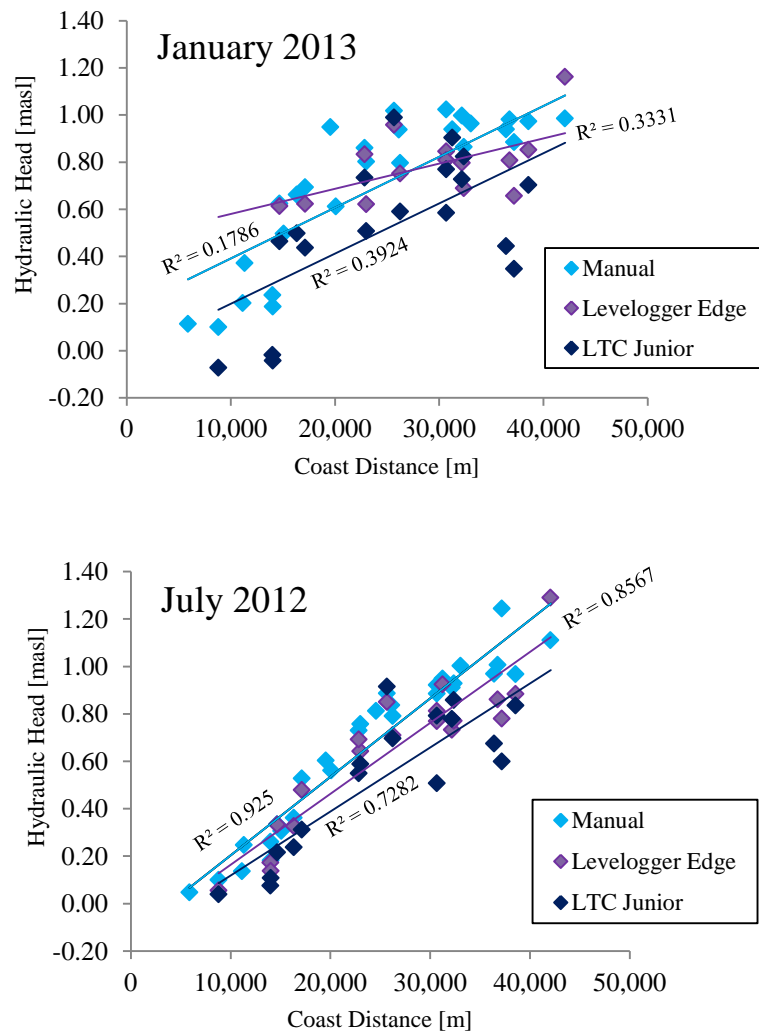


Figure 24: Potentiometric slope obtained from hydraulic heads.

Overall the slope of the potentiometric surface was very low and as Figure 32 depicts the goodness of the linear fit ranged between 0.179 and 0.925 during dry and wet season respectively. In general there was observed a better linear correlation between the parameters during rainy season than in the dry period. The relation depends on the location of precipitation events, the hydraulic conductivity and aquifer recharge among others. The decreasing potentiometric surface towards the coast determines the regional groundwater flow pattern.

To obtain the hydraulic gradients for different sections of the study area, the change in hydraulic head per unit distance between various wells in almost perpendicular direction to the coastline was calculated from the data of the manual and automatic water table measurements. It has to be emphasized that the groundwater flow in the study area is not strictly perpendicular to the coastline but the presented determination of the hydraulic gradients can give a good approximation. The hydraulic gradients for different month represented below were selected according to their importance in the overall integral analysis of the general pattern of the study area. In general the determined hydraulic gradients for the study area were very low but varied a lot within the study area and differed between the months. Overall the gradients obtained for the coastal study site (Manantiales) were higher and on the whole the manually calculated hydraulic gradients of the most eastern transect (Megalita – Baag) resulted as the highest for all month. Nevertheless there has not been identified a uniform trend for the determined data.

In June the study region at the coastal site received the highest amount of precipitation and Mérida the second highest, the obtained gradients represented in Table 5 are the second lowest after February.

Table 5: Hydraulic gradients for three transects in June.

<b>June 2012</b>	Distance [m]	Hydraulic Gradient	
		Manual	Levellogger Edge
Observatorio – Dzidzilché	23,190	$3.02 \cdot 10^{-5}$	$2.90 \cdot 10^{-5}$
UDS – Sierra Papacal	25,799	$2.68 \cdot 10^{-5}$	$2.18 \cdot 10^{-5}$
Megalita – Baag	14,218	$4.75 \cdot 10^{-5}$	$4.42 \cdot 10^{-5}$

For August less precipitation was registered but the hydraulic gradients resulted slightly higher than the ones obtained for June (Table 6).

Table 6: Hydraulic gradients for four transects in August.

<b>August 2012</b>	Distance [m]	Hydraulic Gradient	
		Manual	Levellogger Edge
Observatorio – Dzidzilché	23,190	$3.72 \cdot 10^{-5}$	$3.09 \cdot 10^{-5}$
UDS – Sierra Papacal	25,799	$3.13 \cdot 10^{-5}$	$3.92 \cdot 10^{-5}$
Megalita – Baag	14,218	$5.08 \cdot 10^{-5}$	$5.07 \cdot 10^{-5}$
Sac-Nicté – Exbasurero 1*	15,955	$3.97 \cdot 10^{-5}$	$3.71 \cdot 10^{-5}$

September is the month of maximum precipitation that was registered during the study period in the meteorological station in Mérida while the station in Progreso received very little rainfall. The calculated hydraulic gradients for this month are based on the highest values registered by the Levelloggers Edge in September (Table 7).

Table 7: Hydraulic gradients for four transects in September.

<b>September 2012</b>	Distance [m]	Hydraulic Gradient
		Levellogger Edge
Observatorio – Dzidzilché	23,190	$3.18 \cdot 10^{-5}$
UDS – Sierra Papacal	25,799	$3.79 \cdot 10^{-5}$
Megalita – Baag	14,218	$4.51 \cdot 10^{-5}$
Sac-Nicté – Exbasurero 1*	15,955	$2.74 \cdot 10^{-5}$

During the dry season in November when only little rain was registered but the overall highest hydraulic heads were reported manually (missing manual measurements for September and October) and the following hydraulic gradients were obtained (Table 8).

Table 8: Hydraulic gradients for three transects in November.

<b>November 2012</b>	Distance [m]	Hydraulic Gradient	
		Manual	Levellogger Edge
Observatorio – Dzidzilché	23,190	$3.57 \cdot 10^{-5}$	$2.90 \cdot 10^{-5}$
UDS – Sierra Papacal	25,799	$2.86 \cdot 10^{-5}$	$3.92 \cdot 10^{-5}$
Megalita – Baag	14,218	$5.5 \cdot 10^{-5}$	$4.99 \cdot 10^{-5}$

For February very few precipitation events were registered and the overall lowest hydraulic gradients are represented in Table 9.

Table 9: Hydraulic gradients for three transects in February.

<b>February 2013</b>	Distance [m]	Hydraulic Gradient Levellogger Edge
Observatorio – Dzidzilché	23,190	$1.76 \cdot 10^{-5}$
UDS – Sierra Papacal	25,799	$2.75 \cdot 10^{-5}$
Megalita – Baag	14,218	$2.89 \cdot 10^{-5}$

On a whole the hydraulic gradients obtained from the observation wells ranged between  $18 \text{ mm km}^{-1}$  and  $55 \text{ mm km}^{-1}$ .

Figure 25 depicts the maps of hydraulic gradients obtained with the help of the software Surfer 9 for the month August 2012, November 2012, January 2013 and May 2013. It becomes clear that in the northern and central part of the study area, at a distance of approximately 15-25 km from the coastline the overall steepest hydraulic gradients were determined; this is in accordance with the manual calculated gradients between the wells Megalita and Baag. Probably the steep hydraulic gradients in this zone are due to a reduced horizontal component of the hydraulic conductivity. The smallest hydraulic gradients were obtained for the southern part of the study area. In general for November the highest gradients were identified while during August the overall lowest gradients were reported. Comparing to the manual calculated transect gradients the ones obtained with Surfer 9 varied over a wider range. Table 10 shows the values between those hydraulic gradients ranged for the four month.

Table 10: Ranges of hydraulic gradients (dimensionless) obtained for the study area from the interpolated manual measurements of hydraulic heads.

Month	Maximum Gradient	Minimum Gradient
August 2012	$8.19 \cdot 10^{-5}$	$1.60 \cdot 10^{-7}$
November 2012	$1.56 \cdot 10^{-4}$	$6.42 \cdot 10^{-7}$
January 2013	$1.06 \cdot 10^{-4}$	$1.69 \cdot 10^{-7}$
May 2013	$1.17 \cdot 10^{-4}$	$3.48 \cdot 10^{-7}$

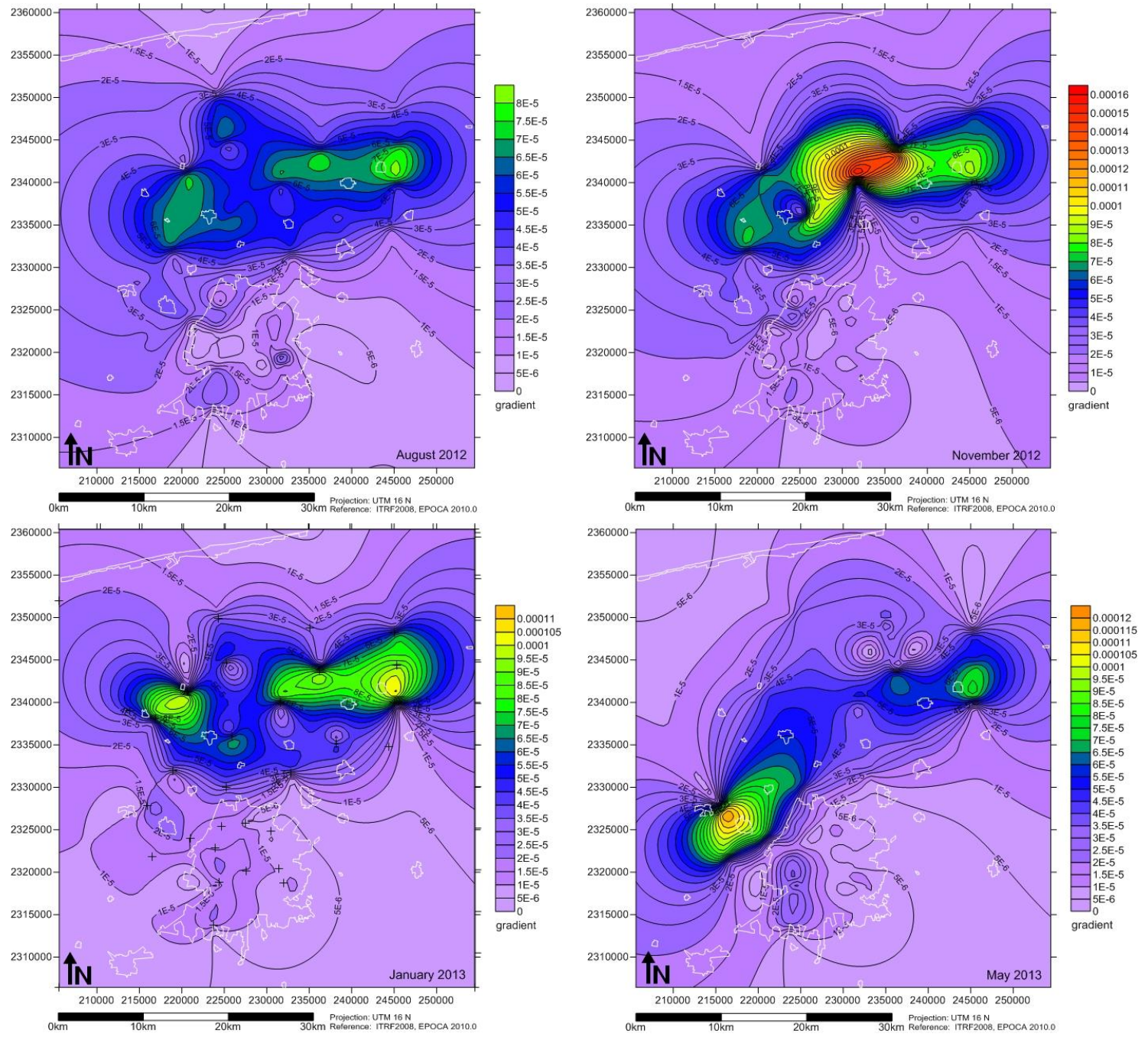


Figure 25: Hydraulic gradient maps for four month.

#### 4.1.4 Artesian wells

For the manual hydraulic head measurements realized at the coastal study sites at the flowing artesian wells Manantiales and Exbasurero the assumption of correlation between hydraulic head and distance to the coastline is depicted in Figure 26. Comparing to the observation wells during wet season an overall lower correlation was determined, this probably indicates that the flow system that discharges at the coastline is not the same like the one of the continental observation wells and furthermore stronger tidal influences have to be considered near the coast. The best linear fit was adjusted to the data from the measurement on June 5, 2012 where the overall highest hydraulic heads were registered.

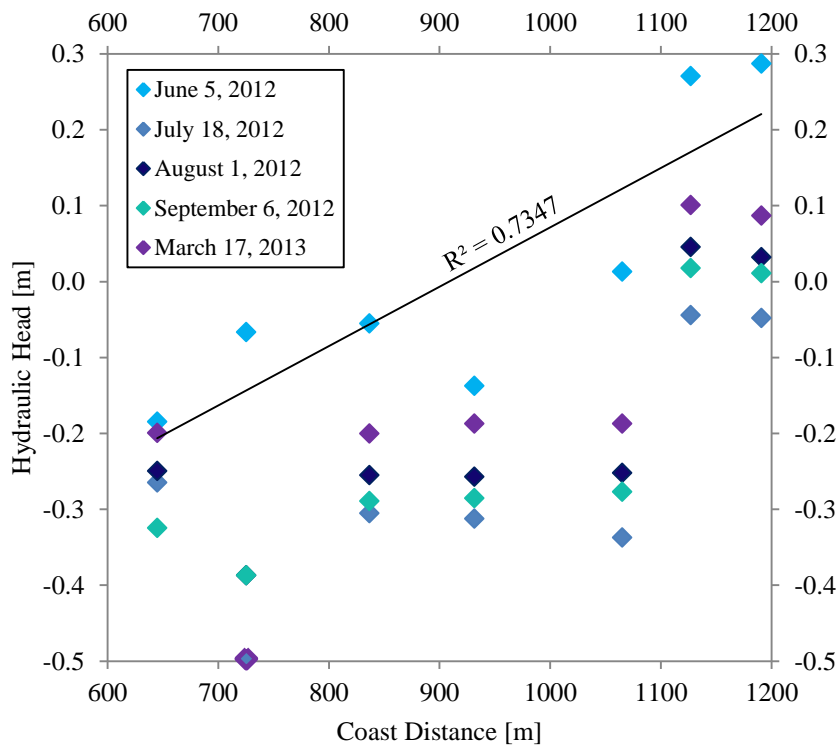


Figure 26: Hydraulic heads related to the coast distance.

The hydraulic gradients that were calculated between Manantial 1 and Manantial 8, the two flowing artesian wells furthest apart from each other (555.91 m) were higher than the ones obtained between the previously described observation wells as they are located in the discharge zone and calculated on a very small scale and only for a small fraction of the study area. The hydraulic gradients obtained from the ascending water in the artesian wells ranged between  $39 \text{ cm km}^{-1}$  and  $85 \text{ cm km}^{-1}$  (Table 11).

Table 11: Hydraulic gradients for study area of the artesian wells Manantiales.

Manantial 1 - Manantial 8 Distance 555.91 m	Hydraulic Gradient
June 5, 2012	$8.48 \cdot 10^{-4}$
July 18, 2012	$3.89 \cdot 10^{-4}$
August 1, 2012	$5.06 \cdot 10^{-4}$
September 6, 2012	$6.04 \cdot 10^{-4}$
March 17, 2013	$5.15 \cdot 10^{-4}$

Furthermore there has to be considered that the hydraulic gradients near the coast varied a lot and even inverse gradients were observed for the data obtained from the artesian wells at the study site Exbasurero (Table 12).

Table 12: Hydraulic gradients for study area of the artesian wells Exbasurero.

Exbasurero 1 - Exbasurero 4 Distance 283.32 m	Hydraulic Gradient
July 18, 2012	$7.06 \cdot 10^{-5}$
August 16, 2012	$-1.94 \cdot 10^{-4}$
September 6, 2012	0
March 17, 2013	$8.82 \cdot 10^{-5}$

Hourly measurements over a period of 12 hours, in two campaigns (July 2012 and March 2013) were performed in four of the flowing artesian wells of the discharge area to register the fluctuation of the hydraulic heads. This was done manually with the help of PVC-tube and measuring tape and the hydraulic heads of the study site Manantiales showed an overall uniform course over the day (Figure 27).

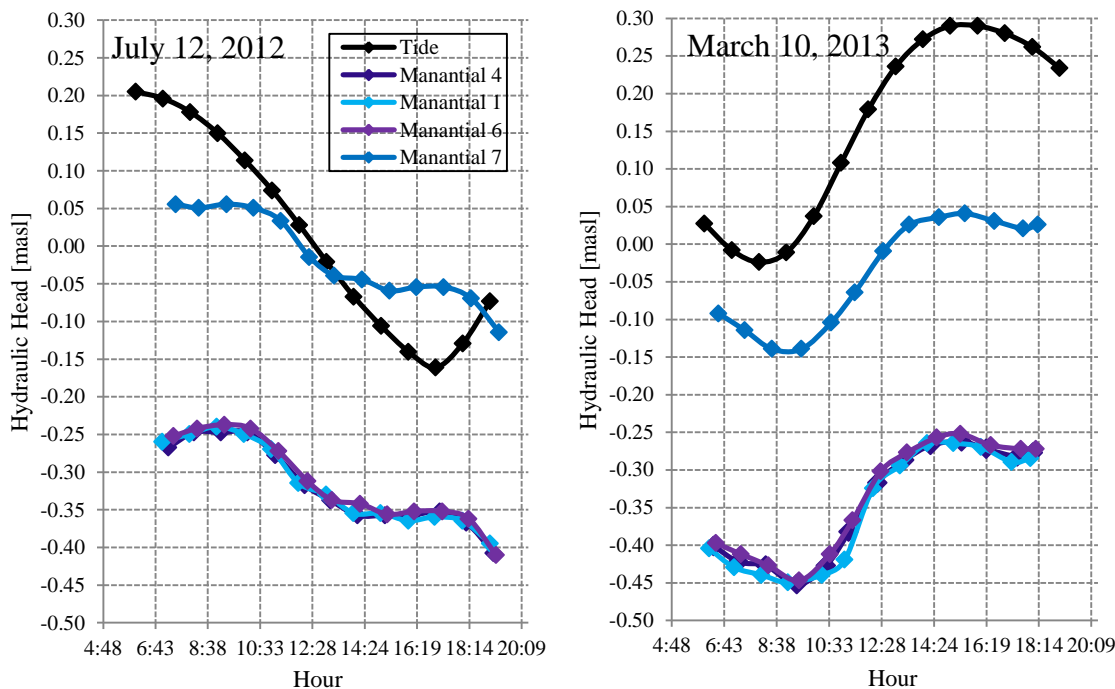


Figure 27: Hydraulic heads during 12 hours measurement and tidal curve, tide data from MAR V1.0 J.I. (Gonzales, 2011).

The graphic outlines that the curves of the tide show an inverse course for the two measurement periods, whose pattern are followed by the flowing hydraulic heads. The measurements of the hydraulic heads in the four artesian wells throughout a day showed, that daily fluctuation can be clearly linked to the influence of the ocean tide. On July 12, 2012 during the rainy season, the moon was one day after entering the last quarter of the lunar cycle before new moon. For March 10, 2013 the moon phase already advanced and the measurements were realized one day before new moon. This difference in the moon phases during the measurements is clearly reflected in the curves of the elevation of groundwater head in the flowing artesian springs as well. There could be observed a difference between the tidal curve direction of the registration period in July 2012 and the measured values during low tide between 14:00 hours and 19:00 hours. The tidal graph decreases to the lowest tide (-0.16 masl) at 17:00 hours and then rises again whereas the water level in the artesian wells remains almost constant till 17:00 and starts decreasing afterwards.

The highest hydraulic heads were determined for Manantial 7, the artesian well of the four monitored springs that is the most distant to the coast (1,127 m) and reaches the highest altitude (-0.204 masl). With exception of this artesian well all hydraulic heads were

registered below sea level. The maximum tidal range over the two measurement campaigns was of 35.7 cm and 31.4 m in July 2012 and March 2013 respectively. The hydraulic head range of the four artesian wells was relatively lower between 15.5 and 19.5 cm. There could be observed little difference between rainy and dry season, apart from the inverse course due to inverse tidal influence. In general the variations of the discharging aquifer were slightly more pronounced in dry season during March even though the variations of the tide were bigger in July.

During the measurement in March 2013 the discharge of the four flowing wells was documented with a flowmeter, unfortunately the device failed in June 2012 before completing the measurements. The depiction of the spring hydrograph over the course of one day in Figure 28 clearly indicates that discharge is conforming to tidal and hydraulic head course as well.

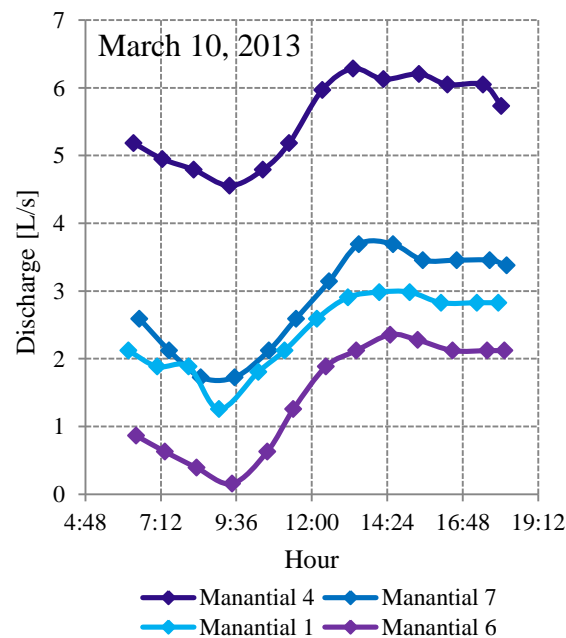


Figure 28: Groundwater discharge variations due to tidal influence.

In Figure 29 a zoom to the data registered during the first three days of operation (17.06.2012-19.06.2012) of the Levelogger Edge in the observation well Baag is shown with the tides for this period. There could be observed that the hydraulic heads reported with the datalogger are following a sine curve but slightly shifted. This discrepancy may be effect of the different measurement intervals as the levelogger registers data only every six hours while tide is given hourly. The maximum variation of the water table within these three days was 3 cm while the tide varied up to 65 cm. Observation well Baag is located at a distance of 8.796 km from the coastline and the influence of tide over the groundwater

flow system is supposed to be still perceptible. Comparing to observation well Dzidzilché located 14.028 km from the coastline (Figure 30) there could be identified higher tidal influence in Baag whereas in Dzidzilché hydraulic heads showed a slightly decreasing trend.

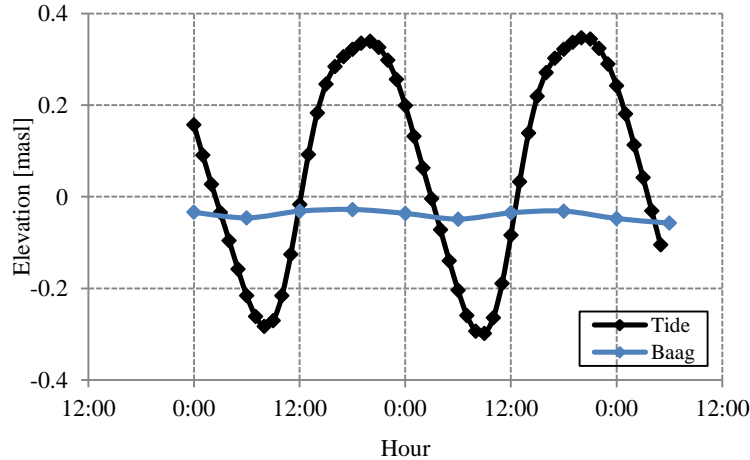


Figure 29: Zoom to three datalogger registration days of water levels in Baag compared to tide.

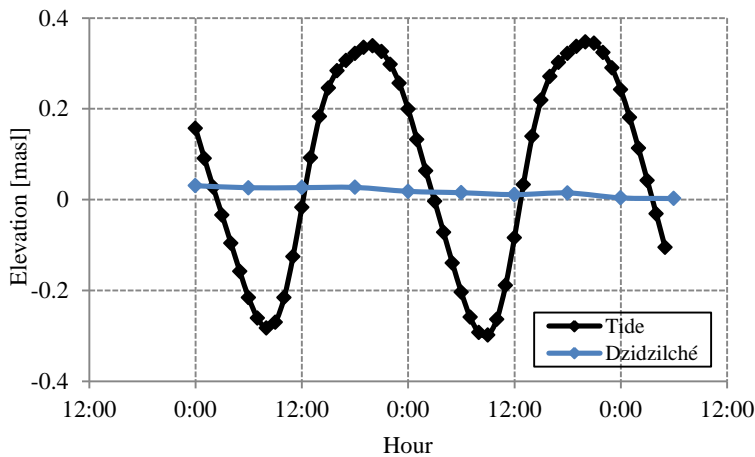


Figure 30: Zoom to three datalogger registration days of water levels in Dzidzilché compared to tide.

According to Beddows et al. (2002) water circulates more than 9 km inland and tidal rise can still be measured at that distance, Villasuso Pino et al. (2011) suggested that tidal influences disappear for a greater distance than 13 km from the coast.

Figure 31 and Figure 32 show the variations of all the measured hydraulic heads for the study area Manantiales and Exbasurero over the whole study period. They include measurements ante (am) and post meridiem (pm) and depict that due to the tidal influence more similar to the curve depicted for July 12, 2012 (Figure 27) the hydraulic heads reached higher elevations in the morning than in the afternoon. Except for the measurement

dates July 9, 2012 and September 6, 2013 were the tide performed inversely, like in March. Generally for all artesian wells from the two study sites similar pattern were observed throughout the study period, ranging the hydraulic heads between 0.29 masl and -0.45 masl.

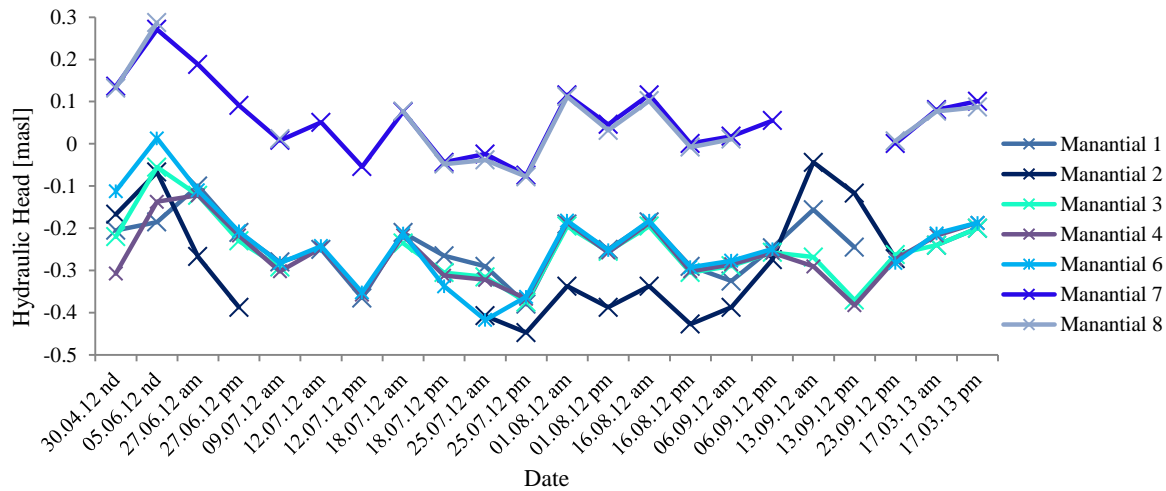


Figure 31: Variation of hydraulic heads in the artesian wells Manantiales during the whole study period.

For the artesian wells 7 and 8, the two furthest from the shoreline, over the whole study period the highest and almost uniform hydraulic heads were registered. The artesian wells 3 and 6 performed very similar but presenting lower hydraulic heads.

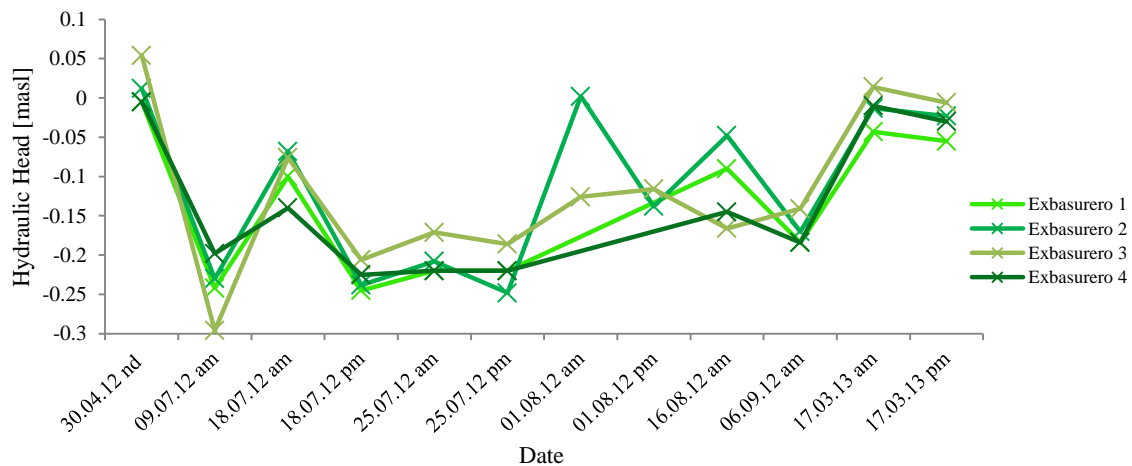


Figure 32: Variation of hydraulic heads in the artesian wells Exbasurero during the whole study period.

Regarding the amounts of precipitation registered in the meteorological station of Progreso and Mérida around the measurement dates there could not be made any solid conclusion about the influence of the natural aquifer recharge due to rainfall on the artesian wells. The water level fluctuation in the confined aquifer is overall strongly governed by the tides.

## 4.2 Hydrochemistry

Regarding the chemistry of the water moving through the hydrological cycle in the study area, the analysis of groundwater, precipitation, coastal lagoon and ocean water is described in the following part.

### 4.2.1 Hydrolab

Water quality profiles (parameter versus depth) were recorded in the observation wells for up to six measurement dates. In this section the results are discussed in general terms focusing on the general pattern as well as on exceptional cases.

Analyzing the electrical conductivity profiles there could not be detected a sharp interface between fresh and saline groundwater but a dynamic transition zone. For the purposes of this thesis, the depth below the water table where the mixing of freshwater and saltwater begins (halocline) was defined as the area where the groundwater starts to exceed  $1,400 \mu\text{S cm}^{-1}$  for electrical conductivity or presents more than  $1,000 \text{ mg L}^{-1}$  of total dissolved solids. In general the electrical conductivity showed a very pronounced rise after reaching values of approximately  $1,400 \mu\text{S cm}^{-1}$  (brackish water) increasing through the whole extent of the mixing zone till reaching concentrations for saltwater. This value corresponds to the permissible limit for drinking water established in the NOM-127-SSA1-1994 (Secretaría de Salud, 2000). Table 13 presents the specifications for some common chemical classification of waters at  $25^\circ\text{C}$ , according to Robinove et al. (1958) and Moody et al. (1988).

Table 13: Common chemical classification of waters reproduced and combined according to Robinove et al. (1958) and Moody et al. (1988).

Class	Electrical conductivity [ $\mu\text{S cm}^{-1}$ ]	Total Dissolved Solids [ $\text{mg L}^{-1}$ ]
Drinking water	< 1,400	< 1,000
Slightly saline/Brackish	1,400 – 4,000	1,000 – 3,000
Moderately saline/Brackish	4,000 – 14,000	3,000 – 10,000
Saline	14,000 – 50,000	10,000 – 35,000
Briny	> 50,000	> 35,000

Some observation wells showed slightly saline water below the water table (Contenedores, Predeco, San Miguel, Sierra Papacal, Cheuman and Dzidzilché) and therefore the steep increase in electrical conductivity due to increased mixing of fresh and saline water was

determined at higher electrical conductivity values ranging between  $1,900 \mu\text{S cm}^{-1}$  and  $4,000 \mu\text{S cm}^{-1}$ . Consequently the horizontally aquifer zoning in the different observation wells was not determined at the same depth and evidently the saltwater influence decreases towards the continent but overall similar behavior was detected in all the observation wells of the study zone.

Figure 33 depicts the vertical zonation of the different aquifer layers schematically.

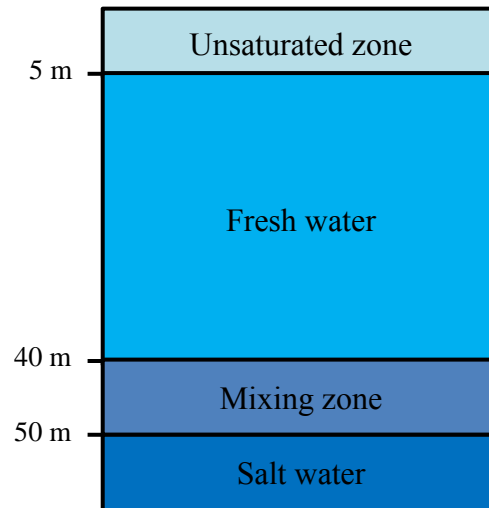


Figure 33: Schematical vertical zonation of the aquifer waters layers with different salt content.

Figure 34 shows the typical quality profiles for the deepest observation well (Matemáticas) located in the center of the study area, giving rise to the identification of the characteristic vertical water zoning of the aquifer. The sudden rise of electrical conductivity reaching values greater than  $2,000 \mu\text{S cm}^{-1}$  at a depth of approximately 40 m below water table indicates the beginning of the fresh-saltwater mixing zone. With increasing depth the conductivity values increased rapidly till reaching saline water concentrations ( $10,000 \mu\text{S cm}^{-1}$ ) at a depth of 46 m and the subjacent layers with values similar to seawater ( $49,000 \mu\text{S cm}^{-1}$ ) at 54 m approximately. The electrical conductivity curves for the different month almost matched perfectly showing very little variation at maximum depth. As the concentration of Total Dissolved Solids (TDS) is directly linked to electrical conductivity, the profile showed the same curve shape. Generally there could be clearly observed that all the measured parameters (Temperature, TDS, pH, ORP, DO) follow similar patterns to those of the electrical conductivity showing an abrupt change at the depth where the beginning of the fresh-saltwater mixing zone is located as well.

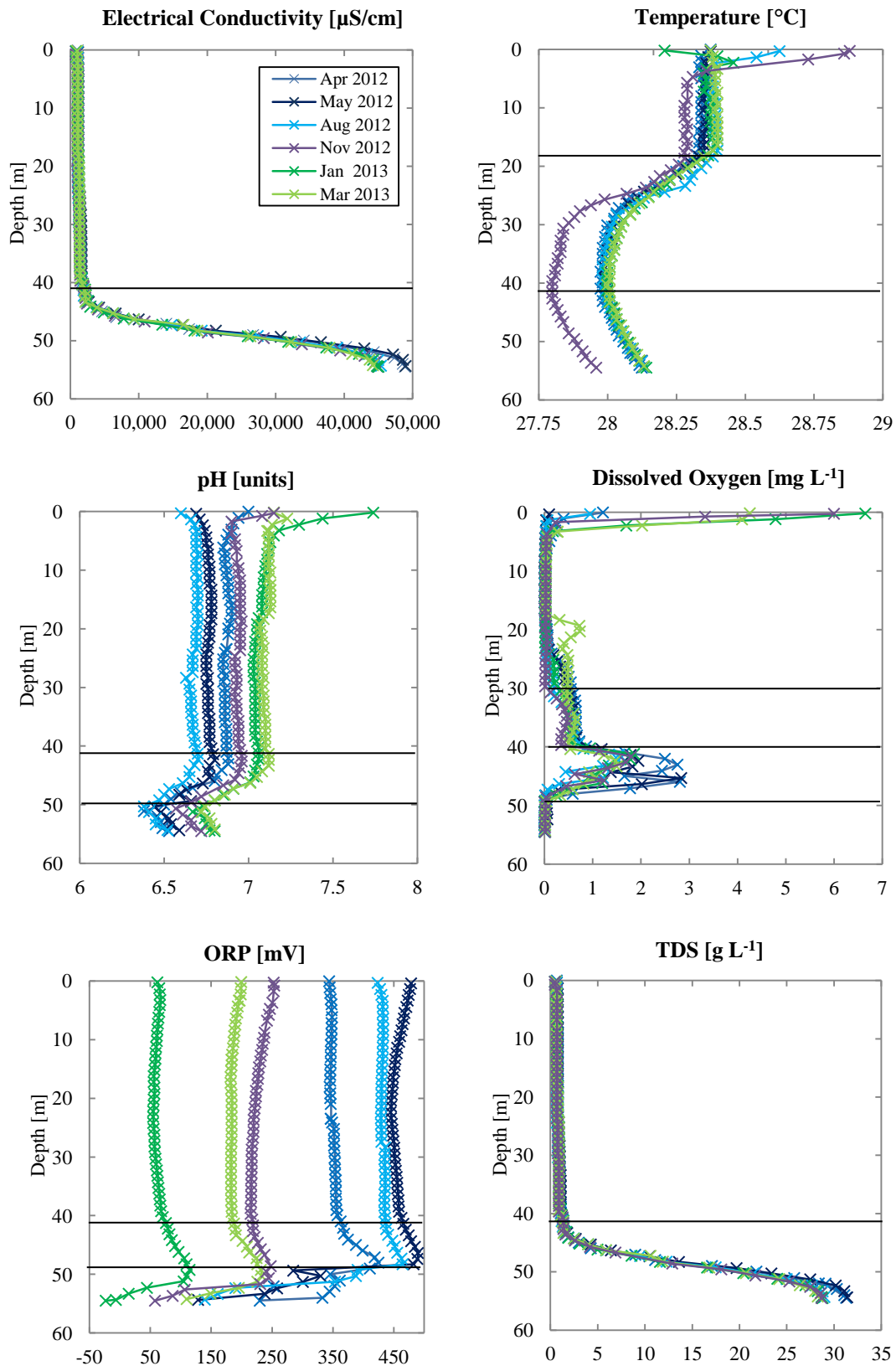


Figure 34: Quality profiles of the observation well Matemáticas.

It should be emphasized that all the registered quality parameters followed similar patterns showing a sudden change of direction at depth of 41 m. Water temperature below the water table (2-3 m) ranged between 28 and 29 °C, reflecting recharge water temperature warmer in August and November and colder in January. Dissolved oxygen and pH are also showed significant temporal changes, suggesting several infiltration events. Temperature below this upper layer (3-20 m) remained almost constant ( $\approx 28.3$  °C). From this depth on the temperature decreased with increasing depth to a minimum value of 27.77 °C at 40 m. In accordance with the beginning of the fresh-saltwater mixing zone the temperature started to increase as the saltwater is warmer. Eliminating some outlier values in January during the measurements in the observation well Matemáticas the pH values varied between 7.15 (March) and 6.6 (August) before reaching the mixing zone. Considering the accuracy of the Hydrolab of 0.2 units this variations were evaluated as relatively low. Reaching the mixing zone at 41 m the pH started to decrease till reaching a depth of 50 m and below this depth the pH increased again: mixing of fresh and saline water, both in equilibrium with calcite produce an undersaturated mixed water, the dissolution of additional calcite causes the pH values to increase. The Oxidation-Reduction Potential (ORP) showed a relatively constant behavior until 40 m where it started to increase till 50 m to reverse again. The lower ORP at high saltwater concentration indicated a decreasing oxidation potential due to very low dissolved oxygen concentration. Over the whole study period the ORP was relatively low and fluctuated in the range of 445 mV (May 2012) and -23 mV (January 2013) reaching negative potential and consequently predominant biochemical reduction processes only in January. The amount of dissolved oxygen near the water table that is in contact with the atmosphere was relatively high achieving values up to 85 % (January) but steeply falling to values near zero within the first 5 m of groundwater. This indicates water circulation and the presence of preferential flow paths. Between 20 m and the mixing zone the DO increased again falling to almost zero at a depth of 50 m where the maximum electrical conductivity was reached. Overall in the described well the seasonal variability was not very significant.

Table 14 represents for all observation wells the mean depth were the fresh-saltwater mixing zone begins, the approximate thickness of this transition zone and the maximum electrical conductivity reached at greatest depth.

Table 14: Depth and thickness of fresh-saltwater mixing zone. a: only in January and March electrical conductivity  $\geq 1,400 \mu\text{S cm}^{-1}$  was registered, b: only in August electrical conductivity  $\geq 1,400 \mu\text{S cm}^{-1}$ , c: the mixing zone continues outside the scope of the observation well.

ID	Well	Coast Distance [m]	Elevation [masl]	Depth [m]	Depth Mixing Zone [m]	Thickness [m]	Maximum EC [ $\mu\text{S cm}^{-1}$ ]	Depth Max. EC [m]
25	Contenedores	5,886	1.268	10.98	7.50	2 <sup>c</sup>	2,861	9.0
3	Baag	8,796	3.680	36.99	17.0	3	5,206	32.0
29	Vázquez	11,143	4.182	20.30			1,144	15.0
24	Predeco	11,330	3.977	25.60	17.0	5	9,565	21.5
2	Granjas Crío	14,013	4.930	42.26	12.0	7	6,191	36.5
5	Dzizilché	14,028	4.492	35.01	2.0	15	8,816	30.5
7	San Miguel	14,670	4.034	40.26	15.0	20	49,269	35.0
28	X'luch	15,084	4.487	24.69	10.0	10 <sup>c</sup>	6,351	20.0
6	Sierra Papacal	16,338	4.233	39.57	16.5	20	42,572	35.5
4	Sac-Nicté	17,142	5.004	51.74	11.0	15	14,907	45.5
27	Hda. Too	19,560	5.888	41.56	22.0	13 <sup>c</sup>	6,134	35.5
23	Komchén	20,089	5.132	36.16	2.0		1,818	31.0
8	Cheuman	22,853	4.560	45.82	21.0	25 <sup>c</sup>	17,631	45.0
1	Megalita	23,000	6.712	51.52	22.0	3	4,410	44.0
26	Mococha	24,603	7.242	49.27	27.0	3	4,397	42.0
16	Tixcuytun	25,668	6.157	56.19	41.0	8	15,698	49.5
22	Matemáticas	26,138	6.407	62.20	40.0	10	49,004	54.5
9	Ucú	26,258	4.781	58.03	22.0	20	35,981	51.0
13	Tecnológico	30,672	7.682	49.90	30.0	10	16,279	43.0
20	Chenku	30,687	6.701	41.24	31.0 <sup>a</sup>		2,012	34.5
10	Anicabil	31,255	7.408	28.08	13.0 <sup>b</sup>		1,416	20.5
14	Sagarpa	32,184	8.097	55.77	30.0	15 <sup>c</sup>	14,707	47.0
18	Chalmuch	32,372	7.189	50.94	22.5	18	14,028	43.5
21	Conagua	33,047	7.593	56.37	32.0	16 <sup>c</sup>	30,159	48.0
12	Bomberos	36,413	8.569	43.30	33.5		2,280	34.5
15	Pacabtun	36,768	8.581	51.72	30.0	15 <sup>c</sup>	11,742	44.0
17	Observatorio	37,174	9.064	53.29	25.0	15	15,555	45.0
19	Acuaparque	38,559	8.443	55.52	42.0	7 <sup>c</sup>	12,646	47.0
11	UDS	42,076	9.795	60.04	35.0	15 <sup>c</sup>	31,864	49.0

Overall the mixing zone showed dissimilar thickness in the observation wells presenting values between 2 and 25 m and varied due to the different months. The maximum electrical conductivity value at well depth is assumed to depend on the seasonality (90 % showed the highest values in the dry season, the majority in May). During May in the majority of the observation wells the water was determined brackish ( $1,400 \mu\text{S cm}^{-1}$ ) below the water table. The overall highest electrical conductivity ( $49,269 \mu\text{S cm}^{-1}$ ) was registered in April 2012 at the bottom (35 m) of the observation well San Miguel located about 15 km from the coast. The water was determined almost briny ( $> 50,000 \mu\text{S cm}^{-1}$ ) and similar to the electrical conductivity measured for ocean water at Chicxulub in April 2012 ( $54,300 \mu\text{S cm}^{-1}$ ).

For some observation wells in the northwestern part (Dzidzilché, Sierra Papacal, San Miguel, Tixcuytun, Komché, Predeco and Contenedores) of the study area the freshwater lens was absent in April and May 2012 as registered conductivity exceeded  $1,400 \mu\text{S cm}^{-1}$  at the water table. On the other hand for the coastal observation well Vázquez during the whole investigation the mixing zone wasn't detected. In the observation well Anicabil electrical conductivity values above the drinking water standard were only reported in August 2012 at 13 m depth.

The electrical conductivity values at the bottom of the observation wells were very different over the entire study zone. In general there could not be identified clear spatial relations neither to coast distance nor elevation or depth of the observation well. Nevertheless analyzing the depth of the mixing zone of four transects almost perpendicular to the coastline from the west to the east of the study area (Chalmuch – Ucú – San Miguel; Unidad Deportiva del Sur – Cheuman – Sierra Papacal; Bomberos – Tecnológico – Predeco – Contenedores and Mococho – Hda. Too – X'Luch) Figure 35 was obtained. There might be recognized a logarithmic correlation between the depth of the mixing zone and coastal distance in three transects and one linear relationship but it has to be emphasized that to make representative assumptions this behavior has to be ascertained including more data for each transect and analyzing by long-term monitoring.

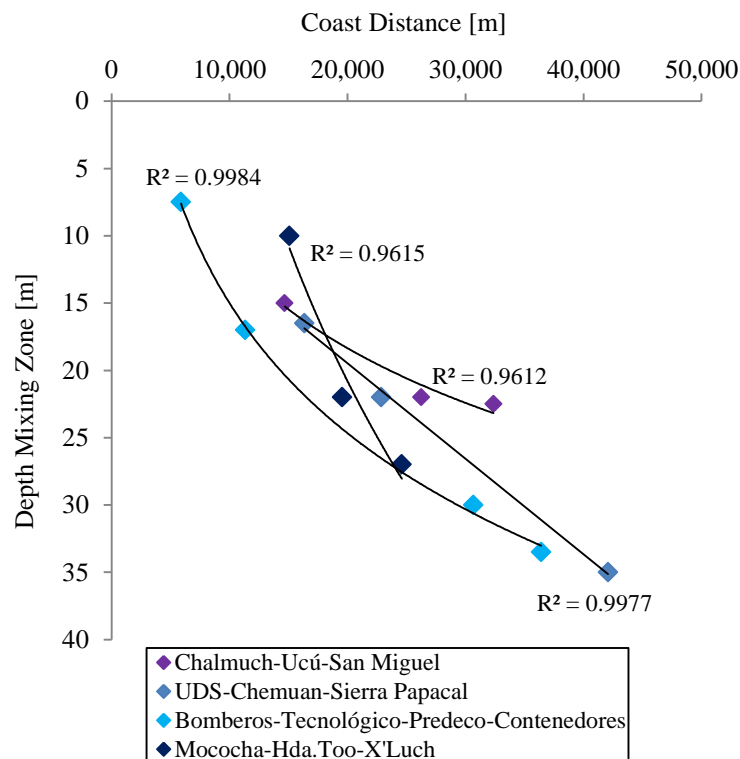


Figure 35: Relation between mixing zone depth and coast distance of four transects.

Figure 36 depicts selected conductivity profiles for the observation wells Anicabil, Bomberos, Cheuman, Dzidzilché, Ucú and Sierra Papacal, the majority located outside the town center in the western part of the study area, showing behavior that worth being visualized. Overall the obtained electrical conductivity profiles did not show pronounced variations between the different months of the study period and a uniform trend or relationship with respect to meteorological pattern could not be identified from the Hydrolab measurements.

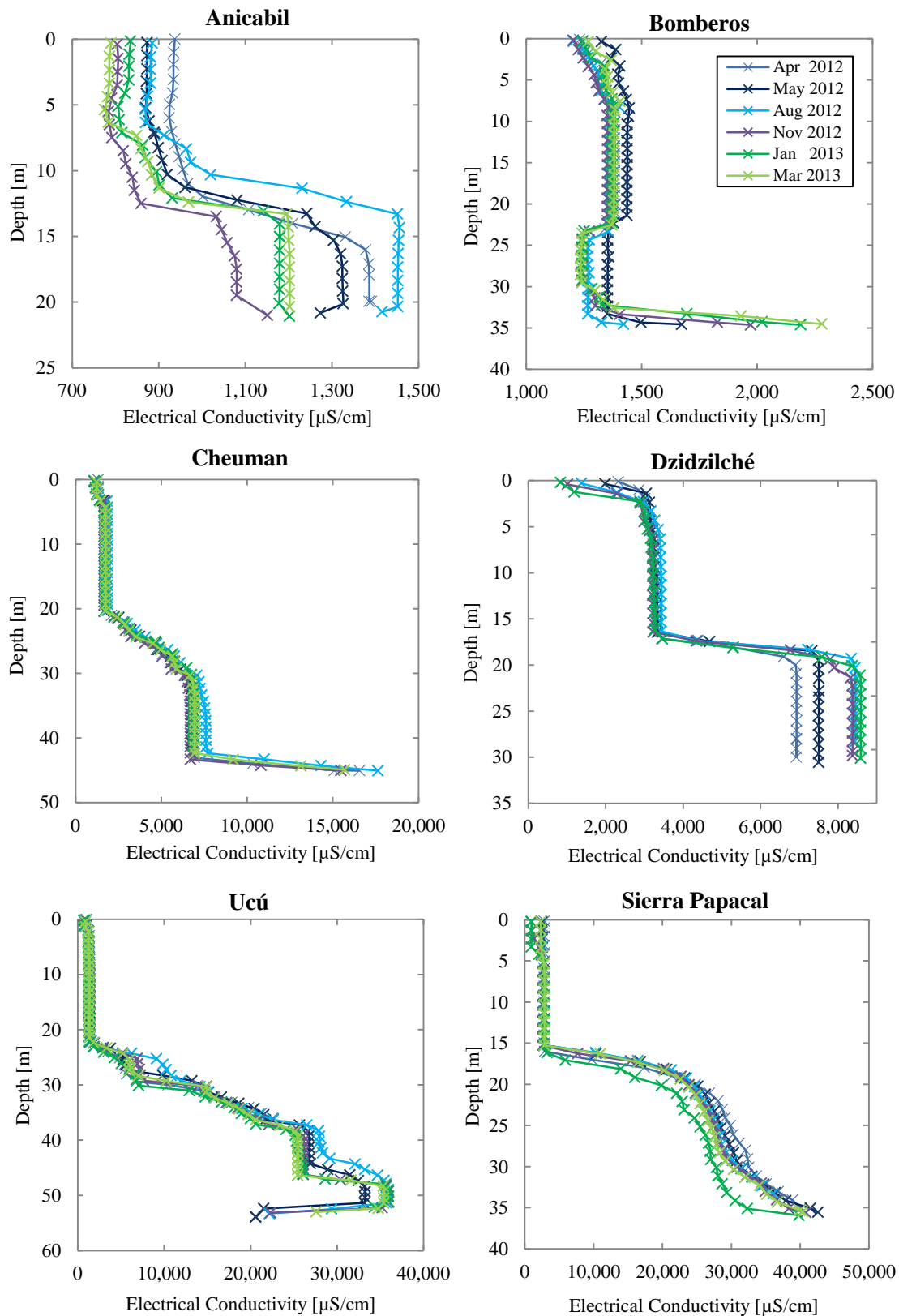


Figure 36: Electrical conductivity profiles for six observation wells.

Regarding the Hydrolab measurements in the artesian wells, it could be identified the same pattern for the electrical conductivity in all seven wells including all measurements over the study period from April 2012 to March 2013. Figure 37 shows the electrical conductivity of the measurements carried out with the Hydrolab ante merediam. The electrical conductivity slightly increased from the artesian well Manantial 1 to Manantial 6 (from the coast to the continent) and decreased between the artesian wells Manantial 6 and Manantial 8. The highest electrical conductivities for all artesian wells were reported for August 1, 2012, reaching Manantial 6 the overall highest conductivity of  $4,614 \mu\text{S cm}^{-1}$ . For the measurements in March 2013 during the dry period the lowest electrical conductivities were reported  $2,830$  and  $2,980 \mu\text{S cm}^{-1}$ , having in mind that no data were obtained from October 2012 to February 2013.

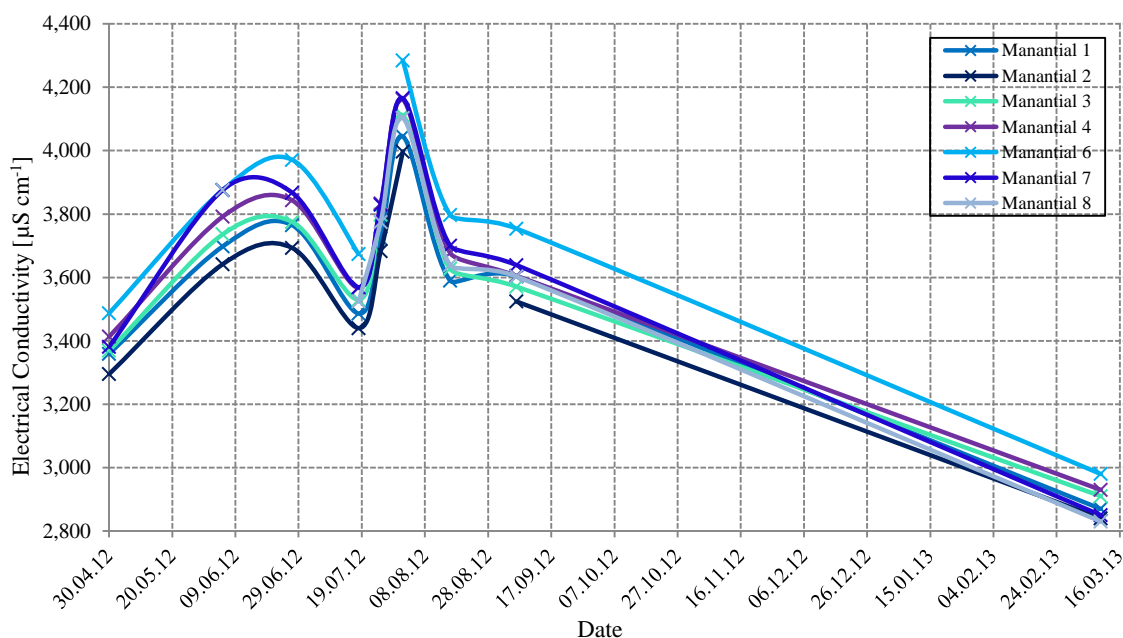


Figure 37: Evolution of the electrical conductivity measured with the Hydrolab in the artesian wells during the investigation period.

The electrical conductivity measured in the lagoon water around the discharging artesian wells reached values up to  $92,610 \mu\text{S cm}^{-1}$  higher than the electrical conductivity determined for seawater at Chicxulub in April 2012 ( $54,300 \mu\text{S cm}^{-1}$ ).

### 4.2.2 Sampling

For the more exhaustive water quality analysis two sampling campaigns (September 2012 and February 2013) were analyzed.

For groundwater, the ion balance error of the analytical results should not exceed  $\pm 5\%$ , only if the total dissolved solids (TDS) value is reported less than  $5 \text{ mg L}^{-1}$  higher errors are acceptable (UNEP/WHO, 1996) but this was not the case in the present analysis. Figure 38 shows the results of the major ion balances for the two sampling campaigns in September and February resulting about 4 % and 1/3 of the samples out of the range of 5 % respectively. Consequently totally 17.5 % of the sample results did not fall within the analytical range being  $> 5\%$  but  $< 8\%$  and let suspect errors of analytical technique or transcription of the data, nevertheless all data were considered. A detailed table of the analytical results of the laboratory analysis with cation and anion concentrations and respective errors can be found in the Appendix 2 to 5.

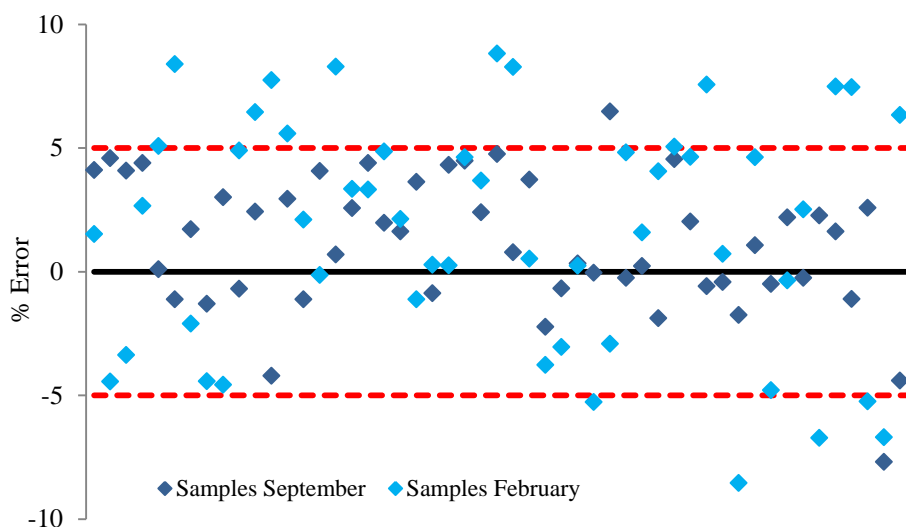


Figure 38: Errors resulting from the major ion balance of all water samples.

As samples were taken at different depth and classified in (i) shallow ( $< 20 \text{ m}$ ), (ii) intermediate ( $\geq 20 < 30 \text{ m}$ ) and deep samples ( $\geq 30 \text{ m}$ ) in the following section the results of the different sample classes are analyzed.

Discrepancies of up to 48 % were detected between the electrical conductivity values that have been determined in situ with the Hydrolab and in the laboratory. This can probably be attributed to the fact that during the sampling process with the sampling bottle water mixing inside the well was produced and overall the extracted deep samples did not always

correspond to the same water as analyzed in situ. All shallow samples (< 20 m) that were outside norm limit for sodium and chloride also presented high electrical conductivity so that is appears safe to assume, that sea water mixing causes the high NaCl values already in the shallow water horizons of the aquifer.

In general 50 % of the shallow samples that were taken in the majority within a distance of 16 km from the coastline, already presented brackish groundwater at shallow depth while the other half were classified as fresh water. Surprisingly three of the five coast nearest wells (Baag, Crío and Vázquez) presented relatively low results for electrical conductivity and Total Dissolved Solids (TDS) for both sampling campaigns, providing fresh water at a sampling depth of 10 m.

Only for three of the observation wells where the intermediate samples were taken, brackish water ( $> 1400 \mu\text{S cm}^{-1}$ ) was detected, the remaining intermediate samples showed fresh water and overall fair water quality, disregarding the bacteriological analysis. Intermediate samples classified as brackish water were obtained from the observation well Granjas Crío for the two sampling campaigns, Tecnológico (September) and Chalmuch (February).

In general the electrical conductivity was slightly higher during September sampling than in February. Table 15 shows the results of obtained electrical conductivity, TDS and the standard ions sodium ( $\text{Na}^+$ ) and chloride ( $\text{Cl}^-$ ) of the shallow samples. The numbers represented in bold letters indicate concentrations above the Mexican drinking water standard NOM-127-SSA1-1994 (Secretaría de Salud, 2000).

Table 15: Electrical conductivity, TDS, sodium and chloride for the shallow samples during both sampling campaigns. In bold are values above drinking water standard.

Well	Sampling Date	Sampling Depth [m]	Coast Distance [m]	EC (Lab) [ $\mu\text{S cm}^{-1}$ ]	TDS [ $\text{mg L}^{-1}$ ]	$\text{Na}^+$ [ $\text{mg L}^{-1}$ ]	$\text{Cl}^-$ [ $\text{mg L}^{-1}$ ]
Contenedores	26.09.2012	6	5,886	1,850	<b>1,258</b>	193	<b>372</b>
Baag	21.09.2012	10	8,796	1,148	754	121	115
Vázquez	02.10.2012	10	11,143	1,047	722	85	99
Predeco	26.09.2012	15	11,330	1,736	<b>1,198</b>	151	<b>255</b>
Granjas Crío	21.09.2012	10	14,013	1,148	796	95	159
Dzidzilché	26.09.2012	10	14,028	2,700	<b>1,811</b>	<b>314</b>	<b>469</b>
San Miguel	22.09.2012	10	14,670	2,840	<b>2,100</b>	<b>370</b>	<b>667</b>
X'luch	02.10.2012	15	15,084	3,310	<b>2,416</b>	<b>347</b>	<b>644</b>
Sierra Papacal	22.09.2012	10	16,338	2,570	<b>1,850</b>	<b>303</b>	<b>567</b>
Cheuman	22.09.2012	10	22,853	1,358	892	131	156
Ucú	24.09.2012	10	26,258	1,323	965	165	194
Anicabil	24.09.2012	10	31,255	836	620	52	76
Contenedores	16.02.2013	6	5,886	1,768	870	<b>221</b>	<b>345</b>
Baag	14.02.2013	10	8,796	1,110	551	83	144
Vázquez	14.02.2013	10	11,143	1,039	521	68	117
Predeco	14.02.2013	15	11,330	1,603	801	164	<b>284</b>
Granjas Crío	14.02.2013	10	14,013	1,108	557	80	117
Dzidzilché	16.02.2013	10	14,028	2,720	<b>1,360</b>	<b>402</b>	<b>595</b>
San Miguel	16.02.2013	10	14,670	2,790	<b>1,420</b>	<b>627</b>	<b>705</b>
X'luch	14.02.2013	15	15,084	2,150	<b>1,070</b>	<b>264</b>	<b>433</b>
Sierra Papacal	16.02.2013	10	16,338	2,400	<b>1,170</b>	<b>331</b>	<b>518</b>
Cheuman	16.02.2013	10	22,853	1,404	703	155	236
Ucú	16.02.2013	10	26,258	1,304	644	117	<b>284</b>
Anicabil	15.02.2013	10	31,255	830	414	54	55
Limit [ $\text{mg L}^{-1}$ ]					1,000	200	250

From Table 15 results indicate that 37 % of the shallow samples exceeded the drinking water standard for TDS, 37 % for  $\text{Na}^+$  and 54 % for  $\text{Cl}^-$ . For the intermediate samples resulted that 19 % for TDS, 11 % for  $\text{Na}^+$  and  $\text{Cl}^-$  did not comply with the norm (Table 16). Water from the deep samples as well as the samples from the artesian wells (Manantiales and Exbasurero) showed very high amounts of TDS,  $\text{Na}^+$  and  $\text{Cl}^-$  consequently all the samples exceeded the drinking water standard. The deep sample obtained from the observation well Tixcuytun in February 2013 showed surprisingly low amounts of calcium and sodium ions at a sampling depth of 45 m and consequently the lowest hardness regarding deep samples ( $394 \text{ mg L}^{-1}$  of  $\text{CaCO}_3$ ).

Table 16: Electrical conductivity, TDS, sodium and chloride for the intermediate samples during both sampling campaigns. In bold are values above drinking water standard.

Well	Sampling Date	Sampling Depth [m]	Coast Distance [m]	EC (Lab) [ $\mu\text{S cm}^{-1}$ ]	TDS [ $\text{mg L}^{-1}$ ]	Na <sup>+</sup> [ $\text{mg L}^{-1}$ ]	Cl <sup>-</sup> [ $\text{mg L}^{-1}$ ]
Acuaparque	24.09.2012	25	38,559	1,006	734	56	159
Bomberos	25.09.2012	25	36,413	1,324	894	122	143
Chalmuch	24.09.2012	25	32,372	1,317	1,000	99	160
Chenku	25.09.2012	20	30,687	1,207	796	122	152
Conagua	25.09.2012	20	33,047	1,097	750	89	99
Granjas Crio	21.09.2012	25	14,013	5,270	<b>3,795</b>	<b>651</b>	<b>1,471</b>
Komchén	26.09.2012	20	20,089	1,508	<b>1,085</b>	128	241
Matematicas	02.10.2012	20	26,138	1,086	784	71	119
Megalita	21.09.2012	20	23,000	1,273	850	86	172
Mococha	02.10.2012	20	24,603	1,138	785	95	123
Observatorio	24.09.2012	20	37,174	1,302	<b>1,021</b>	81	143
Pacabtun	24.09.2012	20	36,768	852	579	68	89
Sac-Nicte	23.09.2012	20	17,142	1,687	<b>1,214</b>	121	230
Sagarpa	25.09.2012	20	32,184	1,159	754	120	171
Tecnológico	25.09.2012	20	30,672	2,140	<b>1,390</b>	<b>250</b>	<b>464</b>
Tixcuytun	25.09.2012	20	25,668	1,291	884	146	163
Hda. Too	02.10.2012	20	19,560	1,265	872	124	183
UDS	24.09.2012	20	42,076	1,382	967	139	155
Acuaparque	15.02.2013	25	38,559	1,013	511	75	137
Bomberos	19.02.2013	25	36,413	1,253	632	111	147
Chalmuch	15.02.2013	25	32,372	2,430	<b>1,210</b>	<b>342</b>	<b>549</b>
Chenku	19.02.2013	20	30,687	1,194	592	115	158
Conagua	19.02.2013	20	33,047	1,082	538	90	116
Granjas Crio	14.02.2013	25	14,013	4,520	<b>2,210</b>	<b>577</b>	<b>1,468</b>
Komchén	14.02.2013	20	20,089	1,458	725	144	230
Matematicas	15.02.2013	20	26,138	1,213	606	104	162
Megalita	14.02.2013	20	23,000	1,166	580	96	172
Mococha	14.02.2013	20	24,603	1,045	527	103	133
Observatorio	15.02.2013	20	37,174	1,248	627	115	192
Pacabtun	15.02.2013	20	36,768	925	462	70	104
Sac-Nicte	14.02.2013	20	17,142	1,330	661	121	189
Sagarpa	15.02.2013	20	32,184	1,174	584	101	126
Tecnológico	19.02.2013	20	30,672	1,112	555	105	147
Tixcuytun	19.02.2013	20	25,668	1,184	591	97	137
Hda. Too	14.02.2013	20	19,560	1,256	626	108	158
UDS	15.02.2013	20	42,076	1,335	665	119	179
Limit [ $\text{mg L}^{-1}$ ]					1,000	200	250

Based on the commonly used classification by Sawyer (1960) the water samples were classified by their hardness according to Table 17.

Table 17: Water classification according to hardness, reproduced after Sawyer (1960).

CaCO <sub>3</sub> equivalent [mg L <sup>-1</sup> ]	Classification
< 75	Soft
75 – 150	Moderately hard
150 – 300	Hard
> 300	Very Hard

All groundwater samples resulted hard (9%) or very hard (91%) ranging between 228 and 4624 mg L<sup>-1</sup> of CaCO<sub>3</sub>. The recollected precipitation water was classified as soft for the sample obtained in Progreso in January 2012 and moderately hard for the remaining samples. In general the discharging water from the artesian springs had lower hardness than the deep groundwater samples. Overall the hardness increased with depth and the discharging water of the flowing artesian wells showed values in the range of those determined at the observation wells for shallow and intermediate depth. Table 18 summarizes the ranges of alkalinity, hardness and pH for the different sample classes that were determined ex-situ. The ranges of hardness and alkalinity were higher during rainy season than dry season, while the pH performed inversely. However the groundwater samples from September showed less variability between the observation wells regarding both, alkalinity and pH (laboratory).

According to the NOM-127-SSA1-1994 (Secretaría de Salud, 2000) the given limit value for hardness is 500 mg L<sup>-1</sup>. Almost 30% of the shallow samples exceeded this limit while only 8% of the intermediate samples showed higher values (Table 18).

Table 18: Alkalinity, hardness and pH for the different sample classes and sampling campaigns. a: the sampling date was 13.04.2012, b: the pH was measured in-situ.

Sample Location	Hardness	September	Alkalinity	Hardness	February	Alkalinity
	CaCO <sub>3</sub> [mg L <sup>-1</sup> ]	pH	CaCO <sub>3</sub> [mg L <sup>-1</sup> ]	CaCO <sub>3</sub> [mg L <sup>-1</sup> ]	pH	CaCO <sub>3</sub> [mg L <sup>-1</sup> ]
Shallow wells	302–838	6.97–7.64	300–509	243–512	7.07–7.98	126–385
Intermediate wells	275–1182	7.20–7.94	232–382	245–1453	7.14–7.92	223–385
Deep wells	1026–4624	6.47–7.27	248–352	228–3034	7.01–8.19	116–399
Artesian wells	589–712	7.19–7.52	344–410	470–586	7.32–8.20	223–404
Precipitation	25–98	4.24–7.17	39	82–94	4.88–6.99	58–77
Lagoon	682	7.54	394	249	7.51	223
Ocean	7161 <sup>a</sup>	8.01 <sup>b</sup>	251			

The higher amount of water samples exceeding the hardness limit from shallow depth is very probably related to the closer location of the wells to the ocean. Totally about 44 % of the groundwater samples (including the flowing artesian wells) counted with hardness  $> 500$  mg  $L^{-1}$  and were also regarded as brackish water.

The Piper diagrams were used to depict the evolution and changes in the composition of main ions during wet and dry seasons within the study zone. There could be identified seven different water types whose proportions for the shallow and intermediate samples are shown in Figure 39 and 40 respectively.

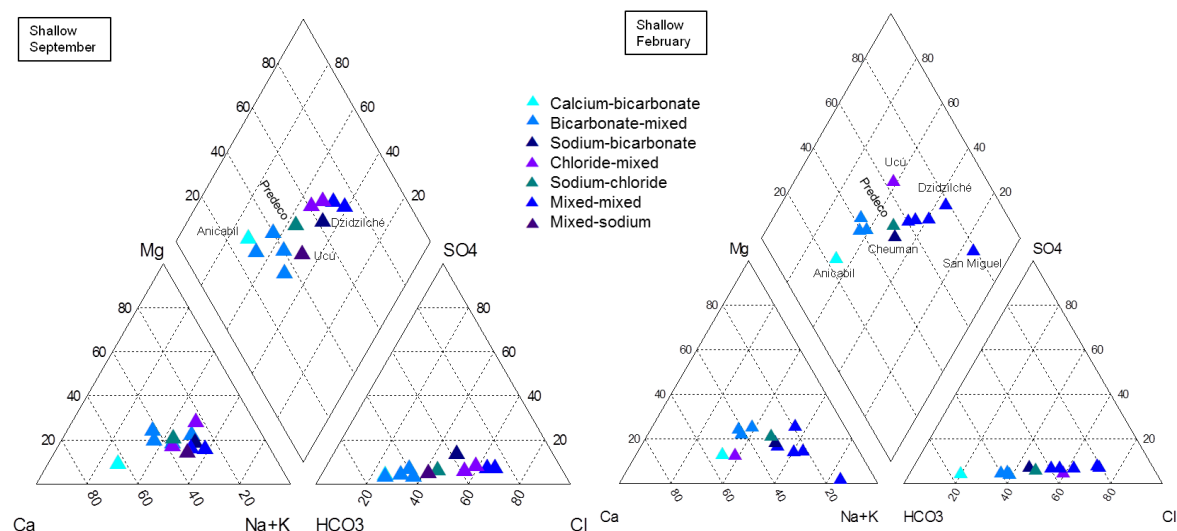


Figure 39: Water types of the shallow samples from September 2012 and February 2013.

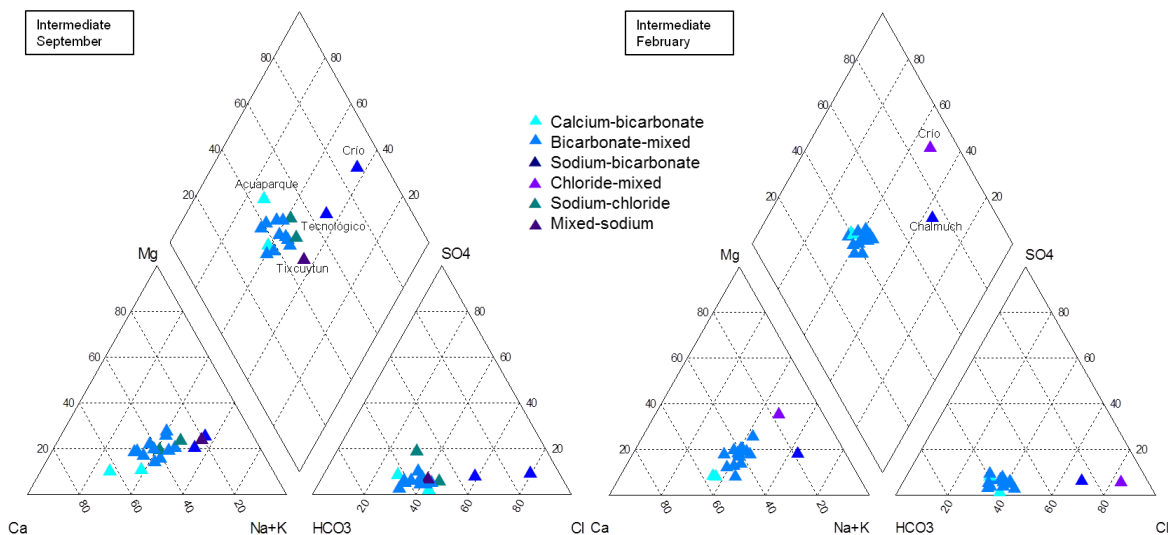


Figure 40: Water types of the intermediate samples from September 2012 and February 2013.

In the dry season less precipitation water percolates through the subsoil that could dissolve minerals that reach groundwater, the element concentration of the majority of the samples was very similar. During September the highest amount of rainfall was registered for the meteorological observatory in Mérida and is supposed to enhance chemical processes occurring between mixing waters and soil or rocks before the precipitation recharges the aquifer that could lead to the diversification of the samples. The composition of the intermediate samples resulted very homogeneous for the February sampling campaign (with the exception of the wells Granjas Crío and Chalmuch) indicating that they are well mixed. Less homogeneity of water composition in the September samples suggests the stronger influence of recharge during rainy season.

In the Piper diagram of the deep samples (Figure 41, left) only sodium-chloride water types are identified for the two sampling campaigns, as well as for the samples from the artesian wells (Figure 41, right). Between the precipitation samples from the meteorological station in Progreso and the ones from Mérida significant differences were identified. Mérida precipitation samples were classified as mixed-calcium water type for both sampling campaigns whereas the samples recollected closed to the port city Progreso were of chloride-mixed (September 2012) and mixed-mixed type (February 2013). The samples from Progreso were richer in sodium-chloride and more similar to the samples from the artesian wells, this is related more than likely to the proximity to the shoreline.

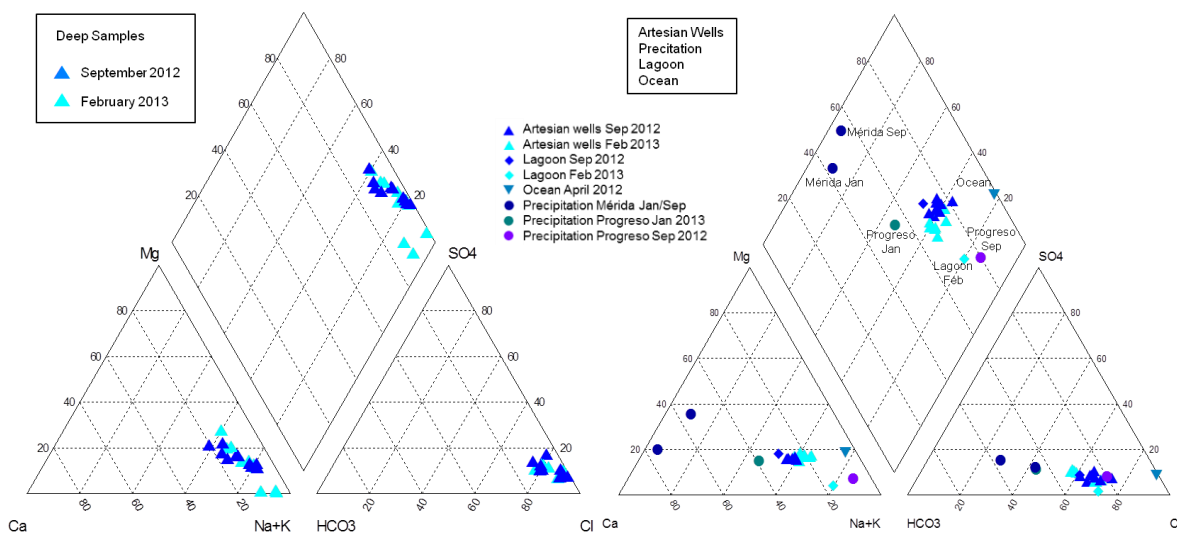


Figure 41: Water types of the deep samples (left) and the samples from artesian wells, precipitation, lagoon and ocean water (right).

There should be emphasized that the meteorological data obtained for the month of the sampling campaigns evidenced the two different climate subtypes, receiving September the highest precipitation amount for Mérida while in Progreso was registered much fewer rainfall. During the movement of air masses inland the aerosol concentrations of the atmosphere, that predetermine the composition of precipitation water, are fractionated and fundamentally changed. At the coastal site (Progreso) the composition of the precipitation samples was comparable to diluted sea water. Moving inland the air mass absorbs dust and gases, modifying the composition. As in the Mérida precipitation samples calcite predominated, it is assumed, that limestone particles, probably derived from the quarries, were washed out of the air.

In Figure 42 the percentages of the different water types documented in the two sampling campaigns can be appreciated.

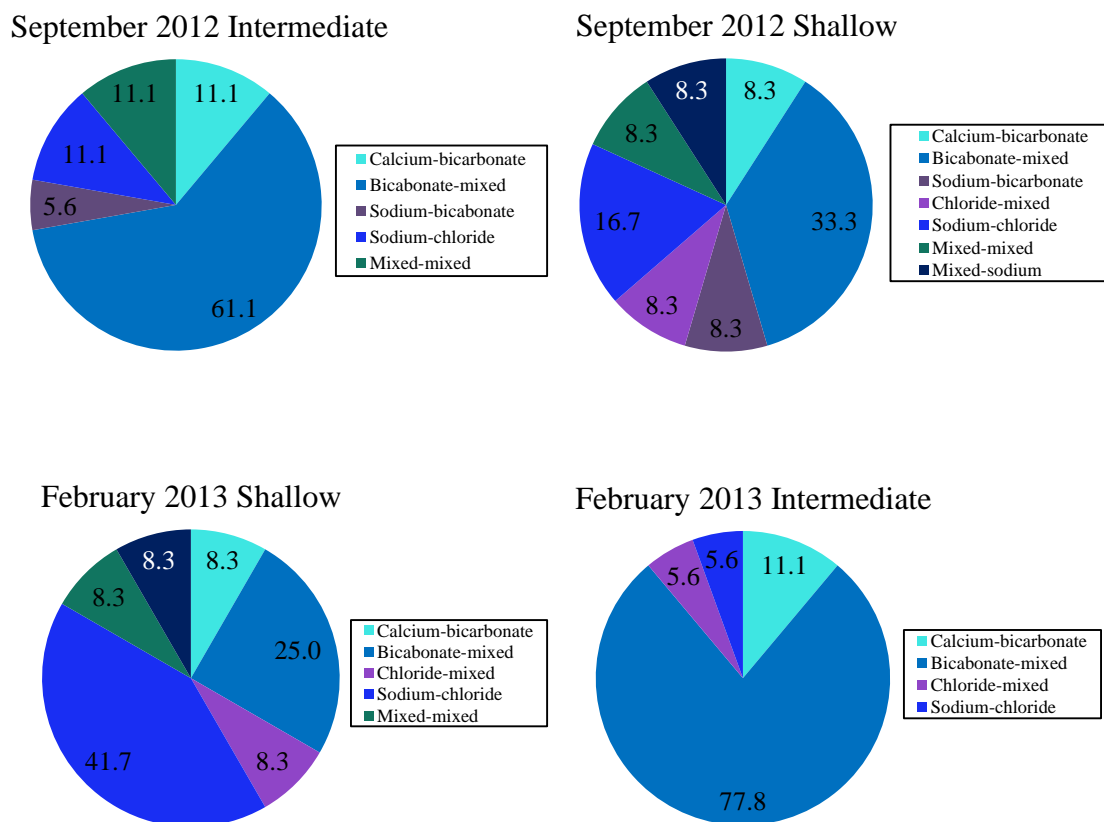


Figure 42: Percentages of different water types for the shallow and intermediate water samples.

Up to seven water types could be distinguished in the shallow samples. The predominant water type in September 2012 was bicarbonate-mixed ( $\text{HCO}_3\text{-Na-Ca-Cl}$ ) suggesting that dissolution of carbonates and mixing with saline water are dominating water chemistry. In February 2013 the NaCl-type had the highest percentage, reflecting the dominant effect of mixture with saline water, while the rest of the families remained constant. The intermediate samples in September 2012 were also dominated by the bicarbonate-mixed type, even increasing the percentage in February 2013. Furthermore the sodium-bicarbonate type ( $\text{Na-HCO}_3$ ) and the mixed type ( $\text{Na-Ca-Mg-Cl-HCO}_3$ ) were only registered in September while in February the chloride-mixed type ( $\text{Ca-Na-Mg-HCO}_3\text{-Cl}$ ) appeared. The water type with calcium bicarbonate ( $\text{Ca-HCO}_3$ ) as dominant chemical compound was considered as those representing the freshwater lens. Its proportion was higher in the more continental intermediate samples (11 %) than in the shallow but more coastal samples and did not change between the different seasons. This water type could be evidenced in the shallow samples only for the observation wells Anicabil and Baag that are located in the central-western part and in the north of the study area respectively. For the intermediate samples the calcium bicarbonate type was detected in the observation wells Acuaparque and Conagua for both sampling campaigns.

In Table 19 the percentage of samples with concentrations above Mexico's drinking water standards (NOM-127-SSA1-1994) are represented.

Table 19: Percentage of samples with concentrations above Mexico's drinking water standard.

Parameters exceeded	Limit [ $\text{mg L}^{-1}$ ]	Shallow [%]	Intermediate [%]	Deep [%]	Artesian Wells [%]	Lagoon [%]
TDS	1000	41.7	19.4	100	100	100
Hardness	500	29.2	8.3	90	87.5	50
$\text{Na}^+$	200	37.5	11.1	100	100	100
$\text{Cl}^-$	250	54.2	11.1	100	100	100
$\text{N-NO}_3$	10		19.4			
$\text{SO}_4^{=}$	400			75		
As	0.05			5		
Hg	0.001			60	18.7	50
Pb	0.01	4.2		35		

High concentrations of the heavy metals, mercury and lead (Hg, Pb) and metalloid arsenic (As) were identified in several samples. High lead concentrations ( $0.018 \text{ mg L}^{-1}$ ) above the drinking water standard were detected in one of the shallow samples from Dzidzilché (February 2013) and in the deep water samples of the observation wells Matemáticas,

Pacabtun, Sac-Nicté, San Miguel, Sierra Papacal, Ucu and Unidad Deportiva del Sur, the majority in the February campaign as well (up to  $0.068 \text{ mg L}^{-1}$  for Unidad Deportiva del Sur in February 2013). In the deep September 2012 sample from San Miguel  $0.068 \text{ mg L}^{-1}$  of arsenic were reported. Excess in mercury occurred in twelve of the deep samples (September and February) as well as in the two samples from the artesian wells Exbasurero 1 and 4, for Manantial 2 and for the lagoon water in February 2013.

High  $\text{N-NO}_3$  concentrations above Mexico's drinking water standard ( $10 \text{ mg L}^{-1}$ ) were identified in four observation wells (intermediate samples); Bomberos in downtown Mérida city showed the highest concentration ( $20.8 \text{ mg L}^{-1}$ ), probably indicating the effect of induced recharge with wastewater in the urban area. High sulfate concentrations above the drinking water standard ( $400 \text{ mg L}^{-1}$ ), ranging between 433 and  $1969 \text{ mg L}^{-1}$  were detected in almost all deep samples for one or both of the sampling campaigns with the exception of the observation well Pacabtún.

Additionally a bacteriological analysis was done for September 2012 water samples. The identification of colony forming units (CFU) for all observation wells at all sampled depth was evidenced. The total coliforms ranged between 20 and 5800 CFU while the amount of fecal coliform bacteria lied between 10 and 5300 CFU being Unidad Deportiva del Sur (47 m) the observation well with the lowest bacterial load and Cheuman (10 m) the highest polluted. Overall the shallow samples showed higher amounts of microbial contaminants than the deeper ones indicating contamination by sewage infiltration from shallow septic tanks. The concentration values of coliforms for all samples can be found in Appendix 6.

Disregarding the bacterial contamination; about 50 % of the intermediate samples showed good water quality. Without including the bacteriological analysis totally 54 % of the 24 shallow samples from the two sampling campaigns exceeded at least for one parameter the drinking water standard indicated in norm NOM-127-SSA1-1994 and should be classified as unsuitable for human consumption. For the intermediate samples 36 % of the 36 samples exceeded the limit for at least one parameter. For the majority of the shallow and intermediate samples (42 % and 11 % respectively) however there were identified three or more (up to five) chemical parameters out of the norm.

As for all the deep samples important mixture with saline water was detected, deep groundwater resources are not useful from this perspective alone. The presence of coliforms leads to the unsuitability of all water samples. Without considering the bacteria indicator some of the fresh water samples could have been of good to fair quality. The following tables 20-23 show the samples with parameters that exceeded the Mexican drinking water standard. The element concentrations of the samples can be found in Appendix 7 to 10.

Table 20: Shallow samples, parameters exceeding the Mexican drinking water standards. February samples were not analyzed regarding coliform bacteria.

Well	Samle date	Sample Depth [m]	Parameters exceeded
Anicabil	24.09.2012	10	Coliforms
Baag	21.09.2012	10	Coliforms
Cheuman	22.09.2012	10	Coliforms
Contenedores	26.09.2012	6	Cl <sup>-</sup> , TDS, Hardness, Coliforms
Granjas Crio	21.09.2012	10	Coliforms
Dzidzilché	26.09.2012	10	Na <sup>+</sup> , Cl <sup>-</sup> , TDS, Hardness, Coliforms
Predeco	26.09.2012	15	Na <sup>+</sup> , Cl <sup>-</sup> , TDS, Hardness, Coliforms
San Miguel	22.09.2012	10	Na <sup>+</sup> , Cl <sup>-</sup> , TDS, Hardness, Coliforms
Sierra Papacal	22.09.2012	10	Na <sup>+</sup> , Cl <sup>-</sup> , TDS, Hardness, Coliforms
Ucú	24.09.2012	10	Coliforms
Vazquez	02.10.2012	10	Coliforms
X'luch	02.10.2012	15	Na <sup>+</sup> , Cl <sup>-</sup> , TDS, Hardness, Coliforms
Contenedores	16.02.2013	6	Na <sup>+</sup> , Cl <sup>-</sup>
Dzidzilché	16.02.2013	10	Na <sup>+</sup> , Cl <sup>-</sup> , Pb, TDS, Hardness
Predeco	14.02.2013	15	Na <sup>+</sup> , Cl <sup>-</sup>
San Miguel	16.02.2013	10	Na <sup>+</sup> , Cl <sup>-</sup> , TDS
Sierra Papacal	16.02.2013	10	Na <sup>+</sup> , Cl <sup>-</sup> , TDS
Ucú	16.02.2013	10	Cl <sup>-</sup>
X'luch	14.02.2013	15	Na <sup>+</sup> , Cl <sup>-</sup> , TDS

Table 21: Intermediate samples, parameters exceeding the Mexican drinking water standards. February samples were not analyzed regarding coliform bacteria.

Well	Samle date	Sample Depth [m]	Parameters exceeded
Acuaparque	24.09.2012	25	Coliforms
Bomberos	25.09.2012	25	Coliforms
Chalmuch	24.09.2012	25	N-NO <sub>3</sub> , Coliforms
Chenku	25.09.2012	20	Coliforms
Conagua	25.09.2012	20	Coliforms
Granjas Crío	21.09.2012	25	Na <sup>+</sup> , Cl <sup>-</sup> , TDS, Hardness, Coliforms
Komchen	26.09.2012	20	TDS, Coliforms
Matemáticas	02.10.2012	20	N-NO <sub>3</sub> , Coliforms
Megalita	21.09.2012	20	Coliforms
Mococha	02.10.2012	20	Coliforms
Observatorio	24.09.2012	20	TDS, Coliforms
Pacabtun	24.09.2012	20	N-NO <sub>3</sub> , Coliforms
Sac-Nicte	23.09.2012	20	TDS, Coliforms
Sagarpa	25.09.2012	20	Coliforms
Tecnológico	25.09.2012	20	Na <sup>+</sup> , Cl <sup>-</sup> , TDS, Hardness, Coliforms
Tixcuytun	25.09.2012	20	Coliforms
Hda. Too	02.10.2012	20	Coliforms
UDS	24.09.2012	20	Coliforms

Well	Samle date	Sample Depth [m]	Parameters exceeded
Bomberos	19.02.2013	25	N-NO <sub>3</sub>
Chalmuch	15.02.2013	25	Na <sup>+</sup> , Cl <sup>-</sup> , TDS
Chenku	19.02.2013	20	N-NO <sub>3</sub>
Crio	14.02.2013	25	Na <sup>+</sup> , Cl <sup>-</sup> , TDS, Hardness
Pacabtun	15.02.2013	20	N-NO <sub>3</sub>

Table 22: Deep samples, parameters exceeding the Mexican drinking water standards. February samples were not analyzed regarding coliform bacteria.

Well	Samle date	Sample Depth [m]	Parameters exceeded
Conagua	25.09.2012	43	Na <sup>+</sup> , Cl <sup>-</sup> , SO <sub>4</sub> <sup>=</sup> , Hg, TDS, Hardness, Coliforms
Matematicas	02.10.2012	50	Na <sup>+</sup> , Cl <sup>-</sup> , SO <sub>4</sub> <sup>=</sup> , Hg, Pb, TDS, Hardness, Coliforms
Pacabtun	25.09.2012	36	Na <sup>+</sup> , Cl <sup>-</sup> , SO <sub>4</sub> <sup>=</sup> , Pb, TDS, Hardness, Coliforms
Sac-Nicte	23.09.2012	36	Na <sup>+</sup> , Cl <sup>-</sup> , TDS, Hardness, Coliforms
Sagarpa	25.09.2012	30	Na <sup>+</sup> , Cl <sup>-</sup> , SO <sub>4</sub> <sup>=</sup> , Hg, TDS, Hardness, Coliforms
San Miguel	22.09.2012	30	Na <sup>+</sup> , Cl <sup>-</sup> , SO <sub>4</sub> <sup>=</sup> , TDS, Hardness, Coliforms
Sierra Papacal	22.09.2012	30	Na <sup>+</sup> , Cl <sup>-</sup> , SO <sub>4</sub> <sup>=</sup> , Hg, TDS, Hardness, Coliforms
Tixcuytun	25.09.2012	45	Na <sup>+</sup> , Cl <sup>-</sup> , TDS, Hardness, Coliforms
Ucú	24.09.2012	35	Na <sup>+</sup> , Cl <sup>-</sup> , SO <sub>4</sub> <sup>=</sup> , Hg, TDS, Hardness, Coliforms
UDS	24.09.2012	47	Na <sup>+</sup> , Cl <sup>-</sup> , SO <sub>4</sub> <sup>=</sup> , Hg, TDS, Hardness, Coliforms
Conagua	19.02.2013	45	Na <sup>+</sup> , Cl <sup>-</sup> , TDS
Matematicas	15.02.2013	50	Na <sup>+</sup> , Cl <sup>-</sup> , SO <sub>4</sub> <sup>=</sup> , Hg, TDS, Hardness
Pacabtun	15.02.2013	40	Na <sup>+</sup> , Cl <sup>-</sup> , Hg, TDS, Hardness
Sac-Nicte	14.02.2013	40	Na <sup>+</sup> , Cl <sup>-</sup> , SO <sub>4</sub> <sup>=</sup> , Hg, Pb, TDS, Hardness
Sagarpa	15.02.2013	40	Na <sup>+</sup> , Cl <sup>-</sup> , SO <sub>4</sub> <sup>=</sup> , TDS, Hardness
San Miguel	16.02.2013	30	Na <sup>+</sup> , Cl <sup>-</sup> , SO <sub>4</sub> <sup>=</sup> , Hg, Pb, As, TDS, Hardness,
Sierra Papacal	16.02.2013	30	Na <sup>+</sup> , Cl <sup>-</sup> , SO <sub>4</sub> <sup>=</sup> , Hg, Pb, TDS, Hardness
Tixcuytun	19.02.2013	45	Na <sup>+</sup> , Cl <sup>-</sup> , TDS
Ucú	16.02.2013	35	Na <sup>+</sup> , Cl <sup>-</sup> , SO <sub>4</sub> <sup>=</sup> , Hg, Pb, TDS, Hardness
UDS	15.02.2013	47	Na <sup>+</sup> , Cl <sup>-</sup> , SO <sub>4</sub> <sup>=</sup> , Hg, Pb, TDS, Hardness

Table 23: Artesian wells samples, parameters exceeding the Mexican drinking water standards. February samples were not analyzed regarding coliform bacteria.

Well	Samle date	Sample Depth [m]	Parameters exceeded
Manantial 2	23.09.2012	1	Na <sup>+</sup> , Cl <sup>-</sup> , TDS Hardness
Manantial 3	23.09.2012	1	Na <sup>+</sup> , Cl <sup>-</sup> , TDS Hardness
Manantial 4	23.09.2012	1	Na <sup>+</sup> , Cl <sup>-</sup> , TDS Hardness
Manantial 6	22.09.2012	1	Na <sup>+</sup> , Cl <sup>-</sup> , TDS Hardness
Manantial 7	22.09.2012	1	Na <sup>+</sup> , Cl <sup>-</sup> , TDS Hardness
Manantial 8	22.09.2012	1	Na <sup>+</sup> , Cl <sup>-</sup> , TDS Hardness
Exbasurero 1	22.09.2012	1	Na <sup>+</sup> , Cl <sup>-</sup> , TDS Hardness
Exbasurero 4	22.09.2012	1	Na <sup>+</sup> , Cl <sup>-</sup> , TDS Hardness
Manantial 2	19.02.2013	1	Na <sup>+</sup> , Cl <sup>-</sup> , Hg, TDS, Hardness
Manantial 3	19.02.2013	1	Na <sup>+</sup> , Cl <sup>-</sup> , TDS Hardness
Manantial 4	19.02.2013	1	Na <sup>+</sup> , Cl <sup>-</sup> , TDS Hardness
Manantial 6	19.02.2013	1	Na <sup>+</sup> , Cl <sup>-</sup> , TDS Hardness
Manantial 7	19.02.2013	1	Na <sup>+</sup> , Cl <sup>-</sup> , TDS
Manantial 8	19.02.2013	1	Na <sup>+</sup> , Cl <sup>-</sup> , TDS Hardness
Exbasurero 1	19.02.2013	1	Na <sup>+</sup> , Cl <sup>-</sup> , Hg, TDS, Hardness
Exbasurero 4	19.02.2013	1	Na <sup>+</sup> , Cl <sup>-</sup> , Hg, TDS, Hardness

## 5 Discussion & Conceptual Model

From the integral analysis of the study area and the documented dynamics of the karst aquifer in interaction with intrinsic and extrinsic factors a conceptual model (Figure 43) of the functioning and dynamic behavior of the study area was developed and is described below. The conceptual model aims to integrate and explain the dynamic conditions of the groundwater flow system, seasonal, tidal changes and recharge/discharge relationships.

The majority of the investigated hydraulic and chemical parameters showed a connection with the meteorological conditions but in close proximity to the coastline where the aquitard can be found, tidal influences were predominant. It is suggested that the groundwater flow is governed by two different systems that are recharge or discharge dominated. Overall the precipitation has important influence over the water table of the Yucatán karst aquifer and also the water composition and the zoning of the groundwater layers, in some wells more pronounced than in others. The flow direction and hydraulic gradients change locally between the different month and is supposed to be highly governed by recharge and the heterogeneity of the karst environment.

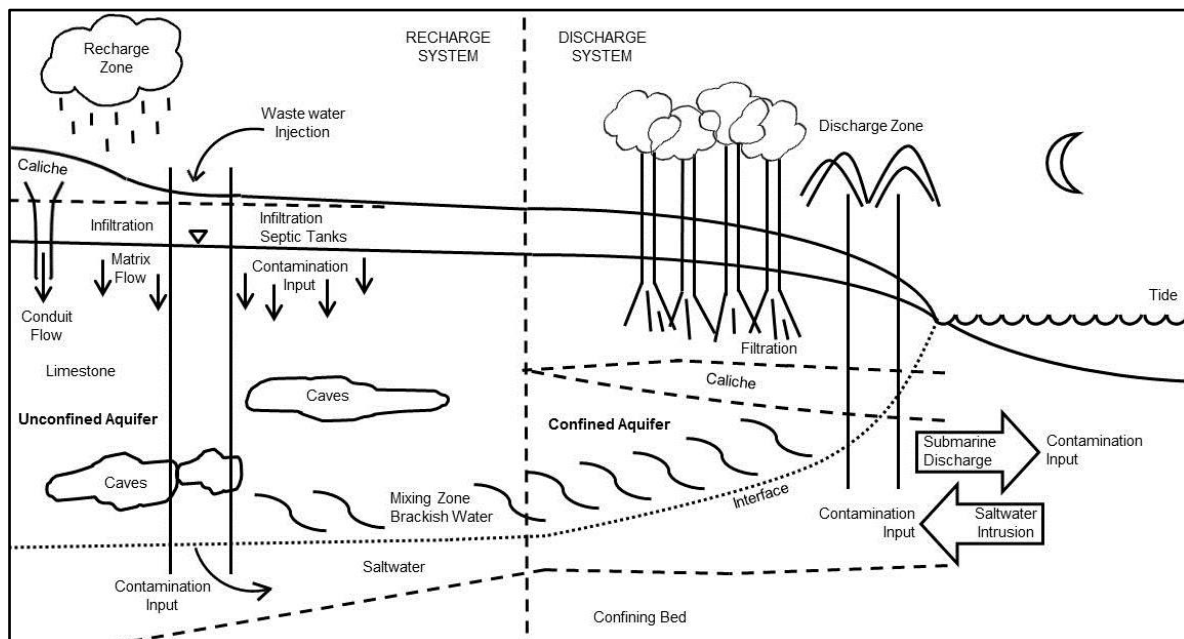


Figure 43: Conceptual model of the study area.

## 5.1 Water Quality

Overall anthropogenic activities and natural processes are spatially and temporally distributed unequally throughout the study area producing modification of water quality. Groundwater recharge mainly occurs inland where the water composition it is modified due to human activities and the groundwater that partly reaches the wetlands, or discharges to the ocean is suspected to alter coastal ecosystems dynamics.

Studying the evolution of the major element concentrations and the water types of the samples during wet and dry season it was documented that the recharging precipitation water in September lets increase the number of different water types in the shallow and intermediate samples. In the intermediate samples the prevalent bicarbonate-mixed water type evolved due to interaction with the predominant soluble limestone of this geological layer. For the dry season the percentage of sodium-chloride water type and bicarbonate-mixed type increased for the shallow and intermediate samples respectively. The trend of the shallow groundwater to the sodium-chloride water type indicates progressive mixing with saltwater already at shallow depth in the more coastal observation wells.

Normally it would be suspected that during the rainy season more limestone is dissolved due to higher amounts of precipitation interacting with the subsoil but the intermediate samples surprisingly showed that it was the other way round and in February the amount bicarbonate-mixed type in the water samples increased. Analyzing the shallow samples there was observed this assumed decrease of bicarbonate-mixed water types from wet to dry season. For the shallow samples the percentage of sodium-chloride dominated water samples was lower during rainy season and let assume the effect of dilution due to increased recharge of the shallow groundwater layers. During dry season increased mixing with saltwater was documented in the shallow groundwater layers. This observation could be explained by the lower discharge that was measured in the coastal region during dry season, saltwater could penetrate further inland. However it has to be taken into account, that higher discharge could also be related to high tides. On the other hand in the intermediate and more continental samples there was noted a reduction of sodium-chloride water type and electrical conductivity during dry season that let assume less fresh-saltwater mixing.

It has to be taken into account that the samples could not be taken at the same depth exactly for the two sampling campaigns and due to changing geology this could affect the water concentrations. The water types for all flowing artesian wells were identified as sodium-chloride and did not change within the study period. However the analysis of the principal ions showed the lowest calcium concentrations and electrical conductivities for Manatial 7 the artesian well with the highest hydraulic head. Less dissolved calcium in the water let assume, that less dissolution process preformed in the geological media and probably the caliche layer

around Manantial 7 is more extend and impermeable confining the aquifer at higher pressure that leads to the particular rise of discharging groundwater.

Comparing the water hardness and alkalinity throughout the study area there was registered a relatively wide spread between the observation wells while the values for the artesian wells showed less variations. The pronounced variations for the observation wells could be related to different grades of karsticity and local changing geology that originate different chemical reactions modifying the water composition and also different land use practices can affect these parameters. Comparing the samples of the dry and wet season it was difficult to predict a certain trend.

The results of the investigations concerning water quality by analyzing the standard ion concentrations of sodium, chloride, sulfate and nitrate as indicators for seawater intrusion, wastewater pollution and contamination due to agricultural practices showed a very irregular occurrence of the elements in the different water samples obtained from the observation wells. Nitrate levels that exceeded the drinking water standard were only documented for the intermediate samples during both dry and wet season in observation wells located within the densely populated urban area of Mérida or very closed to it. In the less populated regions lower N-NO<sub>3</sub> concentrations were detected. This outcome is in accordance with the investigation of nitrate concentrations of Pacheco and Cabrera (1997) for a small study area north of Mérida during 1983-1986. The groundwater contamination with nitrate is presumably attributable to sewage injection or uncontrolled infiltration from septic tanks and the use of fertilizers in agricultural activities. However the high seasonally variation and important differences in nitrate concentrations from adjacent observation wells that were observed by Pacheco and Cabrera (1997) could not be established with certainty from this investigation.

The ranges of hardness and alkalinity were higher during rainy season than dry season, while the pH performed inversely probably indicating dissolution or precipitation processes. However the groundwater samples from September showed less variability between the different observation wells regarding both, alkalinity and pH. During the rainy season the higher amount of aquifer recharge by precipitation and the mixing of waters with different saturation in calcite, is assumed to facilitate dissolution of limestone that is responsible for higher alkalinity and hardness during wet season.

Due to spatially unevenly distributed land use and industrial practices also the occurrence of heavy metals in the groundwater samples was irregular. Regarding the groundwater pollution by heavy metals and primarily the high and norm-exceeding concentrations of mercury and lead in the deep water samples it is assumed the authorized or unauthorized injection of not or insufficiently treated industrial wastewater to the aquifer. Another source could be the use of artificial fertilizers or pesticides that contain Hg but as the heavy metals lead and mercury

were only identified in the deep saltwater samples (with exception of the well Dzidzilché) the presumption suggests that their origin lies in the injected wastewater from domestic and industrial use from the municipal deep wells. This statement is supported by the fact that the concentrations varied a lot between adjacent observation wells and let suppose point-source pollution. Another important source could be the lixiviation of heavy metals due to leakages in the landfills. One important big urban solid waste landfill is located in the municipality of Mérida about 20 km to the west (CDM, 2007) near the observation well Chalmuch. Its placement above the Yucatán karst aquifer and the risk of contaminated leachate infiltration constitutes a severe hazard for the groundwater and ecosystems. The mercury and lead concentrations of the deep samples from the three most western located observation wells Ucu, Sierra Papacal and San Miguel exceeded the limits established in the drinking water norm for almost all samples. Due to the obtained equipotential maps that confirm that groundwater is directed from the location of the landfill to the north and towards the aforementioned observation wells there can be expressed the cautious assumption that the contamination source lies in the solid waste of the landfill. However the highest concentration of lead ( $68.5 \mu\text{g L}^{-1}$ ) was identified in the most southerly observation well Unidad Deportiva del Sur while the deep sample of February from the well Matemáticas contained the highest amount of mercury ( $29.3 \mu\text{g L}^{-1}$ ). Additionally it should be mentioned that within the study area a lot of small unofficial waste disposal sites were discovered that could be potential contamination sources.

There is unawareness of natural source of the mentioned toxic elements but it is conceivable that groundwater interacting with rocks over a long time shows increased formation of element complexes that favor the mobilization of heavy metals. High concentration of mercury that were found in the samples from the artesian wells Exbasurero, the lagoon water and Manantial 2 ( $2.4\text{-}7.9 \mu\text{g L}^{-1}$ ) during dry season are not supposed to be of natural origin. The described occurrence of heavy metals in the deep continental samples let expect that the contaminated groundwater from the urban areas reaches the coastal ecosystems with important heavy metal load. This fact could even increase the heavy metal content in fish and other marine species and consequently in the food chain. Already Marín, et al. (2000) reported severe contamination of the aquifer due to lead, cadmium and chromium. For the analyzed water samples of this investigation exceeding values for cadmium were only reported for the sample of the observation well Unidad Deportiva del Sur at a depth of 47 m while the chromium values were below drinking water standards. Most of the deep water samples also showed sulfate concentration that exceeded the guideline values and are supposed to come from the mixing with saltwater or from agricultural and industrial origin.

With respect to the water quality profiles obtained with the Hydrolab it was established that the electrical conductivity as a direct indicator for the progression of mixing with saltwater, measurements at the bottom of the well were highly dependent on the specific location within the study area. For instance the observation well San Miguel that lies furthest to the west of the study area presented an electrical conductivity of  $49,000 \mu\text{S cm}^{-1}$  at 35 m depth. On the other hand the observation well Hacienda Too that is located almost at the same latitude as San Miguel but 32 km to the east showed an electrical conductivity of only  $6,000 \mu\text{S cm}^{-1}$  at 35 m below water table. This may be due to their different distance to the diagonal oriented coastline or the heterogenic subsurface with different degrees of karstification and conduits that favor saltwater intrusion.

In some of the observation wells was identified a displacement of the mixing zone upward during the month April, May (2012) and March 2013 probably related with a decrease in groundwater recharge by precipitation and less discharge at the coastal site. In the observation wells near the coastline (Contenedores, Baag, Predeco, Granjas Crío) less variability between the months was identified.

Considering the evolution and transport of contaminants through the aquifer there could not be evidenced a clear pattern. Some of the contaminating elements detected in the observation wells were not registered in the samples from the coastal artesian springs. From the presented equipotential maps it becomes clear that the groundwater flow is from the south of the study area to the north-west and consequently the water that underlies the most continental parts is probably not directed to the artesian wells that were subject of this investigation.

According to (Villasuso et al., 1984) the mixing zone of the aquifer below Mérida is 37 m thick and ranges between a depth of 28 and 65 m. For the present study the average thickness of the mixing zone was estimated as 12 m ranging between 2 and 25 m and was located at depth of 2-25 m, the big differences in the two analyses are probably related to differences in the criteria defining the mixing zone.

Marín et al. (2000) stated that in Mérida a central municipally sewage collection and treatment system is missing and that domestic, industrial and medical wastes are discharged via injection wells directly without treatment to the aquifer. Additionally there are reported 83,000 septic tanks in the area of Mérida and its outskirts that also mostly discharge without treatment directly to the aquifer (Marín et al., 2003). According to the INEGI (2007) the capacity of the residual water treatment plants for the state of Yucatán is of  $8.83 \text{ L day}^{-1}$  per capita and extremely insufficient. Regarding the water quality analysis from this study this situation seems to remain unchanged. Of high importance for a secure and clean water supply is the knowledge about water quality and potential contamination impacts in and around the well fields of water abstraction for human water supply, the abstraction depth and the water treatment procedures. Groundwater for human consumption in the urban and rural zones of

Mérida is abstracted from three well fields (Mérida I, Mérida II and Mérida III) located in the south, south-west and south-east of the city respectively. A fourth well field (Mérida IV) has been recently constructed in order to relieve the well field located closed to the urban areas, but is not operating yet. The principal extraction zone for water supply is the plant Mérida I where water is extracted from 25 wells at a depth of 20 meters below groundwater table (Pacheco-Ávila et al., 2004). The groundwater that is extracted from the well sites is not more than chlorinated before its distribution to the population (Pacheco-Ávila et al., 2004) and probably this treatment is insufficient for the elimination of the bacteriological load (total and fecal coliforms).

To sum it up, besides of the natural (anthropogenic enhanced) contamination caused by saltwater intrusion, the deep samples showed more serious contamination due to heavy metals than shallow and intermediate samples but a natural origin cannot be ruled out. Some of the intermediate samples presented high amounts of nitrate but did present low concentrations of toxic heavy metals.

However in conclusion, as the study area is a well-developed karst terrain the transport pattern and geochemical processes that determine the circulation of water through the subsoil are very complex and dynamic and make scientifically founded statements about spatial distribution of contaminants very difficult. Overall it is assumed that contaminants can travel relatively quickly through the aquifer due to high flow rates. The transport, evolution and concentration of contaminants through the heterogeneous karst aquifer depend on the aquifer characteristics and flow behavior but also on the properties of the contaminants, meteorological influences and whether there are point or diffuse sources.

The groundwater temperature measured in the observation wells and artesian wells with help of dataloggers and Hydrolab decreased towards the shoreline. As the aquifer and the groundwater flow could be described as a system through that energy is displaced, in the discharge zone higher energy and temperature would be expected. Nevertheless the groundwater in the urban areas of Mérida is supposed to be warmer due to the anthropogenic aquifer recharge with wastewater. Additionally the influence of precipitation water that can generate warming of the groundwater is suggested to be stronger landwards. Beddows et al. (2007b) surprisingly reported inverse pattern for their study area in the eastern part of the Yucatán Peninsula near Playa del Carmen.

## 5.2 Hydraulics

The study of the spatial and seasonally changing water table and hydraulic gradients and obtained equipotential regimes of the aquifer let suggest that the study zone is very variable but overall responds quickly to recharge by precipitation. The dynamics that govern the water table elevation or the transformation of rainfall into groundwater often cover a broad spectrum of response time scales (Jan et al., 2013) that can be comparatively quick lasting a few minutes or hours or slow presenting a retarded effect of several days or weeks. In the study area preferential flow paths seem to favor quick groundwater level response a few days after the precipitation event and the degree of karstification is assumed to be very high but heterogeneous throughout the study area. However during the very point measurements over a relative short study period there could not be identified a clear relation between precipitation and the spring discharge and hydraulic heads.

As there is lack of surface streams and water bodies that could drain precipitation water before it reaches the subsoil and infiltrates to groundwater, natural recharge at Yucatán peninsula exclusively depends on rainfall that percolates through the soil matrix or reaches the aquifer through preferential flow path and openings in the subsoil. Therefore natural groundwater recharge can be defined as precipitation minus evapotranspiration. Nevertheless it has to be taken into account that in some regions like the coastal zone were lagoons and flood plains are present the infiltration is mostly inhibited by the impermeable caliche layer and only possible in the outcrop area. Coastal groundwater level response is more directly governed by tides than by precipitation. Furthermore the aquifer of the study area is artificially recharged by anthropogenic injection of wastewater and irrigation-return that is supposed to have little effect on water quantity but significant impact on water quality.

The assumption that the liquid waste that is injected into the deep saline water zone flows offshore is refuted by the discovery of saline water inflow through aquifer conduits that could probably direct the wastewater inland and cause freshwater pollution (Beddows et al., 2007b). All so the overall groundwater flow direction in this study was determined as towards the sea, Beddows et al. (2007b) assumption could be supported regarding the coastal hydraulic gradients that varied a lot between the artesian wells within a very small area and sometimes even reversed.

The hydraulic gradients in general resulted higher during the rainy season, this is assumed to be related to the increasing difference of the hydraulic heads between the southern and northern part of the study area. As the southern region in general receives more rainfall during rainy season than the coastal study site, that influences the water level of the aquifer as aforementioned very directly, the difference between water levels measured in the observation wells increased. During dry season the water slope of the potentiometric surface decreased as

the values equalized and the span of the water table between coastal and continental observation wells decreased. But it should be emphasized that due to the geology and particular geomorphology of karst aquifer the overall low hydraulic gradients should be considered with certain caution. In karst environment low hydraulic gradients cannot be equated with low groundwater flow velocity or constant groundwater circulation as Darcy's Law is not valid and the flow system is characterized by turbulent conduit flow. The different slopes of the water table visualized in the equipotential maps of indicate the gradients variability that express the high dynamic of the flow through the karst aquifer system. Nevertheless it was difficult to identify if there exists clear and universal relation between the spatial distribution of equipotential lines and meteorological pattern that unfortunately were obtained only for two different meteorological stations of the study area.

The analysis demonstrated that the aquifer hydraulics are very dynamic and present a high spatial and temporal variability strongly associated with the heterogeneous structure of the karst aquifer and probably its response to meteorological conditions.

At the scale that was studied during the analysis of this investigation, it is not surprising that the hydraulic gradients varied a lot and no clear trend is apparent. The relatively high hydraulic gradients that were determined for the coastal area may occur because the discharge area is much smaller than the recharge zone. The aquifer confinement because of the cemented caliche layer near the coast may result in reduced hydraulic conductivity and increased gradients.

Summing up over all short response time of groundwater to precipitation events is an indicator of the high degree of karstification (Samani, 2011) that is reflected also by sinkholes and interconnected caves in the Yucatán aquifer. Nevertheless differences in the response behavior of different wells in the study area are assumed to occur due to the high heterogeneity of the karst aquifer system that leads to different percolation times of the recharging water till reaching the water table. As the coastal artesian wells are fed by water from the southern parts of the peninsula it is suggested that the discharge depends on the precipitation variability of the continental part and is also influenced by the particular element concentrations of the precipitation and groundwater that evolves during the circulation through the study area.

## 6 Conclusion & Outlook

The functioning and dynamics of coastal ecosystems are very sensitive to small modifications that can alter the geochemical processes and can lead to far-reaching problems. The important ecosystem services that provide the coastal wetlands with its mangrove forests are of great importance as they avoid coastal erosion and function as a natural filter of water that reaches the coastal zones. However due to steadily increase of settlements, buildings and roads that lead to soil sealing a huge amount of the natural subsoil filters of mangrove vegetation have been eliminated. The population of the Yucatán peninsula and the huge amount of tourists that exert more and more pressure over groundwater resources and the ecosystems are the main threat for the environment. As there is lack of effectiveness or even absence of wastewater treatment plants in Mérida, the groundwater quality is strongly modified by injecting unsuitable artificial recharge. The water reaches the coastal area and changes the nutrient concentration available for the coastal flora and fauna.

The faced contamination problems are well known by the municipality and as the water system entirely depends on groundwater resources (Pacheco-Ávila, et al., 2004) institutions try to avoid to supply the population with contaminated water by moving the extraction well fields to the regions south of the city. Evidently this does not lead to the sustainable management of the Yucatán groundwater resources as it does not reduce the contamination impacts that remain a hazard for the environment and social well-being. Furthermore the current expansion of the urban areas of the capital of the Yucatán state could probably draw pollution sources nearer to the extraction well fields.

This study highly suggests a more exhaustive analysis of heavy metals concentrations in the groundwater below Mérida also in conjunction with other elements to better identify their origin and evolution throughout the region. Little N-NO<sub>3</sub> concentrations in the artesian wells discharge water does not evidence contamination but in combination with low dissolved oxygen values let assume the reduction of nitrates in the coastal area, consequently it is likely that nitrate contamination is hardly perceptible.

A huge legal framework of water management in Mérida exists, Yucatán but as Febles-Patrón and Hoogesteijn (2008) describe there is incongruence, inconsistency and lack of correspondence between the legal framework and groundwater contamination prevention practices. A serious problem still constitutes the uncontrolled infiltration of sewage from the septic tanks. According to Febles-Patrón and Hoogesteijn (2008) more than 90 % of the houses in Mérida drain and dispose of their domestic wastewater through septic tanks and soakaways. Although there were established official lineaments that proscribe wastewater treatment before discharging to the aquifer and technical guidelines for the design,

construction and operation of septic tanks. There exist a huge number of septic tanks that do not comply with the norm (Febles-Patrón and Hoogesteijn, 2008). Overall even the quality of the thin freshwater lens was evaluated as poor in particular due to the high concentrations of coliform bacteria and nitrate. Already in 2003 Morris, et al. (2003) reported groundwater contamination in Mérida with fecal coliforms in the range of 1000 to 4000 CFU per 100 ml. The fecal coliform amounts fluctuate seasonally, being the highest values detected in wet season (Morris et al., 2003). The samples from September 2012 analysed in this investigation could only be compared to a previous sampling campaign in June 2012 where lower coliform counts were identified probably due to lower precipitation amounts as well. Morris et al. (2003) suggest that this variation is provoked due to less attenuation during rainy season because of increased recharge. With an appropriate water treatment (chlorination, ultraviolet radiation, ozonation) removing microorganisms the water could reach good quality. In this study inorganic compounds were evidenced and it would be convenient to analyze groundwater with regard to organic compounds as there is evidence of the use of persistent organic compounds like DDT to control malaria till year 2000 (CEC, 2000).

At least since the 20<sup>th</sup> century various researchers (Escolero, et al., 2000; Pacheco Ávila, et al., 2004) proposed the creation of hydrogeological reserve zones within the Yucatán karst Aquifer to guarantee safe water supply. After two and a half years of exhaustive investigation of various regions of Yucatán, under the direction of the researcher Laura Hernández Terrones of the Scientific Research Center of Yucatán (CICY) in April 2013 finally there has been accepted their proposal for Mexico's first hydrological reserve (AMC, 2013). The suggested reserve is of 312.28 km<sup>2</sup>, located south of Mérida and includes part of the southern region of the Ring of Cenotes (AMC, 2013). According to Hernández Terrones it should provide Mérida with drinking water during the next 25 years. Without doubt the hydrogeological reserve is a very significant achievement of the scientific community for the region and also for Mexico in order to reach the sustainable management of the water resources. However the pollution impacts from anthropogenic sources and activities confirmed during this study put emphasis on the importance of a building ban for the hydrological reserve as well as restrictions for the activities of the residents in this area.

In the study area the implementation of a hydrological reserve is not recommended at all as the freshwater availability is highly restricted to a thin freshwater lens and pollution makes groundwater unsuitable for human water supply. Nevertheless it has to be emphasized that the compliance of good water quality should be of primary importance in the whole peninsula not only with the aim to guarantee safe and healthy water supply but primary to protect the equilibrium of extreme vulnerable ecosystems and its services. But the achievement of the aforementioned goal for the complex and highly dynamic study area is anything but easy. It is

suggested a more exhaustive analysis of the study area with respect to contamination sources and groundwater flow characteristics of the karst aquifer system for instance by groundwater modeling approaches. For the protection of the groundwater resources and the achievement of its sustainable use, the characterization of the dynamics of anthropogenic contamination impacts and the saline interface at local and regional level is highly important in order to generate a solid and reliable scientific basis that permits to establish guidelines for the sustainable operation and management of the karst aquifer.

It is difficult to make reliable and universal statements for a complex system from an analysis over a relatively short period of time including only short-term meteorological pattern. For that reason it is suggested to precede with the continuous measurements with the dataloggers in the observation wells, shortening the measurement intervals to be able to analyze climatological and tidal influences better. There should also be realized continuous measurements in the coastal artesian wells in order to identify the relationship between discharge zone, tidal fluctuation better and perhaps even sea level rise better.

However as the serious water quality problems and the overall vulnerability of the aquifer are a known fact for a long time, the implementation of contamination prevention practices like the adaptation of water treatment plants to the specific pollution and over all the improvement of the septic tanks. It would be desirable the establishment of a central sewage disposal that assures the adequate treatment of the wastewater.

There is another very important point that has to be taken into account to reach the sustainable management of the Yucatán aquifer and that is the achievement of an overall consensus and awareness of the severity of the problems and the importance of the aquifer in the population. With regard to this environmental awareness should be enhanced by environmental education and social participation in decision making processes. Just to give an example there are operating deep official municipal wastewater injection wells because the view is held that by the injection of sewage to the deep saline aquifer levels it is possible to get rid of the wastewater because it finds its way to the ocean. Moreover often the wastewater is insufficiently treated before discharging it to the aquifer.

The complexity and heterogeneity of the coastal karst aquifer system is characterized by a lot of interactions, interrelations and interdependencies between land and ocean, fresh and saline water, groundwater and geology among others. Additionally the complex system is exposed to diverse anthropogenic pressure and impacts and climatological influence that make a sustainable management really challenging.

To sum it up complex resource systems have to be evaluated, analyzed and managed from an interdisciplinary perspective with complex and case specific tools permitting current adaptability of the strategies according to changes and variability in the system.

## 7 References

- Alvarez, L. W., Alvarez, W., Asaro, F., & Michel, H. V. (1980). Extraterrestrial Cause for the Cretaceous-Tertiary Extinction. *Science*, 208, pp. 1095-1108.
- AMC, Academia Mexicana de Ciencias. (2013). Tendrá Yucatán la primera reserva hidrogeológica del país. (A. M. Ciencias, Ed.) Retrieved July 13, 2013, from Boletín AMC/142/13: <http://www.comunicacion.amc.edu.mx/comunicados/tendra-yucatan-la-primera-reserva-hidrogeologica-del-pais/>
- Bauer-Gottwein, P., Gondwe, B. R., Charvet, G., Marín, L. E., Rebolledo-Vieyra, M., & Merediz-Alonso, G. (2011). Review: The Yucatán Peninsula karst aquifer, Mexico. *Hydrogeology Journal*, pp. 507-524.
- Beddows, P. A., Blanchon, P., Escobar, E., & Torres-Talamante, O. (2007a). Los cenotes de la península de Yucatán. *Arqueología mexicana*, 14(83), S. 32-35.
- Beddows, P. A., Smart, P. L., Whitaker, F. F., & Smith, S. L. (2007b). Decoupled fresh-saline groundwater circulation of a coastal carbonate aquifer: Spatial patterns of temperature and specific electrical conductivity. *Journal of Hydrology*, pp. 18–32.
- Beddows, P. A., Smart, P. L., Whitaker, F. F., & Smith, S. L. (2002). Density stratified groundwater circulation on the on the Carribean coast of the Yucatan Peninsula, Mexico. *Hydrogeology and Biology of Post-Paleozoic Carbonate Aquifers*, Charles Town, pp.129-134.eds.
- Caribbean coast of the Yucatan Peninsula, Mexico,. *Journal of Hydrology*, pp. 18–32.
- CDM. (2007). Executive Board. Proactiva Mérida Landfill Gas Capture and Flaring Project: Clean Development Mechanism Project Design Document. Yucatan, Mexico.
- CEC. (2000). Comisión para la Cooperación Ambiental Programa regional de acción y demostración de alternativas sustentables para el control de vectores del paludism sin el uso del DDT en México y America Central.
- Chapin, S. F., Matson, P. A., & Vitousek, P. M. (2011). Changes in the Earth System. In *Principles of Terrestrial Ecosystem Ecology* (2 ed., pp. 401-422). New York, USA: Springer.
- CNA. (2001). Comisión Nacional del Agua. Plan Nacional Hidráulico, 2001–2006. Mexico, D.F.: Nacional Water Commission.
- CONABIO. (2012). Comisión Nacional para el Conocimiento y Uso de la Biodiversidad Manglares de México. Retrieved June 22, 2013, from Biodiversidad Mexicana: <http://www.biodiversidad.gob.mx/ecosistemas/manglares/manglares.html>
- CONAGUA. (2011). Comisión Nacional del Agua. Estadísticas del agua en México, edición 2011. Mexico: SEMARNAT, Secretaría de Medio Ambiente y Recursos Naturales.
- CONAGUA. (2011). Comisión Nacional del Agua. Capítulo 3. Usos del agua. In SEMARNAT, Estadísticas del agua en México, edición 2011.
- CONAGUA. (2011). Comisión Nacional del Agua. Estadísticas del agua en México, edición 2011. In SEMARNAT.
- CONAGUA. (2010). Comisión Nacional del Agua. Estadísticas del Agua en México, edición 2010, p. 249.
- Covington, M. D., Wicks, C., & Saar, M. (2009). What's in a Spring Hydrograph. In *Portland GSA Annual Meeting* (eds.), 176-3.
- Cuevas-Jiménez, A., & Euán-Ávila, J. (2009). Morphodynamics of carbonate beaches in the Yucatán Peninsula. *Ciencias Marinas*, 35(3), pp. 307-320.
- DATATUR. (2013). Compendio Estadístico del Turismo en México 2012. Mexico.

- Elkhatib, H., & Günay, G. (1993). Analysis of sea water intrusion associated with karstic channels beneath Ovacik Plain, southern Turkey. In G. Günay, I. A. Johnson, & B. William (Eds.), *Hydrological Processes in Karst Terranes* (S. 129-133). Wallingfort: International Association of Hydrological Science.
- EPA. (2012). Chapter 5.2 Dissolved Oxygen and Biochemical Oxygen Demand: What is dissolved oxygen and why is it important? Retrieved June 9, 2013, from <http://water.epa.gov/type/rs/monitoring/vms52.cfm>
- EPA. (1896). *Quality Criteria for Water 1986* (Bde. EPA 440/5-86-001). Washington, DC.
- EPA. (2002). *A Lexicon of Cave and Karst Terminology with Special Reference to Environmental Karst Hydrology*. Supercedes EPA/600/R-99/006, 1/99.
- Escolero Fuentes, O. A. (2007). The Hydrology of the Yucatan Peninsula. In L. Holliday, L. Marin, & H. Vaux (Eds.), *Sustainable Management of Groundwater in Mexico, Proceedings of a Workshop* (pp. 62-69). Washington, D.C., USA: The National Academies Press.
- Escolero, O. A., Marín, L. E., Birgit, S., & Julia, P. (2000, September 10). Delimitation of a hydrogeological reserve for a city within a karstic aquifer: the Merida, Yucatan example. (Elsevier, Ed.) *Landscape and Urban Planning*, 51(1), pp. 53-62.
- Escolero, O., Marin, L. E., & Domínguez-Mariani, E. (2006). Dynamic of the freshwater-saltwater interface in a karstic aquifer under extraordinary recharge action: the Merida Yucatan case study.
- Essaid, H. I. (1986). A Comparison of the Coupled Fresh Water-Salt Water Flow and the Ghyben-Herzberg Sharp Interface Approaches to Modeling of Transient Behavior in Coastal Aquifer Systems. (E. S. B.V., Eds.) *Journal of Hydrology*, S. 196-193.
- Febles-Patrón, J. L., & Hoogesteijn, A. (2008). Analysis of the Legal Framework for the Protection of Groundwater in Merida, Yucatan. *Ingeniería*, 12-3, pp. 71-79.
- Field, M. S. (2002). *A Lexicon of Cave and Karst Terminology with Special Reference to Environmental Karst Hydrology* (Bde. EPA/600/R-02/003). (N. C.-W. Office, Eds.) Washington, DC, USA: United States Environmental Protection Agency.
- Ford, D., & Williams, P. (2007). *Karst Hydrogeology and Geomorphology*. John Wiley & Sons, p. 576.
- García Gil, G., & Graniel Castro, E. (2010). Geología. In R. Durán García, & M. E. Méndez González (Eds.), *Biodiversidad y Desarrollo Humano en Yucatán* (p. 496).
- García, E. (2004). *Modificaciones al sistema de clasificación climática de Köppen* (5 ed.). Mexico, D.F.: Instituto de Geografía Universidad Nacional Autónoma de México (UNAM).
- Gerstenhauer, A. (1987). Kalkkrusten und Karstformenschatz auf Yucatán/México, Calcretes and Karst Features on the Yucatán Peninsula/México. *Erdkunde – Archive of Scientific Geography*, 41, pp. 30-37.
- Gfrerer, M., & Lankmayr, E. (2005). DDT degradation during enhanced solid-liquid extractions: A Consideration. *Journal of Chromatography A*, 1072, S. 117-125.
- Giddings, L., & Soto, M. (2003). Rhythms of Precipitation in the Yucatán Peninsula. In A. Gómez-Pompa, M. F. Allen, S. L. Fedick, & J. J. Jiménez-Osonio (Eds.), *The Lowland Maya Area: Three Millennia at the Human-Wildland Interface*, pp. 77-89.
- Gondwe, B. R., Lerer, S., Stisen, S., Marín, L., Rebolledo-Vieyra, M., Merediz-Alonso, G., & Bauer-Gottwein, P. (29. April 2010). Hydrogeology of the south-eastern Yucatan Peninsula: New insights from water level measurements, geochemistry, geophysics and remote sensing. *Journal of Hydrology*(389), pp. 1-17.

- Gonzales, J. I. (2011). MAR V1.0 cicese.edu.mx. (CICESE, Ed.) Retrieved June 12, 2013, from MAR V1.0 2011 Prediccion de Mareas en Mexico: <http://predmar.cicese.mx/calmen.php>
- Granier Castro, E., Vera Manrique, I., González Hita, L., & Cardona Benavides, A. (2005). Dinámica de la Interfase Salina y Calidad del Agua en la Costa Nororiental de Yucatán, Mexico. *Revista Latino-Americana de Hidrogeología*, 5, pp. 39-48.
- Granier, C. E., Morris, L. B., & Carrillo-Rivera, J. J. (1999, April). Effects of urbanization on groundwater resources of Merida, Yucatan, Mexico. *Environmental Geology*, 17(4), pp. 303-312.
- HACH. (2006). Hydrolab DS5X, DS5, and MS5: Water Quality Multiprobes; User Manual. pp. 1-74.
- Herrera-Silveira, J. A., Zaldivar-Jimenez, A., Teutli-Hernández, C., Pérez-Ceballos, R., Caamal, J., & Andueza, T. (2012). Rehabilitación de manglares en el estado de Yucatán sometidos a diferentes condiciones hidrológicas y nivel de impacto: el caso de Celestún y Progreso. Informe Final SNIB-CONABIO. Proyecto GH009. (U. M. Centro de Investigación y de Estudios Avanzados, Eds.), pp. 1-69.
- Hildebrand, A. R., Penfield, G. T., Kring, D. A., Camargo Z., A., Jacobsen, S. B., & Boynton, W. V. (1991). Chicxulub Crater: A possible Cretaceous/Tertiary boundary impact crater on the Yucatán Peninsula, Mexico. *Geology*, 19, pp. 867-871.
- INEGI. (2007). Instituto Nacional de Estadística y Geografía. Retrieved June 7, 2013 von <http://www3.inegi.org.mx/sistemas/mexicocifras/default.aspx?e=31>
- INEGI. (2013). Instituto Nacional de Estadística y Geografía. Retrieved July 17, 2013, from Principales suelos de México: <http://mapserver.inegi.gob.mx/geografia/espanol/datosgeogra/fisigeo/principa.cfm>
- INEGI. (2010). Instituto Nacional de Estadística y Geografía. El sector alimentario en México. Serie estadísticas sectoriales.
- INEGI. (2011). Instituto Nacional de Estadística y Geografía. Panorama sociodemográfico de México - Censo de Población y Vivienda 2010.
- INEGI. (2012). Instituto Nacional de Estadística y Geografía. Perspectiva estadística Yucatán. Diciembre 2012. pp. 1-98.
- IUSS. (2007). Base Referencial Mundial del Recurso Suelo. Un marco conceptual para clasificación, correlación y comunicación internacional. Primera actualización 2007. Informes sobre Recursos Mundiales de Suelos (Vol. 103). (FAO, Ed.) Roma.
- Jan, C.-D., Chen, T.-H., & Huang, H.-M. (2013). Analysis of rainfall-induced quick groundwater-level response by using a Kernel function. *Paddy Water Environment*, 11, pp. 135-144.
- Jan, C.-D., Chen, T.-H., & Huang, H.-M. (2013). Analysis of rainfall-induced quick groundwater-level response by using a Kernel function. *Paddy and Water Environment*, 11, pp. 135-144.
- Kauffer Michel, E. F., & Villanueva Aguilar, C. L. (2011, SEptember). Challenges of Water Management in a Constructed Watershed: The Yucatán Peninsula Watershed in Mexico. *Aqua-LAC*, 3(2), pp. 81-91.
- Kehew, A. E. (2001). Chapter 3: Acid-Base Reactions and the Carbonate System. In P. Hall (Eds.), *Applied Chemical Hydrogeology*, p. 368. New Jersey.
- König, N. (2009). *Handbuch Forstliche Analytik: Eine Loseblatt-Sammlung der Analysemethoden im Forstbereich*. Gutachterausschuss Forstliche Analytik.

- Köppen, W. (1936). Das geographische System der Klimate. In W. Köppen, & R. Geiger, *Handbuch der Klimatologie in fünf Bänden (Vols. I, Part C, pp. 1-43)*. Berlin, Germany: Gebrüder Bornträger.
- LAN. (2012). Ley de Aguas Nacionales. Última Reforma DOF 08-06-2012. Mexico: Cámara de Diputados del H. Congreso de la Unión.
- Lesser, J. A., & Weidie, A. E. (1988). Chapter 28: Region 25, Yucatan Peninsula. In W. Back, J. S. Rosenshein, & P. R. Seaber (Eds.), *The Geology of North America, Hydrogeology (Vols. Vol. O-2, pp. 237-241)*. Colorado: Geological Society of America.
- Loáiciga, H. A., Pingel, T. J., & Elizabeth, S. (2011). Sea Water Intrusion by Sea-Level Rise: Scenarios for the 21st Century. *Groundwater*, pp. 37-47.
- Marín, L. E., & Perry, E. C. (1994). The hydrology and Contamination Potential of Northwestern Yucatán, Mexico. *Geofísica Internacional*, pp. 619-623.
- Marín, L. E., Pacheco, J., & Escolero, O. (2003). Groundwater as a socio-economic constraint: the Yucatan Peninsula, Mexico example. *RMZ - Materials and Geoenvironment*, 50, No. 1, pp. 217-219.
- Marín, L. E., Steinich, B., Pacheco, J., & Escolero, O. A. (2000). Hydrogeology of a contaminated sole-source karst aquifer, Mérida, Yucatán, México. *Geofísica Internacional*, pp. 359-365.
- Mohr, E. C., & van Baren, F. A. (1954). *Tropical Soils. A critical study of soil genesis as related to climate, rock and vegetation*. The Hague.
- Moody, D. W., Carr, J., Chase, E. B., & Paulson, R. W. (1988). *National Water Summary 1986 - Hydrologic Events and Ground-Water Quality*. Water-Supply Paper 2325, United States Geological Survey, Washington, DC 20402.
- Morris, B. L. (1994). *Impact of Urbanisation on Groundwater in Merida, Mexico*. British Geological Survey, p. 23.
- Morris, B. L., Lawrence, A. L., Chilton, P. C., Adams, B., Calow, R. C., & Klinck, B. A. (2003). *Groundwater and its Susceptibility to Degradation: A Global Assessment of the Problem and Options for Management*. (U. N. Programme, Ed.) Early Warning and Assessment Report Series, RS, 03-3, pp. 1-126.
- Neal, C., & Kirchner, J. W. (2000). Sodium and chloride levels in rainfall, mist, streamwater and groundwater at the Plynlimon catchments, mid-Wales: inferences on hydrological and chemical controls. *Hydrology and Earth System Science*, 4(2), S. 295-310.
- NOAA. (2007). National Weather Service, National Hurricane Center. Retrieved May 31, 2013, from <http://web.archive.org/web/20070528163713/http://www.nhc.noaa.gov/pastprofile.shtml>
- Orellana, R., Balam, M., Bañuelos, I., García, E., Gonzalez Iturbe, J., & Vidal, F. J. (1999). Evaluación climática. In A. García de Fuentes, J. Córdoba y Ordóñez, & P. A. Chico Ponce de León (Eds.), *Atlas de Procesos Territoriales en Yucatán*, pp. 163-177. México: Universidad Autónoma de Yucatán.
- Orellana, R., Espadas, C., Conde, C., & Gay, C. (2009). *Atlas Escenarios de Cambio Climático en la Península de Yucatán*. Mérida, Yucatán, México. Retrieved May 2013, from <http://www.cambioclimatico.yucatan.gob.mx/atlas-cambio-climatico/precipitacion-total.php>
- Pacheco A., J., & Cabrera S., A. (1997, February). Groundwater Contamination by Nitrates in the Yucatán Peninsula, Mexico. *Hydrogeology Journal*, 5(2), pp. 47-53.

- Pacheco-Ávila, J., Cabrera Sansores, A., & Pérez Ceballos, R. (2004). Diagnóstico de la calidad del agua subterránea en los sistemas municipales de abastecimiento en el Estado de Yucatán, México. *Ingeniería*, 8-2, pp. 165-179.
- Pacheco-Ávila, J., Cabrera Sansores, A., Calderón Rocher, L., Marín, L., Steinich, B., & Escolero, O. (2004). Delineación de una zona de protección para el abastecimiento de agua en Mérida, Yucatán, México.
- Padilla y Sánchez, R. J. (2007). Evolución geológica del sureste mexicano desde el Mesozoico al presente en el contexto regional del Golfo de México. *Boletín de la Sociedad Geológica Mexicana*(1), pp. 19-42.
- Papadopoulos, M. P. (2011). Optimization Approaches for the Control of Seawater Intrusion and its Environmental Impacts in Coastal Environment. (Y. Publishers, Eds.) *Pacific Journal of Optimization*, pp. 479-502.
- Perry, E., Marín, L., McClain, J., & Velazquez, G. (1995). Ring of Cenotes (sinkholes), northwest Yucatan, Mexico: Its hydrogeologic characteristics and possible association with the Chicxulub impact crater. *Geology*, 23, pp. 17-20.
- Perry, E., Velazquez-Oliman, G., & Marin, L. (2002). The Hydrogeochemistry of the Karst Aquifer System of the Northern Yucatan Peninsula, Mexico. *International Geology Review* (44:3), pp. 191-221.
- Perry, E., Velazquez-Oliman, G., & Socki, R. A. (2003). Hydrogeology of te Yucatán Peninsula. In A. Gómez-Pompa, M. F. Allen, S. L. Fedick, & J. J. Jiménez-Osornio (Eds.), *The Lowland Maya Area: Three Millennia at the Human-Wildland Interface*, pp. 115-138. Food Products Press.
- Pope, K. O., D'Hondt, S. L., & Marshall, C. R. (1998). Meteorite impact and the mass extinction of species at the Cretaceous/Tertiary boundary. *Proceedings of the National Academy of Science of the United States of America*, 95, pp. 11028-11029.
- Pope, K. O., Ocampo, A. C., Kinsland, G. L., & Smith, R. (1996, June). Surface expression of the Chicxulub crater. *Geology*, 24, 527-530.
- Robinove, C. J., Langford, R. H., & Brookhart, J. W. (1958). Saline-Water Resources of North Dakota: A description of the principal saline water aquifers and surface-water bodies, with available analyses. *Geological Survey Water-Supply Paper 1428*, pp. 1-73.
- Samani, N. (2011). Response of karst aquifers to rainfall and evaporation, Maharlou Basin, Iran. *Journal of Cave and Karst Studies*, 63(1), pp. 33-40.
- Sanz, E., Ayora, C., & Carrera, J. (2011, 9(1)). Calcite dissolution by mixing waters: geochemical modeling and flow-through experiments. *Geologica Acta*, pp. 67-77.
- Sawyer, C. N. (1960). *Chemistry for Sanitary Engineers*. New York, USA: McGraw-Hill.
- Scheffer/Schachtschabel, Blume, H.-P., Brümmer, G. W., Horn, R., Kandeler, E., Kögel-Knaber, I., Wilke, B.-M. (2010). *Lehrbuch der Bodenkunde* (16 ed.). Spektrum.
- Schlager, E. (2007). Community Management of Groundwater. In M. Giordano, & K. G. Villholth, *The Agricultural Groundwater Revolution: Opportunities and Threats to Development*. USA: ©CAB International.
- Scott, C. A., & Banister, J. M. (2008). The Dilemma of Water Management 'Regionalization' in Mexico under Centralized Resource Allocation. *Water Resources Development*, Vol. 24, No. 1, pp. 61-74.
- Secretaría de, S. (2000). MODIFICACIÓN a la Norma Oficial Mexicana NOM-127-SSA1-1994, Salud Ambiental. Agua para Uso y Consumo Humano. Límites permisibles de calidad y tratamientos a que debe someterse el agua para su potabilización. *Diario Oficial de la Federación*.

- SEDUMA. (2010). Observatorio de Cambio climático de Yucatán. (G. d. Secretaría de Desarrollo Urbano y Medio Ambiente, Ed.) Retrieved May 31, 2013, from <http://www.cambioclimatico.yucatan.gob.mx/atlas-cambio-climatico/>
- SEMARNAT, S. (2009). Diario Oficial de la Federación. Mexico, D.F.: Organismo del Gobierno Constitucional de los Estados Unidos Mexicanos.
- Sherif, M. M., & Singh V. P. (1999). Effect of climate change on sea water intrusion in coastal aquifers. *Hydrol. Process.* 13.
- Shiklomanov, I. A. (1993). Chapter 2: World fresh water resources. In P. H. Gleick, *Water in Crisis: A Guide to the World's Fresh Water Resources.*
- Solinst. (2012). User Guide: Levellogger Series Software Version 4, pp. 1-78.
- Steinich, B., & Marín, L. E. (1996, July). Hydrogeological Investigations in Northwestern Yucatan, Mexico, Using Resistivity Surveys. *Groundwater*, 34(4), pp. 640–646.
- Steinich, B., & Marín, L. E. (1997). Determination of flow characteristics in the aquifer of the Northwestern Peninsula of Yucatan, Mexico. *Journal of Hydrology*, 191, pp. 315-331.
- UNEP/WHO. (1996). Chapter 14 - Use and Reporting of Monitoring Data. In J. Bartram, & R. Ballance (Eds.), *Water Quality Monitoring – A Practical Guide to the Design and implementation of Freshwater Quality Studies and Monitoring Programmes*, pp. 1-24.
- USGS. (2001). What is Ground Water? U.S. Geological Survey, Open-File Report, 93-643.
- Valiela, I., Bowen, J. L., & York, J. K. (2001). Mangrove Forests: One of the World's Threatened Major Tropical Environments. *BioScience*, 51(10), pp. 807-815.
- Villasuso Pino, M. J., Sánchez y Pinto, I. A., Canul Macario, C., Casares Salazar, R., Baldazo Escobedo, G., Souza Cetina, J., Pech Argüelles, C. (2011). Hydrogeology and Conceptual Model of the Karstic Coastal Aquifer in Northern Yucatan State, Mexico. *Tropical and Subtropical Agroecosystems*(13), pp. 243-260.
- Villasuso, M., González, R., Sánchez, I., & Frias, J. (1984). Alteración de la Interfase Salina por Pruebas de Inyección en Yucatán, Memoria del IV Congreso Nacional de Ingeniería Sanitaria y Ambiental, La Ingeniería Ambiental en el Futuro de Mexico., pp. 79-84.
- Wilder, M., & Romero Lankao, P. (2006). Paradoxes of Decentralization: Water Reform and Social Implications in Mexico. *World Development*, Vol. 34, No. 11, pp. 1977–1995.
- Worthington, S. R., Schindel, G. M., & Alexander, E. C. (2002). Techniques for investigating the extent of karstification in the Edwards Aquifer, Texas. In J. B. Martin, C. M. Wicks, & I. D. Sasowsky (Eds.), *Hydrogeology and Biology of Post-Paleozoic Carbonate Aquifers*, p. 212. Karst Waters Institute, Charles Town, West Virginia.

## 8 Appendix

Appendix 1: Hydraulic heads [masl] obtained manually from the observation wells.

Well	May 12	May/June 12	June 12	July 12	Aug 12	Nov 12	Jan 13	Mar 13	May 13	
1	Megalita	0.7272	0.4722	0.6752	0.7572	0.7722	0.9122	0.8022	0.7472	0.6122
2	Granjas Crío	0.1504	0.1604	0.1304	0.2604	0.2304	0.2854	0.2354	0.2004	0.1304
3	Baag	0.0201	0.0281	0.0001	0.1001	0.0501	0.1301	0.1001	0.0201	0.2801
4	Sac-Nicté	0.4485	0.4235	0.4235	0.5285	0.5435	1.1235	0.6935	0.4735	0.4035
5	Dzizilché	0.0422	0.0472	0.0392	0.1822	0.1422	0.1972	0.1872	0.0722	0.0222
6	Sierra Papacal	0.2325	0.2125	0.2145	0.3625	0.3425	0.3925	0.6625	0.2375	
7	San Miguel	0.1942	0.1942	0.1702	0.3342	0.3042	0.3542	0.6242	0.1942	
8	Cheuman	0.6401	0.6121	0.6101	0.7301	0.7601	0.8201	0.8601	0.6401	
9	Ucú	0.6514	0.6274	0.6114	0.7914	0.7714	0.8364	0.7964	0.6414	0.0414
10	Hda. Anicabil	0.9484	0.7734	0.7824	0.9484	1.0184	1.0684	0.9384	0.8084	0.7084
11	UDS	0.8953	0.8653	0.9053	1.1103	1.1503	1.1303	0.9853	0.8853	0.7753
12	Bomberos	0.8243	0.7993	0.8243	0.9693	1.0193	1.0443	0.9393	0.8243	0.6893
13	Tecnológico	0.8823	0.8043	1.0123	0.9223	0.9923	1.0423	1.0223	0.8523	0.7323
14	Sagarpa	0.8265	0.7965	0.8015	0.9115	0.9965	1.0265	0.9965	0.8465	0.6965
15	Pacabtun		0.8283	0.8463	1.0063	1.0713	1.0713	0.9813	0.8613	0.7213
16	Tixcuytun		0.4269	0.8119	0.8869	0.9569	1.0169	1.0169	0.8419	0.6969
17	Observatorio		0.7794	0.8094	1.2444	1.0044	1.0244	0.8844	1.7144	0.6144
18	Chalmuch		0.8292	0.7392	0.9292	0.9192	0.9592	0.8642	0.7692	0.6392
19	Acuaparque		0.8084	0.8334	0.9684	1.0034	1.0534	0.9734	0.8334	0.6934
20	Chenku		-0.0412	0.7648	0.8858	0.9458	0.9908	-1.0592	0.7908	0.7008
21	Conagua		0.8230	0.8580	1.0030	1.0230	1.0730	0.9630	0.8580	0.753
22	Matemáticas	0.7573	0.7183	0.7293	0.8373	0.8873	0.9423	0.9373	1.7673	0.6473
23	Komchén	0.4920	0.4720	0.4660	0.5620	0.5770	0.5870	0.6120	0.5120	
24	Predeco	0.1966	0.0866	0.7366	0.2466	0.1966	0.2566	0.3716	0.1466	0.0766
25	Contenedores	-0.0021	-0.0621	0.1379	0.0479	-0.1321		0.1129	-0.0621	-0.0621
26	Mococho		0.7422	0.7552	0.8122	0.8922	0.9722	1.9922	0.8222	0.6422
27	Hda. Too	0.6279	0.5879	0.5829	0.6029	0.6679	0.7779	0.9479	0.7229	0.5879
28	X'luch	0.2865	0.2665	0.2485	0.3065	0.3065	0.3965	0.4965	-0.4185	0.2465
29	Vázquez	0.0417	0.0197	0.1047	0.1367	0.1317	0.1517	0.2017	0.0767	0.0417

Appendix 2: Ion concentrations in meq L<sup>-1</sup> for the September 2012 samples.

Well/Depth	Na [meq L <sup>-1</sup> ]	K [meq L <sup>-1</sup> ]	Ca [meq L <sup>-1</sup> ]	Mg [meq L <sup>-1</sup> ]	Cl [meq L <sup>-1</sup> ]	SO <sub>4</sub> <sup>=</sup> [meq L <sup>-1</sup> ]	HCO <sub>3</sub> <sup>-</sup> [meq L <sup>-1</sup> ]	N-NO <sub>3</sub> <sup>-</sup> [meq L <sup>-1</sup> ]
Anicabil-10	2.261	0.436	6.200	0.988	2.130	0.417	6.000	0.557
Baag-10	5.261	0.667	3.250	2.798	3.240	0.563	6.752	0.372
Cheuman-10	5.696	0.846	5.450	2.881	4.400	1.042	7.872	0.393
Contenedores-6	8.391	0.974	7.850	3.786	10.500	1.302	7.260	0.171
Crio-10	4.130	0.410	5.450	2.634	4.480	0.542	7.280	0.300
Dzidzilché-10	13.652	0.667	7.450	5.350	13.230	4.063	10.180	0.264
Predeco-15	6.565	1.308	6.450	3.951	7.200	1.146	7.820	0.679
San Miguel-10	16.087	0.769	7.300	4.856	18.800	2.354	7.120	0.343
Sierra Papacal-10	13.174	0.923	8.250	4.609	16.000	2.042	7.200	0.364
Ucú-10	7.174	0.615	4.900	2.305	5.460	0.771	6.960	0.543
Vasquez-10	3.696	0.256	4.900	2.963	2.800	0.479	7.800	0.279
Xluch-15	15.087	0.564	7.300	9.465	18.170	2.813	10.064	0.336
Acuaparque-25	2.435	0.333	6.550	1.152	4.480	0.292	5.520	0.364
Bomberos-25	5.304	0.718	5.650	2.305	4.030	1.224	6.080	1.486
Chalmuch-25	4.304	0.538	6.250	2.387	4.500	0.896	6.200	0.729
Chenku-20	5.304	0.513	4.030	2.634	4.300	0.917	6.080	0.600
Conagua-20	3.870	0.513	5.750	1.317	2.800	0.896	6.080	0.636
Crio-25	28.304	1.282	9.650	13.992	41.500	5.208	5.600	0.100
Komchen-20	5.565	1.077	6.300	3.292	6.800	0.938	7.040	0.293
Matemáticas-20	3.087	0.333	5.250	2.058	3.360	0.729	6.400	0.729
Megalita-20	3.758	0.538	4.925	2.716	4.860	0.604	6.272	0.364
Mococha-20	4.130	0.333	3.600	3.210	3.470	0.375	7.040	0.314
Observatorio-20	3.522	0.436	5.800	2.387	4.030	0.792	6.720	0.614
Pacabtun-20	2.957	1.000	4.100	1.399	2.500	0.438	4.640	0.729
Sac-Nicte-20	5.261	0.641	6.250	3.128	6.500	0.875	7.640	0.343
Sagarpa-20	5.217	0.487	4.500	2.551	4.810	1.000	6.640	0.250
Tecnológico-20	10.870	0.872	5.400	4.609	13.100	1.927	7.360	0.200
Tixcuytun-20	6.348	0.692	2.590	3.128	4.590	0.813	5.760	0.486
Too-20	5.391	0.282	4.700	3.704	5.160	0.688	7.320	0.350
UDS-20	6.043	0.718	4.090	3.457	4.370	2.813	7.080	0.214
Conagua-45	100.348	2.872	17.000	24.609	115.000	24.792	6.144	0.129
Matemáticas-50	231.522	4.385	18.350	37.942	270.000	26.378	6.120	0.164
Pacabtun-40	37.304	1.385	10.150	10.370	43.500	8.125	6.200	0.136
Sac-Nicte-40	43.043	1.333	10.150	15.473	56.300	7.292	7.040	0.071
Sagarpa-40	42.957	1.487	15.250	15.802	57.000	9.024	6.160	0.079
San Miguel-30	415.348	8.359	34.950	57.531	475.000	38.854	4.960	0.071
Sierra Papacal-30	270.000	6.538	30.400	41.317	297.000	29.167	6.600	0.079
Tixcuytun-45	47.739	1.744	11.600	11.029	56.000	7.289	6.336	0.186
Ucú-35	116.783	1.923	19.000	26.831	149.500	11.801	6.784	0.121
UDS-47	235.304	3.923	26.650	40.329	254.000	30.729	6.000	0.107

Appendix 3: Ion balance errors for the September 2012 samples.

Well/Depth	$\Sigma$ cations [meq L <sup>-1</sup> ]	$\Sigma$ anions [meq L <sup>-1</sup> ]	c - a [meq L <sup>-1</sup> ]	c + a [meq L <sup>-1</sup> ]	% Error
Anicabil-10	9.884	9.104	0.780	18.988	4.110
Baag-10	11.976	10.926	1.050	22.902	4.584
Cheuman-10	14.872	13.707	1.166	28.579	4.079
Contenedores-6	21.002	19.234	1.768	40.235	4.394
Crio-10	12.624	12.602	0.023	25.226	0.090
Dzidzilché-10	27.119	27.737	-0.618	54.856	-1.127
Predeco-15	18.274	16.845	1.429	35.118	4.069
San Miguel-10	29.012	28.617	0.395	57.629	0.685
Sierra Papacal-10	26.956	25.606	1.350	52.562	2.568
Ucú-10	14.994	13.734	1.260	28.728	4.386
Vasquez-10	11.815	11.357	0.458	23.172	1.975
Xluch-15	32.416	31.382	1.034	63.798	1.620
Acuaparque-25	10.470	10.656	-0.186	21.126	-0.879
Bomberos-25	13.977	12.820	1.157	26.797	4.316
Chalmuch-25	13.480	12.325	1.155	25.804	4.476
Chenku-20	12.481	11.897	0.584	24.378	2.396
Conagua-20	11.449	10.412	1.038	21.861	4.746
Crio-25	53.228	52.408	0.820	105.637	0.776
Komchen-20	16.234	15.070	1.164	31.305	3.718
Matematicas-20	10.728	11.218	-0.490	21.946	-2.233
Megalita-20	11.938	12.101	-0.163	24.038	-0.677
Mococha-20	11.274	11.199	0.074	22.473	0.330
Observatorio-20	12.144	12.156	-0.012	24.301	-0.048
Pacabtun-20	9.456	8.306	1.149	17.762	6.471
Sac-Nicte-20	15.279	15.358	-0.079	30.637	-0.256
Sagarpa-20	12.756	12.700	0.056	25.456	0.220
Tecnológico-20	21.750	22.587	-0.837	44.338	-1.887
Tixcuytun-20	12.758	11.648	1.109	24.406	4.545
Too-20	14.077	13.518	0.559	27.595	2.027
UDS-20	14.308	14.477	-0.169	28.785	-0.586
Conagua-45	144.829	146.064	-1.236	290.893	-0.425
Matematicas-50	292.199	302.663	-10.464	594.861	-1.759
Pacabtun-40	59.209	57.961	1.249	117.170	1.066
Sac-Nicte-40	70.000	70.703	-0.703	140.703	-0.500
Sagarpa-40	75.496	72.263	3.233	147.759	2.188
San Miguel-30	516.188	518.886	-2.698	1035.073	-0.261
Sierra Papacal-30	348.255	332.845	15.410	681.101	2.263
Tixcuytun-45	72.112	69.811	2.301	141.922	1.621
Ucú-35	164.537	168.206	-3.669	332.743	-1.103
UDS-47	306.207	290.836	15.370	597.043	2.574

Appendix 4: Ion concentrations in meq L<sup>-1</sup> for the February 2013 samples.

Well/Depth	Na meq L <sup>-1</sup>	K meq L <sup>-1</sup>	Ca meq L <sup>-1</sup>	Mg meq L <sup>-1</sup>	Si meq L <sup>-1</sup>	Fe meq L <sup>-1</sup>	Mn meq L <sup>-1</sup>	CO <sub>3</sub> meq L <sup>-1</sup>	HCO <sub>3</sub> meq L <sup>-1</sup>	Cl meq L <sup>-1</sup>	SO <sub>4</sub> <sup>=</sup> meq L <sup>-1</sup>	N-NO <sub>3</sub> meq L <sup>-1</sup>	F meq L <sup>-1</sup>
Bomberos-25	4.842	0.297	5.452	1.033	1.691	0.002	0.000	0.000	7.437	4.150	0.911	0.750	0.003
Conagua-20	3.895	0.150	6.349	1.043	1.558	0.002	0.000	0.000	6.060	3.261	0.896	0.671	0.004
Chenku-20	4.993	0.158	4.952	1.728	1.523	0.001	0.000	0.000	6.335	4.446	0.859	0.764	0.002
Tixcuytun-45	58.254	1.210	7.172	0.717	1.584	0.003	0.000	0.000	6.886	45.946	6.250	0.250	0.017
Tixcuytun-20	4.215	0.168	5.791	2.294	1.050	0.001	0.000	0.000	7.161	3.854	0.708	0.493	0.003
Tecnológico-20	4.565	0.177	5.202	1.541	1.120	0.001	0.000	0.000	6.335	4.150	0.859	0.271	0.006
Sac-Nicté-40	65.363	1.194	11.946	20.010	3.688	0.002	0.000	0.000	6.886	92.658	12.847	0.057	0.042
Sac-Nicté-20	5.253	0.188	5.260	2.845	1.244	0.000	0.000	0.000	6.886	5.336	0.833	0.371	0.005
Ucú-10	5.095	0.157	6.685	1.834	1.199	0.000	0.000	0.000	4.837	8.003	0.729	0.436	0.003
Ucú-35	141.180	1.437	15.518	26.432	1.950	0.004	0.004	0.000	7.988	141.712	10.764	0.171	0.023
Sierra Papacal-10	14.382	0.328	6.102	3.652	1.026	0.000	0.001	0.000	7.161	14.607	1.745	0.321	0.004
Sierra Papacal-30	234.013	6.035	21.985	38.666	1.346	0.039	0.005	0.000	5.417	311.626	28.472	0.121	0.043
Crio-10	3.487	0.026	3.260	2.367	1.131	0.003	0.000	0.000	5.030	3.314	0.500	0.421	0.014
Crio-25	25.078	0.946	9.192	19.856	3.490	0.001	0.001	0.000	4.958	41.424	3.125	0.093	0.022
UDS-20	5.168	0.174	5.394	2.527	0.769	0.003	0.000	0.000	6.611	5.039	0.729	0.407	0.006
UDS-47	158.393	2.427	24.797	30.027	1.231	0.002	0.004	0.000	7.161	213.426	20.119	0.186	0.045
Chalmuch-25	14.853	0.205	4.238	4.492	1.396	0.000	0.000	0.000	5.611	15.479	1.563	0.300	0.008
Too-20	4.697	0.166	3.630	3.045	2.289	0.001	0.000	0.000	6.385	4.446	0.729	0.314	0.009
Acuaparque-25	3.263	0.048	4.909	0.797	1.496	0.000	0.001	0.275	5.784	3.854	0.188	0.350	0.004
Anicabil-10	2.352	0.061	3.879	0.986	1.439	0.001	0.000	0.000	5.986	1.556	0.397	0.514	0.003
Dzidzilché-10	17.483	0.342	5.992	4.243	0.718	0.002	0.000	0.275	4.958	16.787	2.031	0.264	0.007
Sagarpa-20	4.395	0.144	4.527	2.058	0.682	0.000	0.000	0.000	6.611	3.557	1.125	0.143	0.004
Sagarpa-40	42.085	0.703	8.877	19.580	1.459	0.002	0.004	0.000	5.998	57.775	9.371	0.071	0.020
San Miguel-10	27.268	0.250	4.251	0.797	0.601	0.001	0.000	0.000	5.677	19.901	2.207	0.307	0.002
San Miguel-30	416.478	8.209	21.614	2.328	0.836	0.040	0.014	0.000	4.736	381.532	41.013	0.093	0.045
Mococha-20	4.460	0.101	4.567	1.962	0.452	0.000	0.000	0.000	6.926	3.750	0.438	0.371	0.001
Xluch-15	11.496	0.391	4.018	5.664	1.399	0.000	0.000	0.000	7.696	12.209	1.625	0.471	0.009

Well/Depth	Na meq L <sup>-1</sup>	K meq L <sup>-1</sup>	Ca meq L <sup>-1</sup>	Mg meq L <sup>-1</sup>	Si meq L <sup>-1</sup>	Fe meq L <sup>-1</sup>	Mn meq L <sup>-1</sup>	CO <sub>3</sub> meq L <sup>-1</sup>	HCO <sub>3</sub> meq L <sup>-1</sup>	Cl meq L <sup>-1</sup>	SO <sub>4</sub> <sup>-</sup> meq L <sup>-1</sup>	N-NO <sub>3</sub> meq L <sup>-1</sup>	F meq L <sup>-1</sup>
Matematicas-20	4.510	0.147	4.362	2.383	0.571	0.000	0.000	0.000	6.734	4.578	1.068	0.500	0.032
Matematicas-50	228.396	4.142	20.500	32.519	0.953	0.008	0.010	0.000	5.772	300.866	33.300	0.079	0.055
Puente-2	19.113	0.373	3.990	0.998	0.702	0.000	0.000	0.000	6.809	18.346	0.417	0.171	0.006
Pacabtun-40	43.521	0.847	9.500	13.462	1.523	0.001	0.000	0.000	4.644	50.144	7.813	0.143	0.027
Pacabtun-20	3.030	0.085	3.868	1.028	0.769	0.000	0.000	0.000	5.195	2.930	0.375	0.800	0.008
Vazquez-10	2.941	0.112	3.751	2.266	0.672	0.000	0.000	0.000	4.837	3.314	0.417	0.271	0.001
Komchem-20	6.257	0.345	5.363	2.715	0.513	0.000	0.001	0.000	7.696	6.497	0.500	0.336	0.008
Megalita-20	4.173	0.167	4.801	2.332	0.493	0.001	0.000	0.000	6.926	4.840	0.563	0.386	0.005
Baag-10	3.587	0.153	4.287	2.359	0.514	0.001	0.000	0.000	6.926	4.055	0.604	0.321	0.008
Contenedores-6	9.597	0.318	5.632	3.282	0.615	0.001	0.004	0.000	7.119	9.724	1.383	0.207	0.010
Cheuman-10	6.730	0.305	4.156	2.631	0.503	0.000	0.001	0.000	7.119	6.671	1.167	0.357	0.009
Observatorio-20	5.003	0.191	4.503	2.383	0.456	0.000	0.001	0.000	6.926	5.407	0.896	0.693	0.011
Predeco-15	7.149	0.821	5.053	3.660	0.719	0.000	0.003	0.000	7.696	8.023	1.141	0.586	0.006

Appendix 5: Ion balance errors for the February 2013 samples.

Well/Depth	$\Sigma$ cations [meq L <sup>-1</sup> ]	$\Sigma$ anions [meq L <sup>-1</sup> ]	c - a [meq L <sup>-1</sup> ]	c + a [meq L <sup>-1</sup> ]	% error
Bomberos-25	13.317	13.251	0.066	26.569	0.247
Conagua-20	12.996	10.891	2.105	23.888	8.812
Chenku-20	13.354	12.407	0.947	25.761	3.678
Tixcuytun-45	68.940	59.349	9.591	128.289	7.476
Tixcuytun-20	13.519	12.219	1.300	25.738	5.050
Tecnológico-20	12.606	11.622	0.984	24.228	4.059
Sac-Nicté-40	102.202	112.490	-10.288	214.693	-4.792
Sac-Nicté-20	14.790	13.432	1.358	28.221	4.812
Ucú-10	14.970	14.009	0.961	28.978	3.317
Ucú-35	186.526	160.658	25.867	347.184	7.451
Sierra Papacal-10	25.491	23.839	1.652	49.330	3.348
Sierra Papacal-30	302.090	345.681	-43.591	647.771	-6.729
Crio-10	10.273	9.279	0.993	19.552	5.081
Crio-25	58.564	49.621	8.942	108.185	8.266
UDS-20	14.035	12.792	1.244	26.827	4.635
UDS-47	216.880	240.937	-24.057	457.817	-5.255
Chalmuch-25	25.184	22.961	2.223	48.145	4.618
Too-20	13.828	11.884	1.944	25.711	7.561
Acuaparque-25	10.514	10.455	0.059	20.969	0.280
Anicabil-10	8.718	8.457	0.261	17.175	1.522
Dzidzilché-10	28.779	24.323	4.456	53.103	8.392
Sagarpa-20	11.807	11.440	0.367	23.247	1.579
Sagarpa-40	72.710	73.235	-0.525	145.946	-0.360
San Miguel-10	33.168	28.094	5.074	61.262	8.283
San Miguel-30	449.519	427.418	22.101	876.938	2.520
Mococha-20	11.541	11.486	0.055	23.027	0.237
Xluch-15	22.968	22.011	0.957	44.979	2.127
Matematicas-20	11.973	12.912	-0.939	24.885	-3.773
Matematicas-50	286.528	340.071	-53.543	626.599	-8.545
Puente-2	25.176	25.749	-0.573	50.925	-1.125
Pacabtun-40	68.853	62.771	6.082	131.623	4.621
Pacabtun-20	8.780	9.308	-0.529	18.088	-2.923
Vazquez-10	9.742	8.840	0.903	18.582	4.858
Komchem-20	15.194	15.037	0.157	30.231	0.518
Megalita-20	11.967	12.720	-0.753	24.687	-3.048
Baag-10	10.901	11.915	-1.014	22.816	-4.444
Contenedores-6	19.448	18.443	1.005	37.891	2.653
Cheuman-10	14.325	15.323	-0.999	29.648	-3.369
Observatorio-20	12.536	13.932	-1.396	26.469	-5.274
Predeco-15	17.404	17.452	-0.048	34.857	-0.137

Appendix 6: Coliform concentrations for September 2012 samples.

ID	Location	Sample Depth [m]	Coli Total [CFU 100 ml <sup>-1</sup> ]	Coli Fecal [CFU 100 ml <sup>-1</sup> ]
1	Megalita	20	650	570
2	Granjas Crío	10	1200	800
2	Granjas Crío	25	2500	1800
3	Baag	10	2800	2600
4	Sac-Nicté	20	550	170
4	Sac-Nicté	40	340	280
5	Dzizilché	10	1410	1180
6	Sierra Papacal	10	4700	4100
6	Sierra Papacal	30	430	200
7	San Miguel	10	1480	1350
7	San Miguel	30	1320	630
8	Cheuman	10	5800	5300
9	Ucú	10	2440	2020
9	Ucú	35	1280	550
10	Anicabil	10	1870	1530
11	UDS	20	4340	3900
11	UDS	47	20	10
12	Bomberos	25	3380	1890
13	Tecnológico	20	900	370
14	Sagarpa	20	2000	1630
14	Sagarpa	40	410	280
15	Pacabtun	20	4560	4180
15	Pacabtun	40	2430	1800
16	Tixcuytun	20	2200	1060
16	Tixcuytun	45	460	300
17	Observatorio	20	4210	3100
18	Chalmuch	25	3480	1600
19	Acuaparque	25	3200	2480
20	Chenku	20	1080	720
21	Conagua	20	2750	1200
21	Conagua	45	380	160
22	Matemáticas	20	400	190
22	Matemáticas	50	250	180
23	Komchén	20	610	220
24	Predeco	15	580	430
25	Contenedores	6	1840	970
26	Mococha	20	450	240
27	Hda. Too	20	570	360
28	X`luch	15	840	370
29	Vázquez	10	1420	800

Appendix 7: Element concentrations for shallow samples. In bold values above Mexican drinking water standard.

Well	Sample Date	Sample Depth [m]	TDS [mg L <sup>-1</sup> ]	Na <sup>+</sup> [mg L <sup>-1</sup> ]	Cl <sup>-</sup> [mg L <sup>-1</sup> ]	N-NO <sub>3</sub> [mg L <sup>-1</sup> ]	SO <sub>4</sub> <sup>=</sup> [mg L <sup>-1</sup> ]	As [mg L <sup>-1</sup> ]	Hg [mg L <sup>-1</sup> ]	Pb [mg L <sup>-1</sup> ]	Hardness [mg L <sup>-1</sup> ]
Anicabil	24.09.2012	10	620.00	52.00	75.51	7.81	20.00	0.65	0.12	1.61	359.08
Baag	21.09.2012	10	754.00	121.00	114.87	5.20	27.00	0.93	0.22	0.60	302.34
Cheuman	22.09.2012	10	892.00	131.00	155.99	5.50	50.00	1.55	0.29	0.25	416.33
Contenedores	26.09.2012	6	<b>1258.00</b>	193.00	<b>372.26</b>	2.40	62.50	2.21	0.37	5.77	<b>581.50</b>
Granjas Crio	21.09.2012	10	796.00	95.00	158.83	4.20	26.00	0.60	0.26	0.01	403.98
Dzidzilché	26.09.2012	10	<b>1811.00</b>	314.00	<b>469.04</b>	3.70	195.00	2.95	0.44	2.51	<b>639.77</b>
Predeco	26.09.2012	15	<b>1198.00</b>	151.00	<b>255.26</b>	9.51	55.00	1.60	0.38	5.21	<b>519.81</b>
San Miguel	22.09.2012	10	<b>2100.00</b>	<b>370.00</b>	<b>666.52</b>	4.80	113.00	1.98	0.41	0.50	<b>607.57</b>
Sierra Papacal	22.09.2012	10	<b>1850.00</b>	<b>303.00</b>	<b>567.25</b>	5.10	98.00	2.33	0.37	1.57	<b>642.66</b>
Ucú	24.09.2012	10	965.00	165.00	193.57	7.61	37.00	1.24	0.26	2.24	360.04
Vazquez	02.10.2012	10	722.00	85.00	99.27	3.90	23.00	0.93	0.12	1.80	392.98
X'luch	02.10.2012	15	<b>2416.00</b>	347.00	<b>644.18</b>	4.70	135.00	4.08	0.49	9.74	<b>838.17</b>
Anicabil	15.02.2013	10	414.00	54.10	55.17	7.20	19.04	0.85	0.13	0.04	243.14
Baag	14.02.2013	10	551.00	82.50	143.75	4.50	29.00	1.43	0.51	0.14	332.20
Cheuman	16.02.2013	10	703.00	154.78	236.50	5.00	56.00	2.26	0.21	0.12	339.24
Contenedores	16.02.2013	6	870.00	220.72	<b>344.70</b>	2.90	66.40	2.44	0.22	0.03	445.58
Granjas Crio	14.02.2013	10	557.00	80.20	117.48	5.90	24.00	1.41	0.04	0.27	281.30
Dzidzilché	16.02.2013	10	<b>1360.00</b>	<b>402.11</b>	<b>595.11</b>	3.70	97.50	5.28	0.46	<b>18.52</b>	<b>511.66</b>
Predeco	14.02.2013	15	801.00	164.42	<b>284.42</b>	8.20	54.78	2.14	0.14	0.16	435.59
San Miguel	16.02.2013	10	<b>1420.00</b>	<b>627.18</b>	<b>705.48</b>	4.30	105.95	3.56	0.24	2.87	252.22
Sierra Papacal	16.02.2013	10	<b>1170.00</b>	330.79	<b>517.83</b>	4.50	83.75	3.60	0.29	5.98	487.54
Ucú	16.02.2013	10	644.00	117.19	<b>283.72</b>	6.10	35.00	1.42	0.10	0.04	425.68
Vazquez	14.02.2013	10	521.00	67.65	117.48	3.80	20.00	1.17	0.24	0.01	300.77
X'luch	14.02.2013	15	<b>1070.00</b>	<b>264.41</b>	<b>432.81</b>	6.60	78.00	3.51	0.41	1.50	484.18

Appendix 8: Element concentrations for intermediate samples. In bold values above Mexican drinking water standard.

Well	Sample Date	Sample Depth [m]	TDS [mg L <sup>-1</sup> ]	Na <sup>+</sup> [mg L <sup>-1</sup> ]	Cl <sup>-</sup> [mg L <sup>-1</sup> ]	N-NO <sub>3</sub> [mg L <sup>-1</sup> ]	SO <sub>4</sub> <sup>=</sup> [mg L <sup>-1</sup> ]	As [mg L <sup>-1</sup> ]	Hg [mg L <sup>-1</sup> ]	Pb [mg L <sup>-1</sup> ]	Hardness [mg L <sup>-1</sup> ]
Acuaparque	24.09.2012	25	734.00	56.00	158.83	5.10	14.00	1.03	0.56	4.33	384.80
Bomberos	25.09.2012	25	894.00	122.00	142.88	<b>20.82</b>	58.75	1.00	0.25	0.57	397.50
Chalmuch	24.09.2012	25	1000.00	99.00	159.54	<b>10.21</b>	43.00	0.59	0.34	0.52	431.58
Chenku	25.09.2012	20	796.00	122.00	152.45	8.41	44.00	1.02	0.34	0.34	333.06
Conagua	25.09.2012	20	750.00	89.00	99.27	8.91	43.00	0.44	0.26	0.32	353.08
Granjas Crio	21.09.2012	25	<b>3795.00</b>	<b>651.00</b>	<b>1471.30</b>	1.40	250.00	6.85	0.89	0.01	<b>1182.03</b>
Komchen	26.09.2012	20	<b>1085.00</b>	128.00	241.08	4.10	45.00	1.92	0.37	5.80	479.38
Matematicas	02.10.2012	20	784.00	71.00	119.12	<b>10.21</b>	35.00	0.94	0.33	4.52	365.17
Megalita	21.09.2012	20	850.00	86.44	172.30	5.10	29.00	0.81	0.26	0.21	381.88
Mococha	02.10.2012	20	785.00	95.00	123.02	4.40	18.00	0.84	0.16	3.90	340.41
Observatorio	24.09.2012	20	<b>1021.00</b>	81.00	142.88	8.61	38.00	0.94	0.24	1.00	409.11
Pacabtun	24.09.2012	20	579.00	68.00	88.63	<b>10.21</b>	21.00	0.53	0.34	3.81	274.78
Sac-Nicte	23.09.2012	20	<b>1214.00</b>	121.00	230.44	4.80	42.00	1.27	0.17	0.82	468.65
Sagarpa	25.09.2012	20	754.00	120.00	170.53	3.50	48.00	7.62	0.22	1.72	352.41
Tecnológico	25.09.2012	20	<b>1390.00</b>	<b>250.00</b>	<b>464.43</b>	2.80	92.50	2.94	0.31	0.29	<b>500.31</b>
Tixcuytun	25.09.2012	20	884.00	146.00	162.73	6.81	39.00	1.07	0.28	0.29	285.84
Hda. Too	02.10.2012	20	872.00	124.00	182.94	4.90	33.00	1.78	0.17	6.83	420.05
UDS	24.09.2012	20	967.00	139.00	154.93	3.00	135.00	1.12	0.73	6.56	377.23
Acuaparque	15.02.2013	25	511.00	75.06	136.61	4.90	9.00	1.16	0.07	0.18	285.06
UDS	24.09.2012	20	967.00	139.00	154.93	3.00	135.00	1.12	0.73	6.56	377.23
Acuaparque	15.02.2013	25	511.00	75.06	136.61	4.90	9.00	1.16	0.07	0.18	285.06
Bomberos	19.02.2013	25	632.00	111.37	147.12	<b>10.50</b>	43.75	1.36	0.17	0.03	324.00
Chalmuch	15.02.2013	25	<b>1210.00</b>	<b>341.62</b>	<b>548.74</b>	4.20	75.00	5.16	0.33	11.32	436.55
Chenku	19.02.2013	20	592.00	114.83	157.62	<b>10.70</b>	41.25	1.14	0.13	0.11	333.83
Conagua	19.02.2013	20	538.00	89.58	115.59	9.40	43.00	0.84	0.14	0.05	369.30

Well	Sample Date	Sample Depth [m]	TDS [mg L <sup>-1</sup> ]	Na <sup>+</sup> [mg L <sup>-1</sup> ]	Cl <sup>-</sup> [mg L <sup>-1</sup> ]	N-NO <sub>3</sub> [mg L <sup>-1</sup> ]	SO <sub>4</sub> <sup>=</sup> [mg L <sup>-1</sup> ]	As [mg L <sup>-1</sup> ]	Hg [mg L <sup>-1</sup> ]	Pb [mg L <sup>-1</sup> ]	Hardness [mg L <sup>-1</sup> ]
Crio	14.02.2013	25	<b>2210.00</b>	<b>576.80</b>	<b>1468.46</b>	1.30	150.00	11.09	0.68	11.21	<b>1453.03</b>
Komchen	14.02.2013	20	725.00	143.92	230.32	4.70	24.00	2.07	0.40	0.16	403.73
Matematicas	15.02.2013	20	606.00	103.74	162.30	7.00	51.25	1.39	0.71	0.03	337.14
Megalita	14.02.2013	20	580.00	95.99	171.58	5.40	27.00	1.39	0.27	0.09	356.54
Mococha	14.02.2013	20	527.00	102.58	132.93	5.20	21.00	1.18	0.17	0.13	326.29
Observatorio	15.02.2013	20	627.00	115.06	191.67	9.70	43.00	1.47	0.20	0.08	344.20
Pacabtun	15.02.2013	20	462.00	69.69	103.87	<b>11.20</b>	18.00	0.75	0.33	0.10	244.64
Sac-Nicte	14.02.2013	20	661.00	120.82	189.15	5.20	40.00	1.93	0.14	0.09	405.12
Sagarpa	15.02.2013	20	584.00	101.08	126.10	2.00	54.00	8.98	0.09	0.19	329.14
Tecnológico	19.02.2013	20	555.00	105.00	147.12	3.80	41.25	1.25	0.20	0.18	336.92
Tixcuytun	19.02.2013	20	591.00	96.95	136.61	6.90	34.00	1.35	0.35	0.07	404.06
Hda. Too	14.02.2013	20	626.00	108.03	157.62	4.40	35.00	1.94	0.06	0.21	333.71
UDS	15.02.2013	20	665.00	118.87	178.64	5.70	35.00	1.37	0.32	0.15	395.89

Appendix 9: Element concentrations for deep samples. In bold values above Mexican drinking water standard.

Well	Sample Date	Sample Depth [m]	TDS [mg L <sup>-1</sup> ]	Na <sup>+</sup> [mg L <sup>-1</sup> ]	Cl <sup>-</sup> [mg L <sup>-1</sup> ]	N-NO <sub>3</sub> [mg L <sup>-1</sup> ]	SO <sub>4</sub> <sup>=</sup> [mg L <sup>-1</sup> ]	As [mg L <sup>-1</sup> ]	Hg [mg L <sup>-1</sup> ]	Pb [mg L <sup>-1</sup> ]	Hardness [mg L <sup>-1</sup> ]
Conagua	25.09.2012	45	<b>10380.00</b>	<b>2308.00</b>	<b>4077.10</b>	1.80	<b>1190.00</b>	13.90	<b>2.12</b>	0.01	<b>2080.35</b>
Matematicas	02.10.2012	50	<b>20418.00</b>	<b>5325.00</b>	<b>9572.31</b>	2.30	<b>1266.16</b>	20.68	<b>4.46</b>	<b>40.23</b>	<b>2814.89</b>
Pacabtun	25.09.2012	40	<b>4057.00</b>	<b>858.00</b>	<b>1542.21</b>	1.90	390.00	5.88	1.06	<b>12.71</b>	<b>1025.81</b>
Sac-Nicte	23.09.2012	40	<b>5098.00</b>	<b>990.00</b>	<b>1996.00</b>	1.00	350.00	4.94	0.91	0.01	<b>1281.13</b>
Sagarpa	25.09.2012	40	<b>5400.00</b>	<b>988.00</b>	<b>2020.82</b>	1.10	<b>433.16</b>	25.36	0.75	2.93	<b>1552.32</b>
San Miguel	22.09.2012	30	<b>36950.00</b>	<b>9553.00</b>	<b>16840.18</b>	1.00	<b>1865.00</b>	48.53	0.47	6.63	<b>4624.07</b>
Sierra Papacal	22.09.2012	30	<b>22780.00</b>	<b>6210.00</b>	<b>10529.54</b>	1.10	<b>1400.00</b>	25.12	<b>9.29</b>	0.01	<b>3585.57</b>
Tixcuytun	25.09.2012	45	<b>4822.00</b>	<b>1098.00</b>	<b>1985.37</b>	2.60	349.86	6.34	1.00	0.01	<b>1131.18</b>
Ucú	24.09.2012	35	<b>12577.00</b>	<b>2686.00</b>	<b>5300.22</b>	1.70	<b>566.44</b>	31.53	<b>1.59</b>	0.01	<b>2291.43</b>
UDS	24.09.2012	47	<b>20755.00</b>	<b>5412.00</b>	<b>9005.06</b>	1.50	<b>1475.00</b>	28.46	<b>1.89</b>	0.01	<b>3348.86</b>
Conagua	19.02.2013	45	<b>3890.00</b>	<b>1590.14</b>	<b>2056.27</b>	3.00	382.95	14.70	0.84	3.28	228.35
Matematicas	15.02.2013	50	<b>18600.00</b>	<b>5253.10</b>	<b>10665.70</b>	1.10	<b>1598.40</b>	25.88	<b>29.30</b>	10.31	<b>2651.72</b>
Pacabtun	15.02.2013	40	<b>3350.00</b>	<b>1000.99</b>	<b>1777.61</b>	2.00	375.00	11.62	<b>1.96</b>	0.99	<b>1148.35</b>
Sac-Nicte	14.02.2013	40	<b>5460.00</b>	<b>1503.34</b>	<b>3284.72</b>	0.80	<b>616.67</b>	10.70	<b>1.82</b>	<b>16.56</b>	<b>1598.31</b>
Sagarpa	15.02.2013	40	<b>3630.00</b>	<b>967.95</b>	<b>2048.12</b>	1.00	<b>449.82</b>	33.30	0.82	4.73	<b>1423.53</b>
San Miguel	16.02.2013	30	<b>22300.00</b>	<b>9579.00</b>	<b>13525.30</b>	1.30	<b>1968.60</b>	<b>67.76</b>	<b>16.23</b>	<b>26.85</b>	<b>1196.04</b>
Sierra Papacal	16.02.2013	30	<b>16600.00</b>	<b>5382.31</b>	<b>11047.15</b>	1.70	<b>1366.67</b>	28.68	<b>2.38</b>	<b>53.04</b>	<b>3033.59</b>
Tixcuytun	19.02.2013	45	<b>3430.00</b>	<b>1339.85</b>	<b>1628.78</b>	3.50	300.00	15.79	1.16	10.71	394.11
Ucú	16.02.2013	35	<b>7779.00</b>	<b>3247.15</b>	<b>5023.69</b>	2.40	<b>516.67</b>	42.82	<b>1.90</b>	<b>31.44</b>	<b>2098.18</b>
UDS	15.02.2013	47	<b>8530.00</b>	<b>3643.04</b>	<b>7565.95</b>	2.60	<b>965.70</b>	24.80	<b>3.97</b>	<b>68.51</b>	<b>2741.58</b>

Appendix 10: Element concentrations for deep samples. In bold values above Mexican drinking water standard.

Well	Sample Date	Sample Depth [m]	TDS [mg L <sup>-1</sup> ]	Na <sup>+</sup> [mg L <sup>-1</sup> ]	Cl <sup>-</sup> [mg L <sup>-1</sup> ]	N-NO <sub>3</sub> [mg L <sup>-1</sup> ]	SO <sub>4</sub> <sup>=</sup> [mg L <sup>-1</sup> ]	As [mg L <sup>-1</sup> ]	Hg [mg L <sup>-1</sup> ]	Pb [mg L <sup>-1</sup> ]	Hardness [mg L <sup>-1</sup> ]
Manantial 2	23.09.2012	1	<b>2023.00</b>	<b>349.00</b>	<b>588.17</b>	2.90	110.00	2.91	0.35	1.43	<b>626.80</b>
Manantial 3	23.09.2012	1	<b>1988.00</b>	<b>348.00</b>	<b>683.53</b>	2.70	147.50	2.14	0.44	1.89	<b>635.17</b>
Manantial 4	23.09.2012	1	<b>2215.00</b>	<b>369.00</b>	<b>648.79</b>	2.70	117.50	1.92	0.37	3.58	<b>618.43</b>
Manantial 6	22.09.2012	1	<b>1985.00</b>	<b>383.00</b>	<b>811.87</b>	2.70	100.00	2.06	0.91	1.61	<b>615.80</b>
Manantial 7	22.09.2012	1	<b>1910.00</b>	<b>388.00</b>	<b>645.24</b>	2.20	115.00	2.27	0.35	0.01	<b>587.72</b>
Manantial 8	22.09.2012	1	<b>2040.00</b>	<b>366.00</b>	<b>736.71</b>	2.60	112.50	2.21	0.67	6.37	<b>648.40</b>
Exbasurero 1	22.09.2012	1	<b>1940.00</b>	<b>385.00</b>	<b>672.90</b>	3.60	80.00	2.44	0.33	2.42	<b>617.55</b>
Exbasurero 4	22.09.2012	1	<b>2950.00</b>	<b>524.00</b>	<b>1028.14</b>	3.40	140.00	3.37	0.46	2.15	<b>712.40</b>
Manantial 2	19.02.2013	1	<b>1400.00</b>	<b>421.16</b>	<b>850.16</b>	2.30	105.00	4.32	<b>2.40</b>	0.90	<b>586.35</b>
Manantial 3	19.02.2013	1	<b>1440.00</b>	<b>375.00</b>	<b>514.07</b>	2.20	125.00	4.64	0.46	1.41	<b>509.10</b>
Manantial 4	19.02.2013	1	<b>1450.00</b>	<b>370.00</b>	<b>514.07</b>	2.10	130.00	4.77	0.71	6.19	<b>579.97</b>
Manantial 6	19.02.2013	1	<b>1400.00</b>	<b>404.63</b>	<b>534.63</b>	2.20	120.00	3.86	0.42	1.22	<b>551.32</b>
Manantial 7	19.02.2013	1	<b>1300.00</b>	<b>390.58</b>	<b>493.51</b>	2.70	130.00	4.45	0.80	4.74	470.16
Manantial 8	19.02.2013	1	<b>1330.00</b>	<b>334.00</b>	<b>493.51</b>	2.50	120.00	3.75	1.09	0.82	496.43
Exbasurero 1	19.02.2013	1	<b>1460.00</b>	<b>434.44</b>	<b>772.88</b>	3.50	87.50	3.07	<b>7.86</b>	2.97	<b>527.16</b>
Exbasurero 4	19.02.2013	1	<b>1320.00</b>	<b>388.03</b>	<b>772.88</b>	3.80	90.00	3.10	<b>4.78</b>	3.52	<b>572.28</b>